DISSECTION OF THE FACTORS INVOLVED IN CHROMATIN REMODELLING AND DNA DAMAGE RESPONSE PATHWAY IN HYPOXIC CONDITIONS

A THESIS SUBMITTED TO THE UNIVERSITY OF MANCHESTER FOR THE DEGREE OF DOCTOR OF PHILOSOPHY IN THE FACULTY OF BIOLOGY, MEDICINE AND HEALTH

2018

MARIA LIKHATCHEVA

SCHOOL OF HEALTH SCIENCES

TABLE OF CONTENTS

WORD COUNT: 33,170

LIST OF FIGURES

LIST OF TABLES

LIST OF ABBREVIATIONS

Full Name	Abbreviation
National Cancer Institute	NCI
Hypoxia-inducible factor	HIF-1
Erythropoietin	EPO
PER-ARNT-SIM domain	PAS
Basic helix-loop-helix	bHLH
Endothelial PAS domain-containing protein 1	EPAS
Aryl hydrocarbon receptor nuclear translocator	ARNT
Inhibitory PAS domain protein	IPAS
Oxygen dependent degradation domain	ODDD
Prolyl hydroxylase domain enzymes	PHDs
von Hippel-Lindau protein	pVHL
Hypoxia response elements	HRE
Phosphatidylinositol 3-kinase	PI3K
Phosphatidylinositol 3-kinase-related kinases	PIKKs
MutS homolog 2	Msh2
MutS homolog 6	Msh6
Nijmegen breakage syndrome 1	Nbs1
DNA damage response	DDR
Ataxia telangiectasia mutated	ATM
Ataxia telangiectasia-Rad3 related protein	ATR
Protein kinase catalytic subunit	DNA PKcs
Hihistone acetyltransferases	HAT
Histone deacetylases	HDAC
Jumonji C- domain containing iron dependent dioxygenases	JmjC
G9a-like protein 1	GLT
SET Domain Bifurcated 1	SETDB1
Su(Var)3-9 Homolog 1	Suv39H1
Retinoblastoma 1	Rb
Senescence associated heterochromatin foci	SAHF
P300/CBP-associated factor	PCAF
NAD-dependent protein deacetylase sirtuin-1	Sirt1
Mouse double minute 2 homolog	MDM2
DNA methyltransferases	DNMT
HDAC inhibitors	HDACi
US Food and Drug Administration	FDA
DOT1-like histone H3K79 methyltransferase	DOT1L
Enhancer of zeste 2 polycomb repressive complex 2 subunit	EZH2
Acute myeloid leukaemia	AML
Mixed-lineage leukaemia	MLL
Reactive oxygen species	ROS
Ionising radiation	IR
Ultraviolet radiation	UV
Mismatch repair	MMR
Nucleotide excision repair	NER
Base-excision repair	BER
Non-homologous end-joining	NHEJ
Homology directed or homologous recombination	HR
Double-stand DNA breaks	DSB
Replication protein A	RPA
Mini chromosome maintenance	MCM
3’single-stranded DNA	ssDNA
Checkpoint kinase 1	Chk1
Checkpoint kinase 2	Chk2
KRAB-associated protein-1	Kap1
Phosphorylation of H2AX on Ser139	γH2AX
Damage checkpoint protein 1	MDC1
IR induced foci	IRIF
60 kDa Tat-interactive protein	Tip60

Mre11-Rad50-Nbs1	MRN
Protein phosphatase 2 A	PP2A
MutL protein homolog 1	MLH1
Cellular homolog of the v-Abl oncogene of the Abelson murine leukemia virus	c-Abl
Breast cancer 1, early onset	BRCA1
Poly (ADP ribose) polymerase	PARP

ABSTRACT

Hypoxia, a common feature of solid tumours, is associated with poor prognosis, a more aggressive tumour phenotype and therapeutic resistance. Tumour hypoxia induces changes in the chromatin structure, with induction of the heterochromatin mark H3K9me3 frequently observed. The upregulation of H3K9me3 was observed with co-incidental upregulation of the methyltransferase Suv39H1 in three (FTC133, U87 and HCT116) different cancer cell lines exposed to hypoxic conditions (0.1% O_2). Thus, it was hypothesised that Suv39H1 was a candidate for the tri- methylation of H3K9 and the first part of this study was focused on investigating the potential regulatory mechanisms. RT-qPCR analysis showed no changes in the levels of Suv39H1 mRNA in hypoxia suggesting a post transcriptional regulation mechanism. In mild hypoxic conditions ($O_2 \geq 1\%$) the cells failed to induce H3K9me3 and Suv39H1. However, treatment with proteasome inhibitor MG132 in mild hypoxia induced Suv39H1 upregulation, suggesting the involvement of the proteasomal pathway in the regulation of Suv39H1 stability in hypoxia.

Under normal oxygen conditions Suv39H1 is degraded via MDM2 dependent ubiquitination, which is blocked by the protein Sirt1. However, the levels of Sirt1 were highly downregulated and MDM2 protein levels were maintained following hypoxic exposure. It has been previously reported that ATM is activated in response to hypoxia and negatively regulates MDM2 activity in response to DNA damage. To test the involvement of ATM and MDM2 in regulating Suv39H1 levels in hypoxia, the ATM specific inhibitor (Ku55933) was used together with MDM2 knockdown under normal oxygen conditions and hypoxia. As predicted, highest levels of Suv39H1 were observed when ATM is catalytically active (hypoxia) and MDM2 inactive (knockdown). The results of this study indicate an important role that ATM has in regulating chromatin structure in response to stress conditions, such as hypoxia, through regulation of MDM2.

As ATM plays a crucial role in the hypoxia induced DNA damage response, the second part of this study was focused on uncovering ATM activation in hypoxia. It has been previously reported that the acetyltransferase Tip60 is involved in ATM activation in response to DNA damage. However, if Tip60 plays a role in the hypoxia induced activation of ATM hasn't been tested to date. In order to do this a Tip60 specific inhibitor, TH1834, was used. FTC133 and HCT116 cells were treated with TH1834 under hypoxic conditions and the levels of the catalytically active form of ATM were assessed by Western blot and IF. The obtained results showed a clear involvement of Tip60 in the hypoxia induced activation of ATM. Finally, as the activation of ATM in hypoxia has been related to S-phase arrest, the cell cycle distribution of FTC133 and HCT116 cells were analysed by FACS. The result showed that ATM activation in FTC133 cells seems independent of S-phase arrest.

Heterochromatin is suggested to be important for cancer cell survival. This study proposes that ATM is involved in maintaining the heterochromatic state under hypoxia. ATM is an extensively researched target for anticancer therapy. Thus, uncovering this mechanism enables new insight into targeting hypoxic tumour cells.

DECLARATION

No portion of the work referred to in the thesis has been submitted in support of an application for another degree or qualification of this or any other university or other institute of learning

COPYRIGHT STATEMENT

ACKNOWLEDGMENTS

Firstly, I would like to thank Professor Kaye Williams, for this opportunity, her support and guidance through my PhD. I'm extremely grateful for all the help and encouragement that she has given me. Her belief and support gave me the necessary direction to be able to achieve each objective of this PhD. She has helped me become a better scientist and always inspired me to be a better person.

I would also like to thank Dr Constantinos Demonacos for all his valuable contributions into this work. His vast knowledge, experience and welcoming approach helped me shape this PhD. Additionally; I must express my gratitude to Dr Roben Gieling for believing in me and providing me with invaluable help with the daily adversities that I faced during this period.

In addition I would like to thank Dr. James Brown (National University of Ireland Galway), for providing the Tip60 inhibitor and for all his help with that part of the project. This research was funded by CONACyT, and I'm very thankful to all the people in Mexico who helped me get here.

Throughout this time I had the opportunity to work alongside very talented scientists in the experimental oncology group, that always had my back and without whom this would have been a much more difficult journey. A very special acknowledgment goes to every one of them.

I'm also very grateful to Dr Alexander Fulton for all his patience and help during the final part of this PhD. Overall these past years have been an invaluable experience that has played an important role in my personal development and growth.

Lastly, I would like to dedicate this to my mother, Larissa Alexandrova, who has always encouraged me to be better. She is my biggest inspiration and the voice inside my head. Her love and support will always be my main source of strength and motivation.

1. INTRODUCTION

1.1. CANCER

Cancer is defined by the National Cancer Institute (NCI) as “A disease in which abnormal cells divide uncontrollably and are able to invade other tissues” [1]. Cancer forms tumours inside a specific organ but can also invade other parts of the body (i.e. metastasise). Cancer is not just one type of disease but many types of diseases that can vary from one patient to another. Even inside a tumour there are molecular and microenviromental differences between different regions of the tumour (i.e. intratumoral variation) [2].

In spite of these differences, every cancer cell has certain characteristics that distinguish them from the non-malignant cells of the same tissue. These characteristics are known as “Hallmarks of Cancer”. In 2000 Hanahan and Weinberg proposed six hallmarks of cancer in order to help provide a logical framework for understanding this type of diseases. These six “Hallmarks of Cancer” were defined based on the theory that cancer arises as a result of the accumulation of specific mutations: mutations that lead to a gain of function in genes, known as oncogenes, and mutations that abolish the normal functions of genes, known as tumour suppressors. These mutations need to occur in certain pathways involved in processes such as: proliferation, angiogenesis, apoptosis, invasion and metastasis [3]. The same authors, in 2011, published a follow-on article in which they described two additional hallmarks that were not present in the first publication. These eight hallmarks of cancer are the following: self-sufficiency in proliferative signalling, disruption of mechanisms that are involved in anti-growth signalling, tissue invasion and metastasis, limitless replication potential, induction of angiogenesis, ability to evade cell death, deregulation of cellular metabolism and energetic pathways, and the capacity to avoid immune destruction. The eight hallmarks of cancer are illustrated in Figure 1.1 [4].

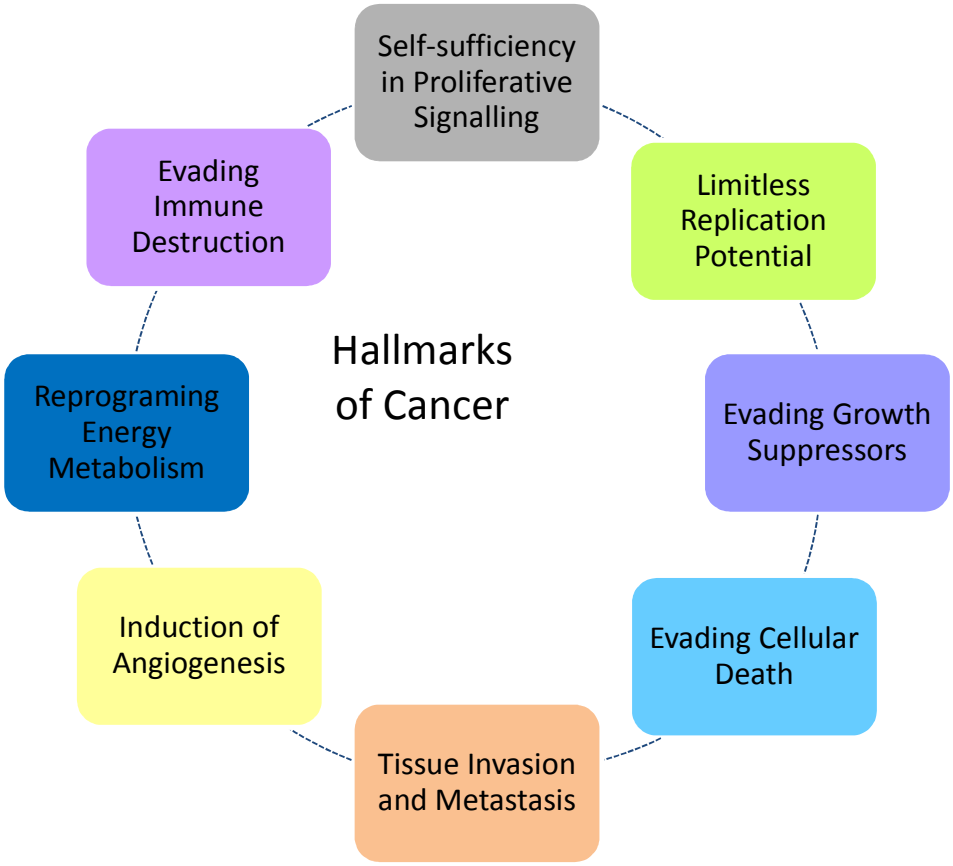

Figure 1.1. Hallmarks of Cancer. Adapted from [4]

1.2. TUMOUR HYPOXIA

Disturbed cell proliferation and angiogenesis are hallmarks of cancer. In solid tumours high proliferation rates as well as aberrant angiogenesis leads to a reduction in the normal levels of oxygen [5]. Normal oxygen levels inside a tissue are around 2-9% (40 mmHg on average). When the oxygen concentration is $\leq$ 2% or $\leq$ 0.02% the tissue is considered hypoxic or anoxic respectively [6]. As a result of aberrant angiogenesis and rapid cell proliferation, the oxygen levels inside a tumour are very variable and dynamic [2]. In order to adapt to hypoxic conditions cancer cells undergo a variety of biological changes that are associated with poor prognosis and more aggressive tumour phenotype. Hypoxia is a driving force behind genomic instability, which is considered another hallmark of cancer [2, 7] and it has been associated with radio and chemo- resistance. Hypoxia-inducible factor (HIF-1) is a transcription factor that is pivotal in the cellular response to oxygen depletion [5].

1.2.1. HYPOXIC INDUCIBLE FACTORS

Hypoxia inducible factors are key players in the regulation of the cellular response to low oxygen concentration. HIF-1 is involved in the regulation of more than one hundred different genes implicated in cellular metabolism, angiogenesis, erythropoiesis, differentiation, apoptosis, cell survival, growth factor signalling, pH regulation, vascular tone, genetic instability, invasion and metastasis [8, 9]. HIF-1 was first identified as a crucial regulator of the expression of erythropoietin (EPO) in response to low oxygen concentration [10]. Since then it has been found that HIF-1 can bind to the promoters of a wide range of different genes associated with the cellular response to hypoxia [11, 12].

HIF-1 is a heterodimer transcriptional factor composed of alpha and beta subunit (HIFα and HIFβ). These two proteins contain the PER-ARNT-SIM (PAS) domain, and belong to the family of basic helix-loop-helix (bHLH) transcription factors. HIF-β is a constitutively-expressed aryl hydrocarbon receptor nuclear translocator (ARNT) protein that is not responsive to cellular oxygen levels.

The HIF-α subunits are regulated by hypoxia. There are three different isoforms of the HIF-α subunit (HIF-1α, HIF-2α and HIF-3α) that are coded in different gene *loci,* and regulated by different promoters. HIF-1α and HIF-2α share a similar structure and are regulated in a similar manner: both of them are subject to oxygen dependent degradation [13]. HIF-1α is present in all types of tissues; while the expression of HIF-2α, also known as EPAS (endothelial PAS domain-containing protein 1), is more tissue specific. The HIF-1α and HIF-2α subunits share common targets but also can regulate the expression of specific genes in different types of cells [14]. The physiological role of the HIF-3α subunit is less clear, but the alternatively spliced isoform of this protein, called inhibitory PAS domain protein (IPAS), can bind to any alpha subunit inhibiting the formation of the active HIFα/β transcriptional factor. It seems that the expression of IPAS is also upregulated under hypoxia, and results in a negative feedback mechanism in the HIF pathway [15].

HIF-α subunits are constitutively expressed in all cells, but have half-lives of less than 5 minutes under normal oxygen conditions. In normal oxygen conditions HIF-α undergoes hydroxylation in two specific proline residues (Pro 405 and Pro 564 within HIF-1α; Pro 405 and Pro 531 within HIF-2α) inside the oxygen dependent degradation domain (ODDD). This hydroxylation is mediated by prolyl hydroxylase domain enzymes (PHDs) [16, 17].

HIF-α hydroxylation is recognised by the von Hippel-Lindau protein (pVHL), which is part of the E3 ubiquitin ligase complex. Hydroxylation of HIF-α thereby triggers ubiquitination and proteasome degradation. Under hypoxic conditions, activity of the hydroxylase enzymes is inhibited, HIF-α is stabilised and translocated to the nucleus where it forms the active HIFα/β (HIF-1) transcriptional factor that recognises and binds to a pentanucleic sequence [5'-(A/G)-CGT(G/C)-3'] of the hypoxia response elements (HRE) within the target genes. HIF-1 is involved in regulating the expression of a large variety of genes [12, 17, 18].

Additionally to an oxygen dependent pathway HIF-1 can also be regulated in an oxygen-independent manner. HIF-1 expression can be induced by oncogene signalling, mutations in tumour suppressors (i.e VHL), growth factors, different hormones, cytokines and the phosphatidylinositol 3-kinase (PI3K)/Akt pathway also plays an important role in HIF-1 regulation [19-21]. Further, phosphatidylinositol 3-kinase-related kinases (PIKKs), a family of Ser/Thr-protein kinases with sequence similarity to PI3Ks are also part of the HIF-1 signalling pathway [2, 22-27].

1.2.2. CONSEQUENCES OF HYPOXIA ON TUMOUR CELLS AND ITS CLINICAL RELEVANCE

Tumour hypoxia is associated with low survival and high incidence of metastasis [28]. This is mainly related to two factors: hypoxic cells are more resistant to chemo and radiotherapy and hypoxia helps to develop more aggressive phenotypes and promote genetic instability [29].

Hypoxia induces a set of events at cellular level. Firstly, it activates HIF-1 signalling pathways that can aid the development and survival of tumours. Processes such as angiogenesis, metastasis, proliferation, migration, metabolism, apoptosis and drug resistance are regulated by HIF-1 [8, 18, 30, 31]. HIF-1 target genes are involved in a wide variety of pathways. An example of HIF-1 target genes and their role in cancer is outlined in Figure 1.2.

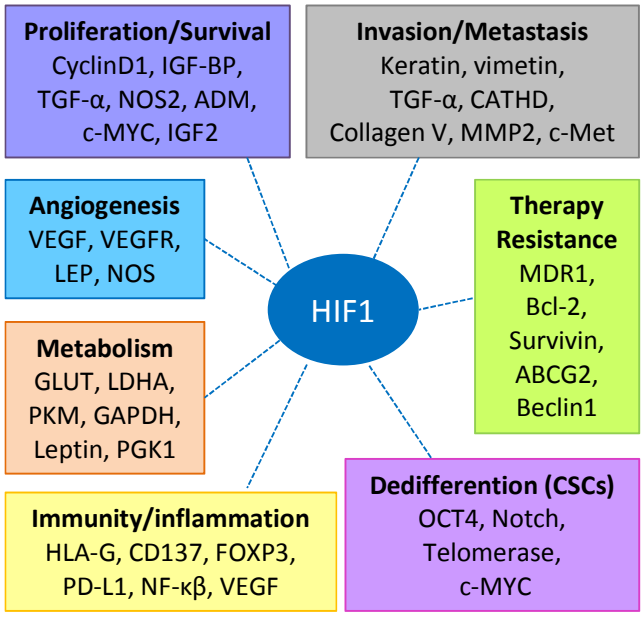

Figure 1.2. Examples of HIF-1 target genes involved in cancer progression. Adapted from [32]

Secondly, hypoxia can inhibit genes involved in the DNA damage repair pathways such as the mismatch repair (Msh2 and Msh6) and Nijmegen breakage syndrome 1 (Nbs1), a protein involved in DNA damage response (DDR), in a HIF-1 dependent fashion [33, 34]. The correlation between HIF-1 and DDR is very complex. Recent evidence suggests that HIF -1 regulated pathways are interconnected with phosphatidylinositol 3-kinase-related kinases (PIKK) family of proteins. The principal members of this family of proteins are: ataxia telangiectasia mutated (ATM), ataxia telangiectasia-Rad3 related protein (ATR) and protein kinase catalytic subunit (DNA-PKcs) [2, 22, 23, 26]. PIKK proteins are the leading initiators and regulators of the DNA damage response. [35].

Thirdly, it is well-known that increased radio-resistance is associated with tumour hypoxia. Molecular oxygen is essential to “fix” the DNA damage induced by radiation and without oxygen you have less DNA damage [36, 37]. In addition to conferring radio-resistance on tumour cells, hypoxia induces the activation of a variety of biological pathways that makes hypoxic cells harder to target using chemotherapy [38].

Finally, recent literature increasingly suggests that hypoxia induces epigenetic events required to initiate the hypoxic response and also maintain the post hypoxic phenotype [39]. These hypoxia induced changes in the chromatin structure can lead to different

cellular outcomes such as the induction of the DDR, resistance to chemotherapy, repression of gene expression, heterochromatin formation and shift in the cell cycle [22, 40].

1.3. CHROMATIN STRUCTURE

The nuclear DNA of the eukaryotic cell is organised in a complex and dynamic structure known as chromatin. The chromatin is composed of DNA and many proteins. Nucleosomes are the basic units of chromatin. Nucleosomes are composed of 147 base pairs of DNA wrapped around an octamer of histones. The core histone octamer is formed by two copies of four different histones: H2A, H2B, H3 and H4. The nucleosomes are linked together by stretches of linker DNA and linker histones such as H1. The arrangements of nucleosomes are further compacted in to secondary and tertiary structures that form the higher order of chromatin [40, 41].

Depending of the level of compaction the regions of chromatin can be divided in two: euchromatin and heterochromatin. Open, less compact, regions of chromatin are called euchromatin. Meanwhile closed and more compact regions of chromatin are considered to be heterochromatic. Generally, lower levels of compaction are associated with active gene transcription and a more compact conformation of chromatin is associated with gene repression [42].

Changes in chromatin structure are dictated by epigenetic modifications and are essential for the majority of cellular process. The main epigenetic mechanisms responsible for regulating the level of compaction of chromatin are DNA methylation and the post-transcriptional modification of histones [40]. DNA can be methylated in repetitive sequences of CpG nucleotides found in genes but also in gene promoters [43]. DNA hypermethylation is usually associated with gene-silencing. On the other hand, DNA hypomethylation is associated with gene expression [44].

Post-transcriptional modification of histones is the fastest way of changing their function. Histone post-transcriptional modifications are covalent modifications that can affect chromosome structure and function. Histones can be phosphorylated on threonine or serine, methylated on arginine or lysine and acetylated or sumoylated or ubiquitinated on lysine residues. Histone modifications usually occur on the N-terminal tail of the histone that hangs from the nucleosome which makes them accessible from its surface [45]. Histone modifications can regulate the levels of chromatin compaction and accessibility in

different ways. Some of these post-transcriptional modifications can directly affect nucleosome interaction and subsequently chromatin compaction [46]. In addition to the direct effects, histone modifications can act indirectly by recruiting different proteins that are involved in blocking the access of remodelling complexes or influence chromatin interaction with transcription factors or chromatin modifiers [47, 48]. The best studied histone modifications are histone acetylation and histone methylation.

Histone acetylation occurs at lysine residues neutralising the positive charge of the N-terminal tail, thereby decreasing its affinity for DNA and altering nucleosome conformation [49]. Additionally, acetylated histones are binding sites for specific bromodomain containing proteins and can enhance the binding of transcriptional factors [50]. The enzymes responsible for regulating histone acetylation are the histone acetyltransferases (HATs) and histone deacetylases (HDACs). Generally, acetylation of histones, by HATs, correlates with active transcription and the removal of acetyl groups, by HDACs, with transcriptional repression and heterochromatin [40].

Histone methylation alters histone hydrophobic and basic properties, changing the affinity for diverse proteins [51]. Histone methylation is mainly associated with heterochromatin but can also be found in euchromatic regions [52]. The dynamic regulation of histone methylation is very important for a variety of cellular process involved in development; ageing and tumour progression. Two main groups of enzymes are responsible for the fine tuning of this post-transcriptional modification: histone demethylases and histone methyltransferases [51].

There are two different families of demethylases that can remove the methyl group from the lysine residues. These are the jumonji C (JmjC)- domain containing, iron dependent dioxygenases and the amine oxidases [53]. Meanwhile, the addition of the methyl group can be catalysed by three families of enzymes. The DOT1-like proteins and the SET-domain containing proteins are capable of methylating lysines and proteins of the arginine N-methyltrasferase family have been shown to methylate arginines [51].

The structure of the chromatin with some of the possible histone modifications are represented in Figure 1.3.

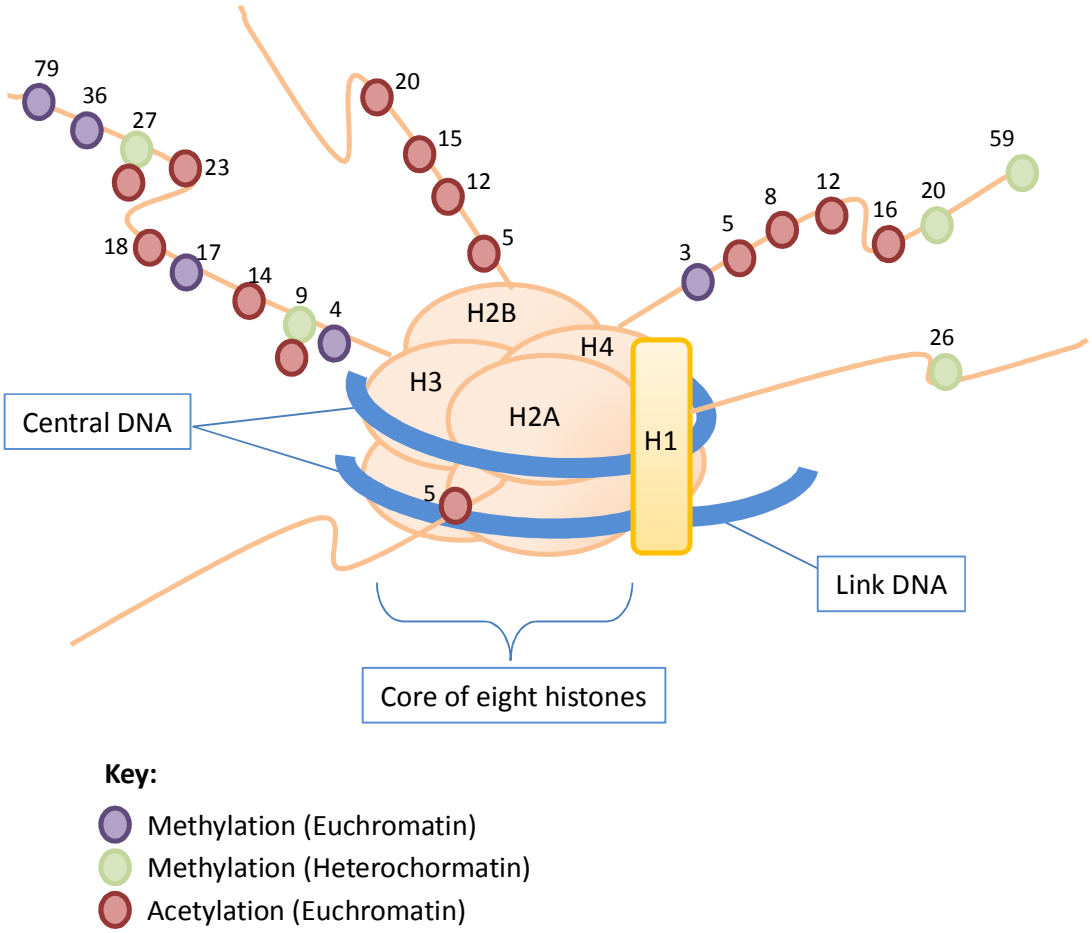

Figure 1.3. Chromatin structure and posttranscriptional modifications of histones.
Adapted from [52] and [54]

1.3.1. HISTONE METHYLATION

Histone methylation is an important post-transcriptional modification that can result in both active and inactive chromatin states [40]. Histones can be methylated at specific arginine (R) or lysine (K) residues: this event changes the level of compaction of the chromatin [55]. Lysine residues can be monomethylated (me1), dimethylated (me2) or trimethylated (me3) on their ε-amine group. Meanwhile, arginine residues can be monomethylated, asymmetrically dimethylated (me2a) or symmetrically dimethylated (me2s) on their guanidinyl group. The location of the methylated residue on a histone and the degree of methylation has been associated with different cellular outcomes [51].

One of the best studied methylation events is the methylation of histone 3 on lysine 9 (H3K9). H3K9 can be monomethylated, dimethylated or trimethylated. Each of these covalent modifications has very distinct distribution and function. H3K9me1 is mainly

found at the transcription site of active genes. Meanwhile, the di- and tri- methylation of K9 of histone 3 are mainly found in the heterochromatic regions of the genome and are more often associated with gene silencing [56, 57].

Recent genome-wide mapping studies have shown that H3K9me3 is not only important for the formation of constitutive heterochromatin but also plays an important role in cell-type-specific regulation of facultative heterochromatin [58]. It has been proposed that H3K9me3 has a protective effect on repetitive gene clusters [57] and plays an important role in the DNA damage response pathway as well as in regulating p53 transcription activity [59, 60].

Different levels of methylation of K9 of histone 3 are catalysed by members of the SET-domain family of methyltransferases. The mono- and di- methylation is usually associated with the action of the methyltransferase G9a and G9a-like protein 1 (GLP). Meanwhile the methyltransferases SET Domain Bifurcated 1 (SETDB1) and the related enzymes Su(Var)3-9 Homolog 1 and 2 (Suv39H1 and Suv39H2 respectively) contribute to the di- and tri- methylation of H3K9 [57].

1.3.2. SET-DOMAIN PROTEIN LYSINE METHYLTRANSFERASES

The SET- domain family of proteins is a group of lysine methyltransferases involved in adding methyl group to the lysine of histones and non-histone proteins. This family of enzymes contains an evolutionary conserved SET domain that was first characterised in *Drosophila melanogaster* [61]. Based on the sequence homology this family of proteins is further classified into subfamilies including: SET1, SET2, PRDM, SMYD and Suv39 [62].

The Suv39 sub-family includes the euchromatic histone-lysine N-methyltransferase 2 (EHMT2) also known as G9a, GLP, Suv39H1, Suv39H2, SETDB1 and SETDB2. This sub-family of proteins are involved in transferring a methyl group from S-adenosyl-L-methionine to ε-amino group on lysine residues of target proteins [63]. As previously mentioned, G9a, GLT and SETDB1 are involved in the catalysis of H3K9me1 and H3K9me2. SETDB1 when associated with the human homolog of mAM (mAM/hAM), a murine ATFa-associated factor, which can also transform H3K9me2 to H3K9me3. Meanwhile, Suv39H1 and Suv39H2 preferentially bind to H3K9me1 to catalyse H3K9me2 and H3K9me3 [57]. It has been shown that Suv39H1, G9a, GLT and SETDB1 can co-exist in the same complex and that its stability is interlinked [64].

Suv39H1 is a nuclear protein involved in regulating cell cycle progression, differentiation and senescence [65]. Suv39H1 is implicated in the G1/S transition by associating with

Retinoblastoma 1 (Rb1) protein and repressing transcription of cyclins such as Cyclin E and Cyclin A2 [66]. In response to various stimuli the cell can enter a non-proliferative state such as senescence. Suv39H1 plays a crucial role in the formation of senescence associated heterochromatin foci (SAHF). SAHF are characteristic heterochromatin structures that are involved in repressing genes involved in proliferation [67].

Similar to Suv39H1, G9a is a nuclear protein. However, G9a has a positive role in proliferation. G9a is involved in repressing the expression of cell cycle inhibitors such as p21 and Rb1. G9a can actively induce the expression of Cyclin D1 by interacting with the acetyltransferase P300/CBP-associated factor (PCAF) [68]. Contrary to G9a and Suv39H1, SETDB1 shows nuclear as well as cytoplasmic localisation [69]. SETDB1s role in proliferation is cell dependent. It has been shown that SETDB1 induces S-phase in myoblasts [70]. However, another study showed that SETDB1 represses proliferation by inhibiting the E2F1 promoter in *Mus musculus* teratocarcinoma cells [71].

Aberrant histone methylation is linked to some developmental disorders and human diseases such as cancer [51, 65]. Consistent with its involvement in repressing genes involved in proliferation, Suv39H1 is considered a tumour suppressor. Suv39H1 activity and stability is regulated by post-transcriptional modifications. An example of this is the negative effect that Pin1 dependent phosphorylation has on Suv39H1 stability. It has been shown that Pin1 can phosphorylate Suv39H1 on Ser16 and that this modification marks Suv39H1 for ubiquitin mediated degradation. Pin1 dependent degradation of Suv39H1 promotes CyclinD1 upregulation and tumour progression [72]. On the other hand, NAD-dependent protein deacetylase sirtuin-1 **(**Sirt1) increases Suv39H1 stability by inhibiting its polyubiquitination and subsequent mouse double minute 2 homolog (MDM2) dependent degradation and thus maintaining genome stability [73].

However, G9a and GLP expression is upregulated in various types of cancer. G9a is involved in tumour progression mainly by negatively regulating tumour suppressors or by activating oncogenes [74]. For instance, silencing of G9a in colorectal carcinoma is co-related with increased DNA damage resulting in upregulation of p21 and other senescence markers [75].

The part that SETDB1 plays in tumourigenesis is less understood. It seems that most of the effects that SETDB1 has in cancer cells are dependent on p53 [65]. A number of studies showed the important role that SETDB1 has in liver carcinogenesis. In liver cancer cells,

SETDB1 is involved in regulating p53 stability. SETDB1 can methylate p53 at Lys 370, which leads to p53 stabilisation and proliferation. In this type of cancer cell, p53 undergoes a specific gain of function mutation (R249S) that endow the mutant protein with a new function involved in cell growth. SETDB1 is overexpressed in liver cancer cells and its silencing induces a G1 cell cycle arrest and subsequently a decrease in proliferation rate of cancer cells [76].

Lysine methyltransferases are critical determinants of cell fate decision and cell cycle. Hence they have emerged as important players in cancer progression. Since these enzymes are reliant on S-adenosyl methionine as a cofactor, their role in linking metabolism to tumourigenesis is important [65]. Hypoxia is a known factor in regulating cell metabolism. Recent studies have shown that hypoxia is also involved in inducing different types of post-transcriptional histone modifications that can lead to the induction or repression of a wide range of genes [39, 40, 77, 78].

1.3.3. HYPOXIA INDUCED CHANGES IN THE CHROMATIN STRUCTURE

It has been suggested that chromatin acts as an oxygen sensor and an active component of the hypoxic response, but the effects of low oxygen conditions on chromatin structure are still poorly understood [13, 78].

In order to respond to hypoxic stress the cells needs to induce or repress the expression of a wide range of genes. This is achievable by inducing a set of epigenetic events on a local and global scale. Hypoxia induces local epigenetic changes on HIF-1 target genes. Local epigenetic changes include increased histone acetylation and decreased histone methylation on the promoters of HIF-1 target genes [79]. Additionally, hypoxia induces global epigenetic changes, including an increase in DNA methylation, an increase in global levels of histone methylation and a global reduction in histone acetylation. This is accomplished by the induction of HDAC, DNA methyltransferases (DNMT) and histone methyltransferases [39]. The hypoxia induced changes in the chromatin structure are summarised in Figure 1.4.

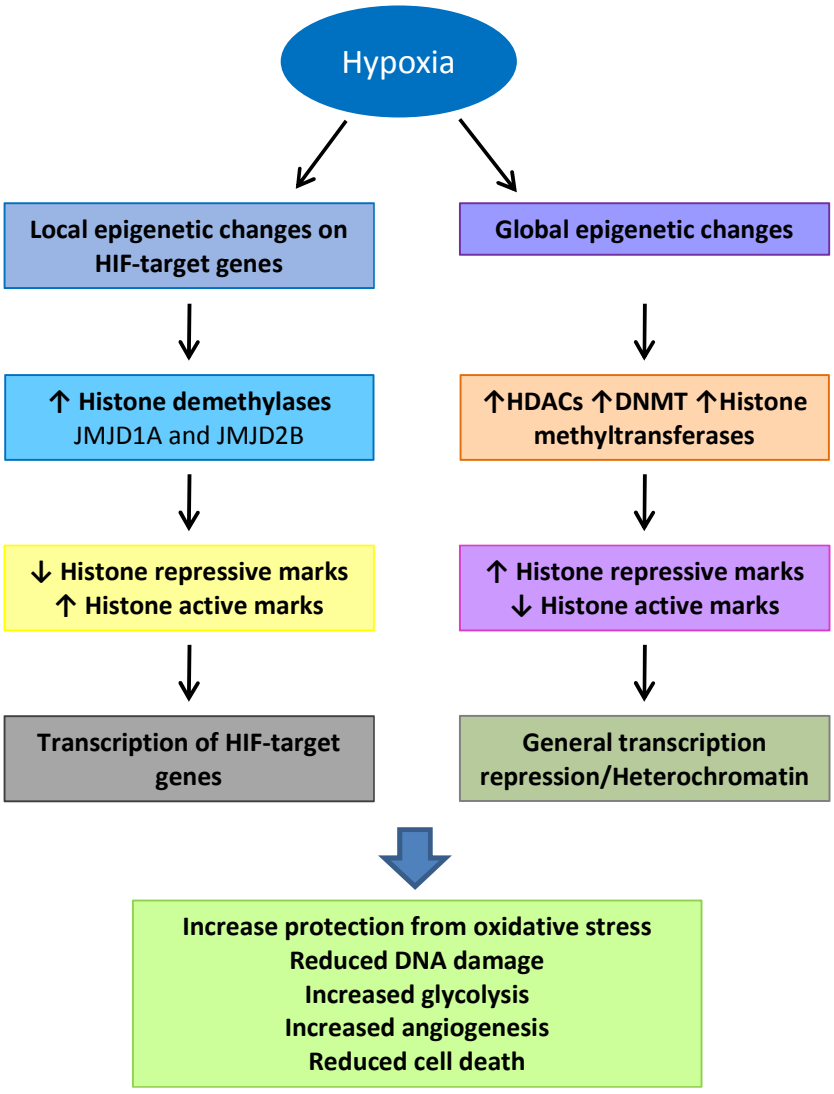

Figure 1.4. Hypoxia induced changes in the chromatin structure. Adapted from [80]

1.3.3.1. HISTONE METHYLATION IN HYPOXIA

Hypoxic induction of some genes is dependent on the status of methylation in histones at the gene promoter. A family of histone lysine/arginine demethylases (JmjC) are direct targets of HIF-1 and their demethylase activity is directly regulated by the levels of molecular oxygen, which makes them less active under hypoxic conditions [81, 82].

A range of global histone methylations has been detected in hypoxia which results in both activation and repression of gene transcription. Hypoxia increases the levels of H3K4me1/2/3 and H3K36me3 (associated with activation of transcription), increases H3K9me2/3 and H3K27me3 (associated with repression and heterochromatin) and

decreases the levels of H3K27me4 (associated with repression of transcription), [39, 55]. Recent studies have suggested that the induction of H3K9me3 in hypoxia is associated with p53-dependent apoptosis and the activation of ATM [22, 83].

It has been suggested that the induction of ATM acts as a tumorigenic barrier by inducing p53-dependent apoptosis in early stages of cancer development and that hypoxia generates a selective pressure for the inactivation of p53 pathways [24, 83-86]. The mechanism by which hypoxia induces the activation of the DDR is not fully understood. However, it has been shown that hypoxia induced replication stress as well as modifications in chromatin structure, specifically H3K9me3, are related to the activation of the DDR [22].

1.3.4. TARGETING EPIGENETIC FACTORS FOR CANCER THERAPY

In the last decade there have been a growing number of studies regarding the epigenetic regulation of cellular phenotype [44, 87]. In cancer, the tumour cell is capable of maintaining abnormal states of self-renewal, by altering the normal state of the genome and the epigenome [88]. Thus, epigenetic abnormalities are involved in cancer initiation and progression. This is exemplified by the number of frequent mutations in genes involved in controlling the epigenome [89]. Considering that epigenetic modifications are reversible, there is a growing interest in using epigenetic therapies in order to reprogram neoplastic cells towards a normal state.

Currently, epigenetic therapy mainly involves inhibitors of DNA methylation and HDAC [87]. Azacitidine is an example of a DNA methylation inhibitor that is used for treating myelodysplastic syndrome and chronic myelomonocytic leukemia [90]. Presently, this drug is being tested for use in solid tumours [91]. HDAC inhibitors (HDACi) shift the balance between acetylation and deacetylation of histones. Lysine deacetylation is a key element of abnormal gene repression in tumour cells [92]. The use of HDACi in cancer therapy is currently under intense research and a variety of HDACi are now in clinical trials [87]. Suberoylanilidehydroxamic acid and depsipeptide, are examples of US Food and Drug Administration (FDA) approved HDACi used for treating cutaneous T cell lymphomas [92].

As previously mentioned, appropriate regulation of histone methylation is necessary to maintain normal biological function. As such, lysine methyltransferases are being intensely investigated as possible therapy targets [93]. Currently inhibitors of the DOT1-like histone H3K79 methyltransferase (DOT1L) as well as the inhibitor for the lysine methyltransferase

6, also known as enhancer of zeste 2 polycomb repressive complex 2 subunit (EZH2), are in clinical trials for acute myeloid leukaemia (AML) and mixed-lineage leukaemia (MLL) respectively [94]. However, methyltransferases may function synergistically in human pathologies [64]. Furthermore, recent studies have identified methyltransferase activity independent functions of these enzymes [95, 96]. Thus, a better understanding of their mechanisms of action and regulation is crucial to develop targeted therapies.

1.4. DNA DAMAGE RESPONSE PATHWAY (DDR)

Human cells are in constant contact with exogenous and endogenous factors that can cause DNA damage. The frequency of DNA damage in human cells is around one million lesions per day. That is why the ability of the cell to respond to damage by DNA repair is very important for genomic stability, and is crucial against the development of pathologies such as cancer [97]. The most important factors that can cause DNA damage are reactive oxygen species (ROS), produced by cellular metabolism, and exogenous sources such as ionising (IR) and ultraviolet (UV) radiation [98].

The cell can respond to DNA damage in three different ways: repair, apoptosis or senescence. This is dependent on the severity and nature of the DNA damage (e.g. nucleotide dimers, single bases, single or double strand DNA breaks) [97]. There are five main molecular pathways that can lead to DNA repair: mismatch repair (MMR), nucleotide excision repair (NER), base-excision repair (BER), non-homologous end-joining (NHEJ) and homology directed or homologous recombination (HR) [98-100].

Double-stand DNA breaks (DSB) are a lethal type of damage that can cause a discontinuity in the genetic code and the formation of abnormal structures [101]. DSB are the simultaneous break of the phosphate backbone of the two DNA stands. DSB arise primarily from stalled replication forks, but also can be generated by direct contact with exogenous agents such as IR or indirectly by the effect of drugs like camptothecin, an inhibitor of topoisomerase function, and by the action of ROS that are produced during aerobic respiration [101]. Cells that escape cell cycle arrest without repairing DSB will eventually suffer mitotic catastrophe and die. Mitotic catastrophe is the main cause of cellular death induced by IR [101]. The cellular response to this type of DNA damage is to rapidly recruit different types of proteins to the chromatin (detailed below). Some of these proteins are involved in DNA repair, while others trigger the DNA damage check points

that delay cell cycle progression and organise DNA repair. Together these events are known as the DNA damage response pathway [102].

In order to repair DSB the cell can undergo two different processes: NHEJ or HR [101]. NHEJ is the most important repair mechanism that is active through all cell cycle phases. This type of DNA repair is an error-prone pathway that can bind the DNA ends back together without any regard of the DNA sequence [25, 35]. On the other hand, HR directed DSB repair is only functional when a second copy of the genome is present, through S and G2 phases of the cell cycle, which makes it a less error prone mechanism of repair [101]. The decision between NHEJ or HR during S and G2 is dependent on the regulation of DNA-resection process and the chromatin structure. Methylation and ubiquitination of the chromatin play a very important, but still very poorly understood role in DNA repair [101].

1.4.1. PHOSPHATIDYLINOSITOL 3-KINASE-RELATED KINASES (PIKKS)

DDR is regulated by a family of phosphoinositide 3-kinase-related protein kinases. PIKKs are primarily responsible for the transduction of the DNA damage response pathway [35]. The PIKKs that are involved in DDR are ATM, ATR and DNA-PKcs [103].

DNA-PKcs is a 469 kDa kinase that plays not only an important role in the DNA damage response, as ATM and ATR, but also in DNA repair. This enzyme is present in cells in the form of an inactive monomer and is activated at the site of DNA damage. DNA-PKcs is recruited to the DNA damage by its interaction with the Ku70/80 complex. DNA-PKcs binds at both ends of DNA break forming a heterotrimeric complex. The interaction between the DNA-PKs bound to each break point promotes repair, by forming a synaptic complex that enables DNA end joining. As a result of this interaction DNA-PKcs undergoes trans-auto phosphorylation in 40 different sites. [103].

ATR is a 300 kDa kinase that is only active through the S and G2 phases of the cell cycle. ATR is activated indirectly by replication protein A (RPA) which is the protein that binds to single strand DNA (ssDNA) that is generated after DNA resection during HR [103]. ATR plays an important role in the DNA damage response as well as in the initiation of DNA replication [35]. ATR is activated in each S-phase of the cell cycle to repair damaged replication forks and regulate replication of origin firing. When the replication of DNA stops and DNA polymerase stalls, the mini chromosome maintenance helicase complex (MCM) continues to unwind the DNA. This generates ssDNA which is coated by RPA, leading to ATR activation. ATR activity is fundamental for the viability of replicating

cells. One of the most important targets of ATR is checkpoint kinase 1 (Chk1), which is a key component of the G2-M transition [35, 103, 104].

ATM is a 315 kDa kinase that is present in the cell in the form of an inactive homo-dimer. In order to be activated ATM needs to be phosphorylated. ATM can undergo trans-auto-phosphorylation (at Ser1981) to be released from the inactive homo-dimer, but this auto-phosphorylation is not sufficient for the full kinase activity [105]. In the inactive homodimeric form, the kinase domain and the internal domain that contains Ser1981 residual of the neighbouring ATM molecule are bound together, preventing the binding of another substrate to the kinase domain. Initial ATM activation occurs within 5 minutes after exposure to a radiation dose as low as 0.5 Gy, which suggests that DNA breaks must signal to ATM molecules at a distance in the cells. ATM is an abundant mainly nuclear protein. A high number of ATM molecules become rapidly activated (phosphorylated) after even a small number of DSB. This suggests that ATM doesn't have to bind directly to the DSB to become activated, but rather DSBs somehow signal to ATM that is not localised to the damage site. Existing data suggests that the initial step of ATM activation is induced by changes in aspects of higher-order chromatin structure [106]. When activated ATM can phosphorylate a great number of proteins including checkpoint kinase 2 (Chk2), which is involved in regulating the cell cycle and KRAB-associated protein-1(Kap1) which is involved in the regulation of epigenetic patterns in order to promote DNA repair [42].

PIKKs have more than 700 target proteins including proteins involved in DNA replication, DNA repair, insulin signalling, RNA splicing, nonsense mediated decay, the spindle check point, tumour suppressors, chromatin remodelling, mitotic spindle and kinetochore proteins. One of the earliest events during DDR is the phosphorylation of H2AX on Ser139 (forming γH2AX) by ATM, ATR and DNA-PKcs [104]. γH2AX recruits mediator of DNA damage checkpoint protein 1 (MDC1) to the site of the DNA damage. MDC1 and γH2AX induce the recruitment of different proteins to the DNA damage site which leads to the generation of IR induced foci (IRIF). The DDR factors that lack an intrinsic affinity for DNA accumulate in large nuclear aggregates that can be detected by fluorescence microscopy as IRIF [102]. A simplified summary of the DNA damage response pathway is presented in the Figure 1.5.

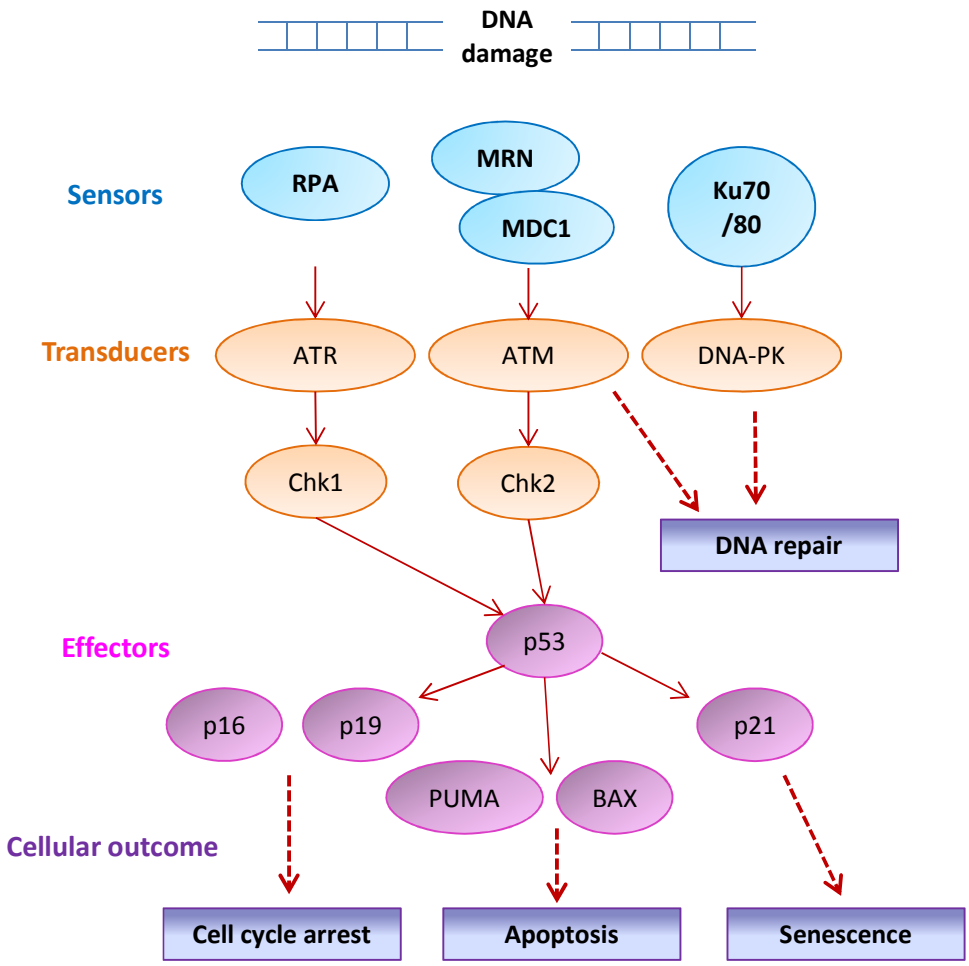

Figure 1.5. DNA damage response pathway. Adapted from [107].

1.4.1.1. Mechanisms of ATM activation

ATM is a key regulator of cell fate as it is involved in regulating cell cycle progression, DNA repair and apoptosis. Active ATM can phosphorylate a plethora of substrates, some of the most important ATM downstream targets are p53, Chk2, Kap1 and H2AX [35, 108]. As previously mentioned ATM exists in the cell in an inactive form, and can be activated by a number of different stress stimuli.

ATM activation in normal oxygen conditions is dependent on the action of the 60 kDa tat-interactive protein acetyltransferase (Tip60) also known as KAT5, that can acetylate ATM at Lys3016. This acetylation is the first step of ATM activation and is necessary for the subsequent ATM trans-auto-phosphorylation [109]. Tip60 is activated by direct interaction with H3K9me3 [109]. It's not very clear if Tip60 recognises and binds to already pre-existent H3K9me3 that are more visible after DNA damage dependent-changes in

chromatin structure or de novo methylations of H3K9 that are induced after DNA damage [59].

Tip60 is part of the MYST family of histone acetyltransferases (HAT) [110]. One of the main functions of Tip60 is the regulation of the levels of DNA accessibility by histone acetylation [111]. However, Tip60 is also involved in acetylating non-histone proteins such as p53 and ATM [112, 113]. Tip60 forms a complex with ATM by binding to the C-terminal region of this protein; this interaction induces Tip60 HAT activity [113]. In response to DNA damage ATM-Tip60 complex co-localize at IRIF where Tip60 interacts with H3K9me3, through its chromodomain, and this interaction further enhances Tip60 HAT activity [59]. Tip60 binding to H3K9me3 is promoted by the phosphorylation of the tyrosine 44 at Tip60 chromodomain by the cellular homolog of the v-Abl oncogene (c-Abl) tyrosine kinase [114]. It has been shown that Tip60 plays an important role in a variety of cellular process such as apoptosis, gene transcription and cell cycle progression [115]. Tip60 dependent acetylation of ATM is a crucial step in the DNA damage and repair pathway.

ATM acetylation is the step that links DNA damage induced chromatin remodelling and DDR [105]. The regulation of ATM activation is very complex. It has been reported that ATM can be catalytically active without being phosphorylated. The Lys 3016 acetylation site of ATM is conserved between different species but this is not true for the phosphorylation site (Ser1981). This might indicate that the acetylated form of ATM has an independent functional role [109].

In order to be fully active the ATM/Tip60 complex needs to be recruited to the site of DNA damage through the interaction with Mre11-Rad50-Nbs1 (MRN) complex; this interaction promotes the auto-phosphorylation of ATM on the Ser367 and Ser2996 residues. ATM phosphorylates MRN which is important for downstream signalling. MRN may also recruit substrates to ATM [104]. The protein phosphatase 2 (PP2A) can dephosphorylate ATM Ser1981, inhibiting its function [116].

ATM can also be activated independently of DNA damage by ROS, heat shock, hypotonic salts and hypoxia [24, 117-119]. Changes in chromatin structure without DNA damage can also induce ATM activation [106]. ATM activation in hypoxia is related to replication stress and chromatin context [22].

1.4.2. DNA DAMAGE RESPONSE PATHWAY IN HYPOXIA

DNA damage and genomic instability are hallmarks of cancer, and hypoxia is a well-known driving force behind it. Current evidence suggests that hypoxia *per se* does not cause any meaningful DNA damage, but damage can occur in response to re-oxygenation [2]. Hypoxia levels inside a tumour vary quite substantially. The intra tumour microenvironment is subject to re-oxygenation periods followed by acute hypoxia while other parts of the tumour might present chronic hypoxia. This has an important clinical effect on the malignant phenotype, for example, by way of inducing resistance to radio or chemotherapy [7]. Hypoxia can also affect the cellular response to DNA damage, which can lead to different results depending on the cellular type and the hypoxic conditions inside the tumour.

The DDR induced in hypoxia differs from the classical pathway where it is induced by DNA damage [25, 86]. Some of the available data indicates that DDR initiated in response to hypoxia serves as a barrier to tumorigenesis in pre-neoplastic cells [120]. However, prolonged exposure to hypoxia can induce downregulation of elements of the DNA damage repair pathway, leading to genomic instability [7].

A study performed in primary human skin fibroblast strain GM05757, showed that DNA repair is compromised under hypoxic conditions. This study makes it very clear that normal fibroblasts are more sensitive to present chromosome abnormalities and have a compromised DNA repair after irradiation, measured through the presence of residual DSBs (using γH2AX and 53BP1 as a marker), if kept under hypoxic conditions [121].

Different types of DNA repair mechanism such as MMR and HR are less functional under hypoxia. Members of the mismatch repair pathways such as Msh2 and Msh6 are directly inhibited by HIF-1α [34]. It has also been reported that MLH1, another component of mismatch repair is repressed in hypoxia in a HIF-1α-independent manner, due to the di-methylation of lysine 9 of histone H3 (H3K9me2) [122]. Additionally, key members of the HR pathway such as breast cancer 1 -early onset (BRCA1) and Rad51 are also downregulated under hypoxia [123].

In spite of this, studies have shown that in hypoxic conditions HR defective cells are more sensitive to IR treatment than cells with mutations in the NHEJ pathway. This might be because HR plays a significant role in cross-link repair, and the formation of DNA-protein cross links is enhanced under hypoxic conditions. Cells in hypoxia are more sensitive to

this type of DNA damage, and when not repaired this damage can be lethal. It's likely that NER proteins are involved in the cross-link repair, but the exact mechanism of DNA-protein cross link repair as well as the involvement of HR is not fully understood [124].

Despite the down regulation of some components of DNA repair mechanism under hypoxia, it is also clear that important elements of the DDR, involved in HR and NHEJ, are upregulated in hypoxia. The expression of Ku70 and DNA-PKcs is induced under hypoxic conditions. It has been shown that DNA-PK as well as ATM is involved in regulating HIF-1α stability in response to hypoxic stress [25, 26, 125].

ATR also plays an important role under hypoxic conditions. ATR is activated under hypoxia as a result of ssDNA formation during replicative stress [27, 84, 85]. The overall result of ATR activation under hypoxia is the phosphorylation of Chk1 and induction of cell cycle arrest. A study performed in colorectal cell lines using an ATR specific inhibitor, VE-821, showed that inhibition of ATR in hypoxia leads to a loss in cancer cells viability and a decrease in HIF-1α mediated signaling [23]. Another study showed that HIF-1α is involved in the expression of ATR binding partner ATR-interacting protein (ATRIP) [126].

Additionally, ATM is also activated in response to hypoxic stress. ATM undergoes auto-phosphorylation and is activated in response to hypoxia in a HIF-1α and MRN independent manner [24]. This is consistent with the fact that Nsb1, a component of MRN, is downregulated in hypoxia [127]. Under these experimental conditions Kap1, Chk2 and DNA-PKcs are also phosphorylated in response to hypoxia in an ATM-dependent manner. The same study reports formation of γH2AX foci in response to hypoxia, without the presence of DNA damage. This is a cell cycle and ATR dependent event, but independent of ATM [24]. The correlation of H2AX and p53 phosphorylation with ATM activity in hypoxia had been previously established by the same group [85].

A study performed in RKO cells shows that the activation of ATM during S phase, in response to replicative stress induced by hypoxia, is dependent on chromatin context, specifically to H3K9me3. Within these studies, the modifications on H3K9 histone were induced by hypoxia through the expression of the histone-lysine methyltransferases Suv39H2 and SETDB2. This study also demonstrated that the use of ATM specific inhibitor (Ku55933) can lead to accumulation of DNA damage in hypoxic cells [22].

The principal aim of the hypoxic induced DDR seems to be the induction of cell cycle arrest, the preservation of replication fork integrity and if there is no subsequent re-oxygenation, induction of p53-dependent apoptosis. The exact mechanism behind the activation of DDR in hypoxia is not fully understood and the involvement of Tip60 in this process hasn't been assessed to date. Available data suggests that hypoxia-induced DDR might function through modification of chromatin structure and that this activation mechanism is different from the one operating in response to DNA damage [22, 25]. There are growing evidences of the role of the chromatin-structure in ATM activation but the exact mechanism is still poorly understood [22]. A study performed in normal oxygen conditions showed that chromatin condensation promotes ATM and ATR activation in a DNA damage independent manner [128], but the effect of the chromatin structure and ATM activation in hypoxia is not clear. It is of high importance to fully understand the process that links the DDR response to hypoxia in order to sensitize cancer cells to hypoxia and treatment.

1.4.3. DNA DAMAGE RESPONSE PATHWAY AS A TARGET FOR CANCER THERAPY

The majority of current strategies for cancer treatment are based on DNA damaging agents, such as radiation or drugs used in chemotherapy. If the induced damage is successfully repaired, the cells will survive. As such, the DDR pathway plays an important role in cancer cell survival and treatment resistance [129, 130]. In order to specifically kill cancer cells, it is important to understand better the specific abnormalities in the DDR pathway that are present in cancer but not in non-malignant cells.

At present there are three known aspects of the DDR in cancer cells that are different from the non-malignant cells: loss of one or more DDR pathways, increase levels of endogenous DNA damage and increased levels of replication stress [129]. Most cancers will have lost some aspects of the DDR pathway during their generation. As mentioned previously, different types of DNA damage will generate the activation of different response pathways and, while there is not a complete redundancy, different repair pathways may compensate for the lack of others. This means that DDR deficiency in a cell will make it more reliable on another repair pathway for survival, which provides a specific target opportunity. This type of approach is known as synthetic lethality [131]. The best studied example of synthetic lethality is the use of poly (ADP ribose) polymerase (PARP) inhibitors in the treatment of BRCA deficient breast cancers [132].

The deregulation of cell proliferation driven, for example by oncogenic stress, is an early step in tumorigenesis [133]. Oncogenic stress has been shown to lead to the activation of DDR [134]. The activation of DDR in premalignant cells has been proposed to serve as a barrier to tumour progression. Cancer cells that were able to progress to form tumours overcome this barrier by the loss of one or more components of the DDR [135]. As a consequence, tumour cells present increased genomic instability and become more dependent on remaining DDR pathways [129]. Additionally, another consequence of oncogenic activation can be the induction of replication stress [136].

Replication stress can be defined as the "uncoupling of the DNA polymerase from the replisome helicase activity" [129]. This leads to the formation of ssDNA at the replication forks, which are coated by RPA which results in the activation of DDR, specifically ATR. The ATR pathway plays an important role in preventing replication fork collapse and, as a consequence, the generation of DSB that can lead to cell death [137]. Considering this, current focus around pharmacological targeting of replication stress has been around ATR and Chk1 inhibitors and several specific inhibitors are currently in clinical trials [129]. However, other factors such as CDKs and Wee1 are also involved in regulating replication origin firing [138] and the clinical use of Wee1 inhibitor, AZD1775, is currently under research [139, 140]. Another important factor that can induce replication stress as well as the activation of the DDR is hypoxia [24, 84].

As mentioned in the previous section, some aspects of the DNA damage repair pathway are downregulated in response to hypoxic stress. This makes hypoxic cells sensitive to synthetic lethality by inhibiting other parts of DDR. The idea of using DDR inhibitors in order to sensitise hypoxic cells to re-oxygenation, chemotherapy or radiotherapy has been proposed by different groups [141, 142]. ATM plays a crucial role in maintaining the integrity of DNA replication forks under hypoxic conditions as well as in regulating origin firing during re-oxygenation [22]. Accordingly, fully understand the mechanism behind hypoxia induced activation of ATM is of high importance in order to sensitise hypoxic tumour cells to treatment.

1.5. OBJECTIVES OF THE STUDY

Hypoxia induced epigenetic changes play an important role in cancer initiation, progression and therapeutic resistance which ultimately impacts patient outcomes. However, the mechanisms behind many of these epigenetic changes are still poorly

understood, despite the potential clinical relevance. The induction of H3K9me3 is observed in response to hypoxia and has been related to the activation of ATM [22]. Despite this, the exact mechanism behind this event is not fully known. Thus, the first aim of this project was to elucidate the mechanism behind the hypoxia induced formation of H3K9me3. In order to achieve this, first the levels of H3K9me3 and the related methyltransferase Suv39H1 were assessed in three different cancer cell lines: FTC13, U87 and HCT116 under hypoxia (0.1% O_2). Considering that the protein stability of Suv39H1 has been related to MDM2 and Sirt1, the levels of these proteins were also studied using the same experimental conditions. Next, the involvement of ATM in regulating MDM2 activity and consequently the protein levels of Suv39H1 in hypoxia was assessed using ATM specific inhibitor Ku55933. Finally, the role that MDM2 and ATM play together in regulating Suv39H1 in hypoxia was studied using MDM2 siRNA together with Ku55933 in FTC133 cell line.

Considering the importance of ATM in the hypoxia induced DDR, the second aim of this project was to evaluate the role of Tip60 in hypoxia induced ATM activation. In order to do this a Tip60 specific inhibitor, TH1834, was used in two different cancer cell lines: FTC133 and HCT116.

2. MATERIALS AND METHODS

2.1. CHEMICALS AND REAGENTS

The reagents used for cell culture, L-Glutamine, Trypsine-EDTA and the cell culture media, were all purchased from Sigma-Aldrich (Poole, Dorset, UK). Phosphate buffer saline (PBS) was purchased from Oxoid (Hampshire, UK). Fetal bovine serum (FBS) was purchased from GIBCO, Invitrogen (GIBCO PRL, Paisley, UK). Dimethyl sulphoxide (DMSO) was purchased from Fisher Scientific (Leicestershire, UK). All tissue culture plates and flasks were purchased from Corning (Flintshire, UK). All other reagents were obtained from Sigma-Aldrich (Poole, Dorset, UK) unless otherwise stated.

2.2. CELL CULTURE

Cell culture was performed using a class II laminar flow microbiological safety cabinet. All cells were grown in a humidified incubator at 37°C supplied with 5% CO_2.

2.2.1. CELL LINES

Three different cell lines were used: FTC133, HCT116 and U87. Cell lines were originally obtained from ATCC and the details are listed in Table 2.1. Mycoplasma testing was carried out routinely at the core facilities at The University of Manchester using MycoAlert™ mycoplasma detection kit (Lonza, Manchester, UK).

Table 2.1. Cell lines description

Cell line	Pathology	Description
FTC133	Human follicular thyroid carcinoma	Obtained from a lymph node metastasis of a 42 year old male [143]
U87	Glioblastoma	Obtained from a malignant glioma of a female patient [144]
HCT116	Colorectal carcinoma	Obtained from a male colorectal carcinoma [145]

2.2.2. CELL LINES MAINTENANCE AND STORAGE

U87 and HCT116 cell lines were grown in RPMI-1640 media supplemented with 10% (v/v) FBS and 1% (v/v) 200 mM L-glutamine solution. FTC133 cell line were grown in Dulbecco's Modified Eagle Medium **(**DMEM) media combined with HAM's F12 (1:1)

supplemented with 10% (v/v) FBS. FTC133 and HCT116 cells were passaged twice-weekly at 1:10 and U87 cell lines were passaged at 1:5. Cell passage was performed first by removing the media and washing gently the cell layer with sterile PBS. To detach the cells 3 mL of Trypsin-EDTA was added to a T175 cell culture flask and incubated for 3 min at 37°C. Next, 7 mL of complete culture media was added to inactivate the Trypsin. An appropriate volume of cell suspension was transferred to a new T175 flask containing the desire volume of complete cell culture media.

In order to maintain cell stocks of lower passage, exponentially growing cells were frozen down and stored at -80°C. Cells were detached and collected from T175 flasks as described above. The cell suspension was centrifuge at 1,400 x rpm for 4 min, the cell culture media was removed and the cell pellet re-suspended in freezing media (50% (v/v) FBS, 40% (v/v) complete cell culture media and 10% (v/v) DMSO). The cell suspension was frozen down in a 1.5 mL cryovials.

2.2.3. CELL COUNTING AND SEEDING

In order to seed a pre-defined number of cells for each experiment, the cell pellet created from an ongoing cell culture (as outlined in section 2.2.2) was re-suspended in 10 mL complete media. The cells were subsequently counted using a TC20 automated cell counter (Bio-Rad Laboratories, Herfordshire, UK). In order to obtain a life cell count an aliquot of cell suspension was diluted in a 1:1 ratio with 0.4% Trypan Blue solution.

2.3. HYPOXIC CONDITIONS

A Whitley H35 Hypoxystation (Don Whitley Scientific Limited, Shipley, UK) was used in order to create the appropriate hypoxic condition (1% or 0.1% O_2, 5% CO_2 and nitrogen balanced). Cells were seeded (as outlined in section 2.2.3) and allowed to adhere to the cell culture dish before being transferred to the hypoxic chamber. Oxygen, carbon dioxide and nitrogen (oxygen-free) gas cylinders were purchased from BOC (The Linde Group, Worsley, UK).

2.4. DRUG TREATMENT

Three different drugs were used: TH1834, a Tip60 specific inhibitor, Ku55933, an ATM specific inhibitor and MG132, proteasome inhibitor. TH1834 was designed and generously provided by Dr. James Brown (National University of Ireland Galway, Galway, Ireland) as described in [146]. Ku55933 was purchased from Sigma-Aldrich. A detailed drug

description is presented in Table 2.2. The cells were treated with one of the drugs and immediately transferred to the hypoxic chamber. Control samples were treated with dimethyl sulphoxide (DMSO) to match the concentration of the highest drug concentration used. For experiments using radiation, cells were first treated with the specified drug for the appropriate amount of time and then irradiated.

Table 2.2. Drug characteristics

Name	Inhibition target	Function
TH1834	Tip60	Directly inhibits Tip60 acetyltransferase activity by binding to the active binding pocket [146].
Ku55933	ATM	Competitive specific ATM kinase inhibitor [147].
MG-132	Proteasome	Reversible 20S proteasome inhibitor that reduces the degradation of ubiquitinated proteins [148].

2.5. IRRADIATION

Cells were irradiated under normal ambient conditions using a Faxitron x-ray (Faxitron Bioptics, AZ, USA). Plates of cells were irradiated with a 4 Gy dose (dose rate of 0.95 Gy/min). The cells were then transferred back into the incubator and lysed after 30 min or 1 hour depending on the experiment.

2.6. WESTERN BLOT

2.6.1. REAGENTS AND BUFFERS

The chemicals used to prepare the solutions were of analytical grade and supplied by Sigma-Aldrich (Poole, Dorset, UK) unless stated otherwise. All NuPAGE™ reagents and gels were purchased from Invitrogen (Parsley, UK). Buffers used for Western blot are detailed in Table 2.3.

Table 2.3. Buffers used for Western Blot

Buffer	Composition
RIPA Lysis buffer	Tris-HCl 50 mM at pH 7.4, NaCl 150 mM, Octylphenoxy poly(ethyleneoxy)ethanol (IGEPAL) 1%, Ethylenediaminetetraacetic acid (EDTA) 1 mM, Protease Inhibitor Cocktail 1 tablet, phenylmethylsulfonyl fluoride (PMSF) 1 mM, Na_3VO_4 1 mM and NaF 1 mM (all the phosphatase inhibitors were added on the day that the lysates were prepared).
SDS-PAGE sample buffer	1 mL 0.5 M Tris-HCl pH 6.8, 0.8 mL glycerol, 1.6 mL 10% (w/v) sodium dodecyl sulphate (SDS), 0.4 mL β-mercaptoethanol, 0.01 g bromophenol blue, 4 mL dH_2O.
NuPAGE™ LDS Sample buffer	1x Lithium dodecyl sulfate (LDS) sample buffer prepared by diluting 4x LDS NuPAGE™ sample buffer and adding 10x NuPAGE™ reducing agent.
SDS-PAGE Running buffer	2.42 g Bis-Tris, 18.75 g glycine, 1 g SDS, made up to 1L in dH_2O.
NuPAGE™ Tris-Acetate SDS Running buffer	1x Tris-Acetate running buffer prepared by diluting 20x NuPAGE™ Tris-Acetate running buffer with dH_2O.
NuPAGE™ MOPS SDS Running buffer	1x 3-(*N*-morpholino)propanesulfonic acid (MOPS) running buffer prepared by diluting 20x NuPAGE™ MOPS SDS running buffer with dH_2O.
NuPAGE™ MES SDS Running buffer	1x 2-(*N*-morpholino)ethanesulfonic acid (MES) running buffer prepared by diluting 20x NuPAGE™ MES SDS running buffer with dH_2O.
Tris/Bicine Transfer buffer	5.24 g Bis-Tris, 4.08 g Bicine, 2.4 g EDTA, made up to 1L in dH_2O
Glycine Transfer buffer:	3.03 g Bis-Tris, 14.41g glycine, 200 mL methanol, made up to 1L in dH_2O.
TBS	1 tablet of Tris Buffered Saline (Sigma Aldrich, UK) in 500 mL of dH_2O.
TBST	0.1% Tween 20 in TBS

2.6.2. CELL LYSATES

Exponentially growing cells were seeded into a 6 cm petri dish at the following cell densities: 4 x 10^5 FTC133 cells, 6 x 10^5 HCT116 cells and 5 x 10^5 U87 cells. The cells were left overnight to attach and treated when they have reached 70% confluency. After treatment the cell were washed with ice-cold PBS and 80 μL of RIPA lysis buffer was added. The cells were scrapped on ice and transfer to a pre-chilled Eppendorf tube. Cell lysates were kept on ice and sonicated twice for 5 seconds at 10 Hz using the Soniprep 150 MSE (Sanyo, UK). Cell lysates were stored overnight at -20 °C and centrifuged the next day at 13,000 rpm for 10 min at 4 °C. The concentration of protein was quantified as described in section 2.7.3 and the supernatants were stored at -20 °C.

2.6.3. PROTEIN QUANTIFICATION

The concentration of proteins in the cell lysates was quantified using the bicinchoninic acid (BCA) assay [149]. Each time a standard curve was generated using protein standards

prepared by performing serial dilutions of bovine serum albumin (BSA) in RIPA buffer. The following concentrations of BSA standards were used: 0.0781, 0.156, 0.3125, 0.625, 1.25, 2.5 and 5 mg/mL. BCA reagent was prepared by diluting 4% (w/v) copper sulphate 1:50 ratio with BCA. The assay was performed by pipetting 5 µL of either cell lysates or BSA standards into a 96-well plate and 200 µL of BCA reagent was added into each well. The plate was incubated for 30 min at 37 °C and the absorbance was measured at 562 nm using a µQuant Microplate Spectrophotometer (BioTek, Potton, UK). The obtained values for the BSA standards were plotted to obtain the standard curve and the protein concentration in each sample were calculated using this standard curve.

2.6.4. GEL ELECOPHORESIS

Three different types of gels were used in order to separate the proteins of the samples according to their molecular weight. SDS-PAGE gels were prepared as detailed in the Table 2.4 and set using Mini-Protein tetra cell (BioRad, Hertfordshire, UK) and run at 120 V with SDS-PAGE running buffer. Two different types of pre-cast gradient gels were used: 3-8% NuPAGE™ Tris-Acetate gels and NuPAGE™ 4-12% Bis-Tris gels. NuPAGE™ gels were run using the Novex Mini-Cell XCell SureLock (Invitrogen, Paisley, UK) either with the NuPAGE™ Tris-Acetate SDS Running buffer, the NuPAGE™ MOPS SDS Running buffer or the NuPAGE™ MES SDS Running buffer. Protein samples (20 or 30 µg) were prepared using either SDS-PAGE sample buffer or the NuPAGE™ LDS sample buffer and boiled at 100 °C or 70 °C for 10 minutes. Finally, the samples were briefly centrifuged and loaded into the gel alongside 10 µL of PageRuler™ Prestained Protein Ladder (Invitrogen, Parsley, UK) and run until the band of blue-coloured sample buffer reached the bottom of the gel.

Table 2.4. SDS-PAGE gels composition

Component	10% Separating gel	15% Separating gel	Staking gel
dH_2O	3.8 mL	2.2 mL	3 mL
1.5 M Tris (pH 8.8)	2.6 mL	2.6 mL	—
0.5 M Tris (pH 6.8)	—	—	1.25 mL
30% Acrylamide/Bis-Acrylamide solution	3.4 mL	5 mL	0.67 µL
20% (w/v) SDS	50 µL	50 µL	25 µL
10% (w/v) APS	50 µL	50 µL	120 µL

TEMED	5 µL	5 µL	12 µL

2.6.5. PROTEIN TRANSFER

Proteins from the gel were transferred to a polyvinyline fluoride (PVDF) membrane (BioRad, Hertfordshire UK) using Mini Trans-Blot® Electrophoretic Transfer Cell (BioRad, UK). PVDF membrane was activated with 100% methanol, washed with dH_2O and submerged in the transfer buffer. Two 3 mm filter papers (Whatman Plc, Brentford, UK) were used to set up the transfer cassette as shown in the Figure 2.1. All transfer components were immersed in pre chilled transfer buffer before being placed into the transfer system. Proteins separated using NuPAGE Bis-tris gels as well as SDS-PAGE gels were transferred for 1 hour at 100 V using Glycine Transfer buffer. Proteins separated using NuPAGE Tris-Acetate gels were transferred overnight at 36 V using Tris-Bicine Transfer buffer. After the transfer was complete, the PVDF membrane was stained using Ponseau S solution (Sigma, Dorset, UK) to test the transfer efficiency of the transfer. To remove the Ponseau S solution the membrane was washed with TBST.

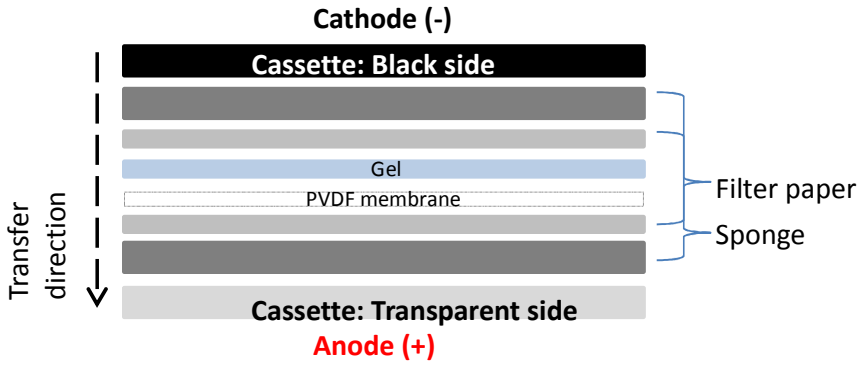

Figure 2.1 Components and assembly of the transfer cassette. Wet-transfer method was used to transfer proteins form the gel into the PVDF membrane. All the elements of the transfer cassette were soaked in pre-chilled transfer buffer. The cassette was assembled and inserted into the BioRad transfer module.

2.6.6. IMMUNOBLOTTING

Membranes were blocked using a blocking buffer (Table 2.5) for 1 hour at room temperature and then incubated with the primary antibody diluted in the corresponding

blocking buffer overnight at 4 °C. The next day the membrane was washed 5 times for 5 minutes with TBST and subsequently incubated for 1 hour at room temperature with a horseradish peroxidase (HRP)-conjugated secondary antibody, diluted in 5% (w/v) non-fat dry milk (Marvel, Spalding, UK). Finally, membranes were washed with TBST 5 times for 5 minutes. The details of all the antibodies used, as well as the corresponding blocking buffer are detailed in the Table 2.5.

Table 2.5. Antibodies used for Western Blot

Antibody	Species	Supplier	Dilution	Diluent/blocking buffer
ATM (Y170)	Rabbit	Abcam	1:5,000	5% (w/v) non-fat dry milk in TBST
ATM-pSer1981 (EP1890Y)	Rabbit	Abcam	1:5,000	5% (w/v) BSA in TBST
HIF-1α	Mouse	BD Transduction *(610958)*	1:1,000	5% (w/v) non-fat dry milk in TBST
Sirt1	Rabbit	Millipore (*#07131)*	1:1,000	3% (w/v) non-fat dry milk in TBST
Tip60 (N-17)	Goat	Santa Cruz	1:200	5% (w/v) non-fat dry milk in TBST
P53-pSer15	Rabbit	Cell signalling (#9284)	1:1,000	5% (w/v) non-fat dry milk in TBST
P53 (PAb240)	Mouse	Abcam	1:1,000	3% (w/v) non-fat dry milk in TBST
H3K9me3	Rabbit	Abcam (ab4441)	1:5,000	5% (w/v) BSA in TBST
H3	Rabbit	Abcam (ab1791)	1:5,000	5% (w/v) BSA in TBST
Suv39H1	Rabbit	Millipore (#07958)	1:1,000	5% (w/v) non-fat dry milk in TBST
MDM2 (EP16677)	Rabbit	Abcam	1:1,000	5% (w/v) non-fat dry milk in TBST
HP1α	Rabbit	Abcam (ab9037)	1:1,000	5% (w/v) non-fat dry milk in TBST
B-actin	Mouse	Sigma	1:5,000	5% (w/v) non-fat dry milk in TBST
Anti-Rabbit HRP	Goat	Sigma	1:5,000	5% (w/v) non-fat dry milk in TBST
Anti-Mouse HRP	Rabbit	Sigma	1:2,500	5% (w/v) non-fat dry milk in TBST
Anti-Goat HRP	Rabbit	Sigma	1:10,000	5% (w/v) non-fat dry milk in TBST

2.6.7. CHEMILUMINESCENT DETECTION OF PROTEINS

The target protein was detected using enhanced chemiluminescent substrate (Clarity Western ECL substrate, Bio-Rad, UK). The membrane was incubated for 1 minute with ECL at room temperature and developed using a ChemiDoc™ XRS + system. ImageLab™ software (BioRad, UK) was used to acquire and analyse the images of the chemiluminescent signal.

2.6.8. DENSITOMETRIC QUANTIFICATION OF PROTEIN EXPRESSION

ImageLab™ software (BioRad, UK) was used to perform the densitometric analysis. The data obtained for the target protein was normalised using a loading control (β-actin). Posttranscriptional modified proteins (e.g. ATM-pS1981) were calculated as a ratio of the total amount of the protein (e.g. ATM). The data obtained from each individual experiment was normalised to the untreated control of the same experiment.

2.6.9. STRIPING AND REPROBING

When probing for post transcriptional modified proteins (e.g. ATM-pS1981), the PVDF membrane was striped using Reblot Plus solution (Merk Millipore, Watford, UK) and re-incubated with the antibody directed against the total form of the protein (e.g. ATM).

2.7. IMMUNOFLUORESCENCE (IF)

2.7.1. SOLUTIONS AND REAGENTS

All the following reagents were of analytical grade and supplied by Sigma-Aldrich (Poole, Dorset, UK). The buffers were prepared as detailed in Table 2.6.

Table 2.6 Solutions used for Immunofluorescence

Solution	Composition
Fixation buffer	10% formalin in PBS (Formalin)
Permeabilisation buffer	0.1% (v/v) Triton-100 in PBS (PBST)
Blocking buffer	3% (w/v) BSA in PBS (BSA/PBS)

2.7.2. CELL FIXING AND STAINING

First, 1.5 x 10^4 cells were seeded onto a sterile cover slip in a 35 mm petri dish containing a total of 2 mL of complete cell culture media and left overnight to attach. Next, the cells were treated as indicated in each experiment and fixed subsequently. The cell culture media was removed, the cells washed with PBS and then incubated for 10 minutes in1 mL of fixation buffer (Table 2.6). All the hypoxic samples were fixed inside the hypoxic station. Fixation buffer was removed from the cells by washing them 3 times with PBS. The cells were permeabilised with 1 mL of permeabilisation buffer (Table 2.6) for 10 min. Cells were then washed with PBS and the non-specific binding sites were blocked by incubating in blocking buffer for 30 min. Staining was performed by incubating the cells overnight at 4°C with the appropriate primary antibody diluted in the blocking buffer.

Cells were washed 3 times with PBS and then incubated with the appropriate secondary antibody for 1 hour in the dark at room temperature. Cover slips were washed 3 times with PBS and then incubated for 3 min with 4',6-diamidino-2-Phenylindole, dihydrochloride (DAPI) (Invitrogen, Paisley, UK) at 1:2,500 in PBS, to visualise the nuclei. Two final washes were performed using PBS and then the coverslips were mounted onto slides using DAKO fluorescent mounting media (DAKO, Ely, UK). Negative controls were included the first time that each experiment was performed, where the sample was incubated with the secondary antibody without the primary antibody. Details of all the antibodies used are listed in Table 2.7.

Table 2.7 Antibodies used for IF

Antibody	Specie	Supplier	Dilution
yH2AX	Mouse	Millipore (#05636)	1:500
53BP1 (BP13)	Rabbit	Abcam	1:250
53BP1 (MAB3802)	Mouse	Abcam	1:250
ATM-Ser1981 (EP1890Y)	Rabbit	Abcam	1:200
AlexaFluor 488	Rabbit	Invitrogen	1:500
Alexa Fluor 568	Mouse	Invitrogen	1:500

2.7.3. FLUORESCENT MICROSCOPY

Microscopy images were collected on a Zeiss Axioimager.D2 upright microscope using a 40x / 0.5 EC Plan-neofluar objective and captured using a Coolsnap HQ2 camera (Photometrics) through Micromanager software v1.4.23. Specific band pass filter sets for DAPI, FITC and Texas red were used to prevent bleed through from one channel to the next. Images were then processed and analysed using Fiji ImageJ software.

In the dose response experiment (*see Chapter 5*) which tested different concentrations of TH1834, the images were captured using a 3D-Histech Pannoramic-250 microscope slide-scanner with a *20x/ 0.30 Plan Achromat* objective (Zeiss) and the DAPI and FITC filter sets. Snapshots of the slide-scans were taken using the Case Viewer software (3D-Histech) and subsequently analysed using Fiji ImageJ software.

2.7.4. DATA ANALYSIS AND FOCI COUNT

All data obtained was analysed using Fiji ImageJ software. The mean fluorescence was quantified using the image obtained with the DAPI staining as a template to delimit all the nuclei present in the image. Incomplete nuclei or nuclei that were in contact with the edges of the image were excluded from the analysis. On average, 100 cells were analysed per each sample to obtain the mean value of fluorescence for the target protein.

Images stained with 53BP1 were analysed by counting the number of foci per cell. This was done using "finding the maxima" function in Fiji ImageJ and manually confirming the obtained results.

2.8. QUANTITATIVE POLYMERASE CHAIN REACTION (QPCR)

2.8.1. RNA EXTRACTION

RNA was extracted using the RNasey kit (Quiagen, Manchester, UK) as specified by the manufacturer. RNA concentration and purity was measured using a NanoDrop Lite spectrophotometer (Thermo Fisher, UK).

2.8.2. REVERSE TRANSCRIPTION OF RNA TO SINGLE STRAND CDNA

Reverse transcription of mRNA to cDNA was performed using High Capacity cDNA Reverse Transcription Kit (Thermo Fisher, UK) following the manufacture instructions. After quantifying the concentration of mRNA, 50 ng of mRNA were converted to cDNA using T100 Thermal cycler (BioRad, UK).

2.8.3. REAL-TIME PCR

Real-time PCR was performed using pre design TaqMan probes for Suv39H1, CA9, MDM2, HRT1 and Actin-β. All TaqMan probes were acquired from Dharmacon (Horizon Discovery, Cambridge, UK). RT-PCR was performed using 1 µg of cDNA of each sample combined with the TaqMan specific probe and TaqMan Fast Advance master mix (Thermo Fisher, UK). The RT-PCR instrument used was a StepOnePlus RT-PCR (Thermo Fisher, UK). The obtained data were analysed using $\Delta\Delta C_T$ method to quantify the relative gene expression [150].

2.9. SIRNA ASSAY

MDM2 knockdown was performed using pre designed ON-TARGETplus SMARTpool siRNA sequences (Dharmacon, Horizont UK). The four target sequences used are:

5’-GCCAGUAUAUUAUGACUAA-3’

5’-GAACAAGAGACCCUGGUUA-3’

5’-GAAUUUAGACAACCUGAAA-3’

5’-GAUGAGAAGCAACAACAUA-3’

The cells were transfected using Lipofectamine2000 (Invitrogen) according to the manufacturer’s instructions. Cells were re-seeded 24 hours post transfection to a new petri dish and treated with drug/hypoxia for 18 hours. Samples were prepared for RT-PCR or Western blot 72 hours post transfection.

2.10. CELL CYCLE ANALYSIS BY FLOW CYTOMETRY

A total of 1 x 10^6 cells were seeded into a 10 cm plate in 10 mL of complete cell culture media. Cells were allowed to attach and placed at the desired oxygen concentration (21%, 1% or 0.1%) for the appropriate amount of time. Cells were detached using 1.5 mL of Trypsin-EDTA and collected into a 15 mL falcon tube and centrifuged at 1,400 x rpm for 5 min. The cell pellet was washed with PBS and centrifuge again at 1,400 x rpm for 5 min and the supernatant discarded. The cell pellet was then re-suspended in 600 μL of ice-cold PBS and fixed by adding 1.4 mL of ice-cold 100% ethanol drop by drop while vortexing the solution. The samples were stored at -20 °C for 24 hours and then stained with propidium iodide (PI). Fixed cells were centrifuged and washed with PBS to remove ethanol and then re-suspended in 400 uL of PBS. 100 μL of PI reagent (1:1 ratio of 1 mg/mL RNAse A and 400 μg/mL PI) was added to the cell solution and incubated at 37°C for 30 min prior to being analysed using a BD LSRFortessa™ cell analyser (BD Bioscience, Oxford, UK). Information from 10,000 events was collected and the cell population were gated to exclude cell debris. ModFit LT™ software was used to analyse the obtained histograms in order to give the percentage of cells in each cell cycle phase.

2.11. STATISTICAL ANALYSIS

Statistical analysis was carried out using Graph pad prism version 7, once the data had been repeated at least three times. When comparing data obtained from experiments with only two different conditions (e.g.: normoxia vs hypoxia) unpaired T-test was used to compare treated and untreated data. When comparing data obtained from experiments with more than one variables (e.g.: normoxia with or without drug vs hypoxia with or without

drug) analysis of variance (ANOVA) was used, and to identify individual differences Sidak's multiple comparisons test was performed. The obtained P-values are represented as follows: a P-value of ≤ 0.05 is represented as *, a P-value of ≤ 0.01 is represented **, a P-value of ≤ 0.001 is represented *** and a P-value of ≤ 0.0001 is represented as ****.

3. CHAPTER3: HYPOXIA INDUCED CHANGES IN THE CHROMATIN STRUCTURE

3.1. INTRODUCTION

It has been previously described that different levels of hypoxia induce changes in the chromatin structure leading to the regulation of various epigenetics events [39, 55, 77, 81]. Histone methylation and acetylation are the two main epigenetic events that are involved in regulating chromatin structure and gene expression [151]. Histone methylation is associated with a more compact form of chromatin, heterochromatin, which is more resilient to different types of DNA damaging events such as radiation and re-oxygenation [152, 153]. One of the main histone epigenetic heterochromatic marks is the tri-methylation of lysine 9 of histone 3 (H3K9me3) [154]. The main ubiquitously expressed methyltransferase responsible for the catalysis of the H3K9me3 mark is Suv39H1 [155, 156]. Suv39H1 has been implicated in promoting heterochromatin formation in response to different types of stress [60, 73, 157]. A global increase in the methylation of H3K9 in hypoxia has been reported in cancer cell lines exposed to different levels of hypoxia [22, 122, 158]. The induction of H3K9me3 in response to hypoxia has been associated with the activation of the DNA damage response pathway [22, 83] and to the regulation of gene expression of various proteins involved in DNA damage repair such as BRAC1 and MLH1 [159, 160]. The induction of Suv39H1 in response to hypoxia has only been previously shown in human fetal lung epithelial cells: in this study the levels of Suv39H1 were correlated with the levels of H3K9me3 under hypoxic conditions [161].

Considering the importance that the heterochromatin mark H3K9me3 plays in regulating different cellular pathways, the levels of H3K9me3, as well as Suv39H1, were analysed in three different cancer cell lines in response to hypoxia conditions (0.1% O_2) and mild hypoxia condition (1% O_2). Additionally RT-PCR was performed to assess the levels of Suv39H1 mRNA in response to hypoxic stress. Finally, the involvement of the proteasomal pathway in regulating the stability of Suv39H1 in hypoxia was studied.

3.2. RESULTS

3.2.1. H3K9ME3 IS UPREGULATED IN RESPONSE TO HYPOXIA

FTC133 cell line was used to evaluate the expression of H3K9me3 in response to hypoxia (0.1% O_2). The cells were incubated for 18 hours in normoxia (21% O_2) or hypoxia prior to immunohistochemical staining of fixed cells. FTC133 cells were stained with H3K9me3 specific antibody and DAPI was used as a nuclear marker. Three independent experiments

were performed and an example image is presented in Figure 3.1. The mean fluorescence of each sample was calculated by analysing the images using ImageJ software as described in the section 2.7. The graph in Figure 3.1 represents the mean fluorescence of each sample normalized with the normoxic control. A significant increase in the levels of H3K9me3 was observed in FTC133 cell line in response to hypoxia.

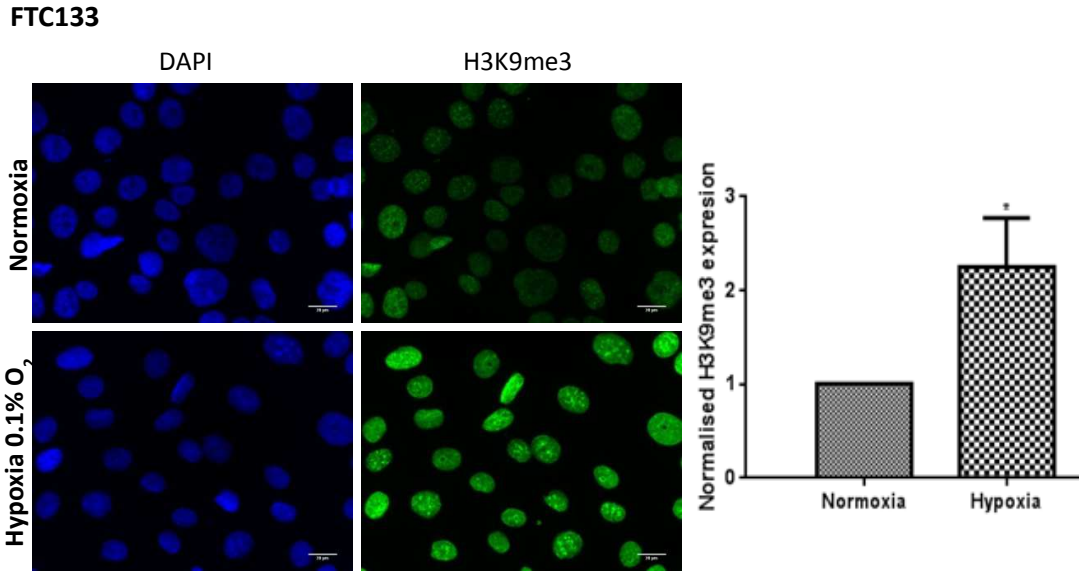

Figure 3.1. The levels of H3K9me3 in response to hypoxia. FTC133 cells were incubated for 18 h in normoxic (21% O_2) or hypoxic (0.1% O_2) conditions and then stained for H3K9me3 (green) and DAPI (blue). The graph represents the normalised expression of H3K9me3 with the normoxic control. Three independent experiments were performed and the bar represents the mean ± SEM.

For further analysis of H3K9me3 expression in response to hypoxia, two different cancer cell lines, FTC133 and U87 were used. The cell lines were incubated for 18 hours in hypoxia or normoxia prior to lysis and Western blot analysis. An example of the Western blot membranes is given in Figure 3.2. Images were analysed by densitometry to calculate the level of H3K9me3 expression in relation to the total levels of H3 and the level of the loading control (β-actin). The graphs represent normalised H3K9me3 expression in relation to the normoxic control (Fig. 3.1). A significant increase of H3K9me3 was detected in response to hypoxia in both cell lines analysed.

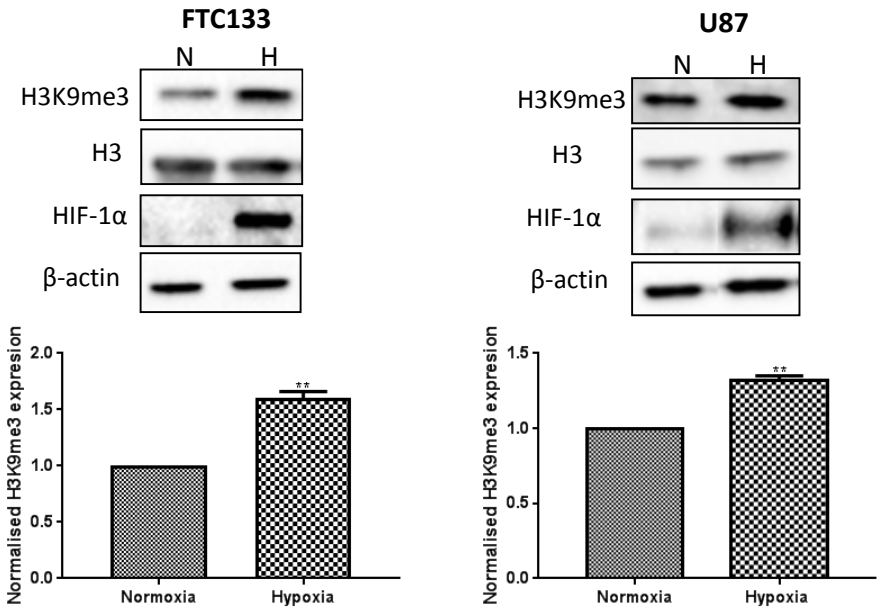

Figure 3.2. The protein expression of H3K9me3 in response to hypoxia. Cells were incubated in normoxia (N; 21% O_2) or hypoxia (H; 0.1% O_2) for 18 hours prior to lysis and Western blotting. HIF-1α was used as a control for hypoxia and β-actin as a loading control. The graphs represent the densitometry of H3K9me3 normalised by total amount of H3, β-actin and the normoxic control. Bars represent the mean ± SEM of three independent experiments.

3.2.2. METHYLTRANSFERASE SUV39H1 IS UPREGULATED IN RESPONSE TO HYPOXIA

To determine whether the levels of the methyltransferase Suv39H1 are also upregulated in response to hypoxia, the expression of Suv39H1 was analysed by Western blot in three different cell lines (FTC133, HCT116 and U87). The cell lines were incubated in normoxia or hypoxia for 18 hours and the results of three independent experiments were analysed by Western blot as described in Section 3.2.1. An example of the Western blot membranes is presented in Figure 3.3A. Graphical representation of normalised Suv39H1 expression against the control is illustrated in Figure 3.3B.

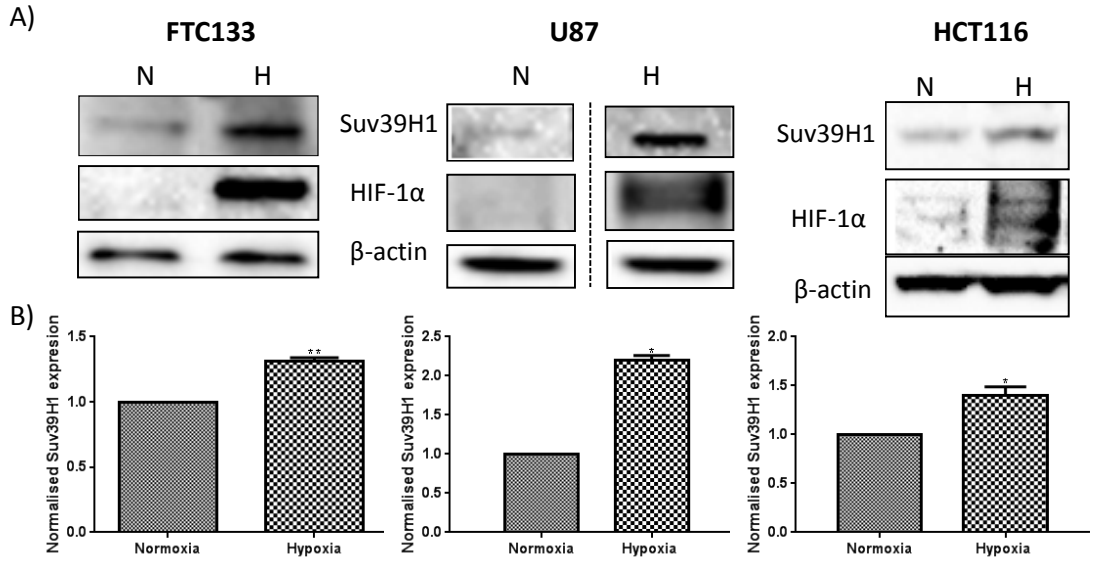

Figure 3.3. The protein expression of Suv39H1 in response to hypoxia. Cells were incubated in normoxic (N; 21% O_2) or hypoxic conditions (H; 0.1% O_2) for 18 hours prior to lysis and Western blotting. HIF-1α was used as a control for hypoxic condition and β-actin as a loading control (A). The graphs represent the densitometry of Suv39H1 expression normalised by the loading control and normoxia. Bars represent the mean ± SEM of three independent experiments (B).

The levels of Suv39H1 were significantly upregulated in response to hypoxia in all the cell lines analysed.

3.2.2.1. mRNA levels of Suv39H1 are not upregulated in response to hypoxia

In order to assess if the observed induction of the protein levels of Suv39H1 is due to an increase in the transcription of the Suv39H1 gene, RNA analysis was performed. RNA was extracted from FTC133, U87 and HCT116 after being exposed for 6 or 18 hours to hypoxic or normoxic conditions. The extracted RNA was converted to cDNA and analysed by RT-PCR using pre-design Taq-man probes for Suv39H1, CA9, HRT1 and β-actin as described in the section 2.8. HRT1 and β-actin were analysed as possible housekeeping genes and CA9 was used as positive control for hypoxia. The obtained data was analysed by the $\Delta\Delta C_T$ method. Firstly, the appropriate housekeeping gene was selected comparing the C_T values of HRT1 and β-actin in normoxia and hypoxia for each cell line obtained in four independent experiments (Fig. 3.4).

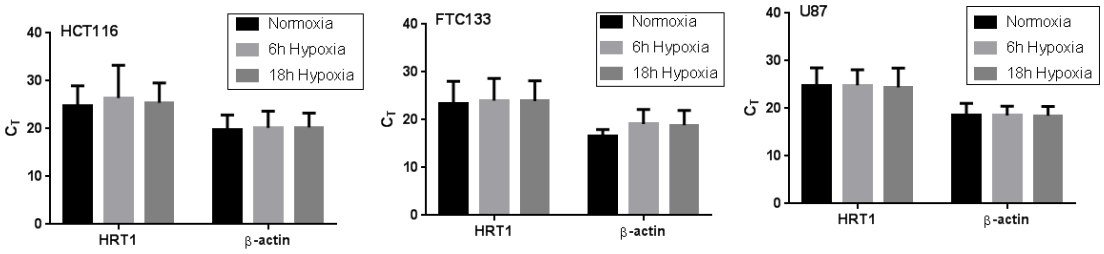

Figure 3.4. C_T values of HRT1 and β-actin in normoxia and hypoxia. HCT116, FTC133, and U87 were exposed for 6 or 18 hours to normoxia (21% O_2) or hypoxia (0.1% O_2). After that time RNA was extracted and analysed by RT-PCR. The C_T of HRT1 and β-actin are shown in the graphs. Bars represent the mean ± SEM of four independent experiments.

Based on the results shown in Figure 3.4 the housekeeping genes were selected for each cell line in order to calculate the relative gene expression of Suv39H1 and CA9. The C_T values of β-actin didn't change in response to hypoxia in U87 and HCT116 cell lines; meanwhile the C_T values of HRT1 were variable. Thus, β-actin was used as the housekeeping gene for U87 and HCT166 cell lines. In FTC133 the C_T values of β-actin were more variable than the levels of HRT1. Thus, HRT1 was used as the housekeeping gene for FTC133. To allow comparison of the level of mRNA expression, values are presented relative to the mRNA expression level in normoxia. The relative gene expression of Suv39H1 and CA9 of four independent experiments is represented in Figure 3.5.

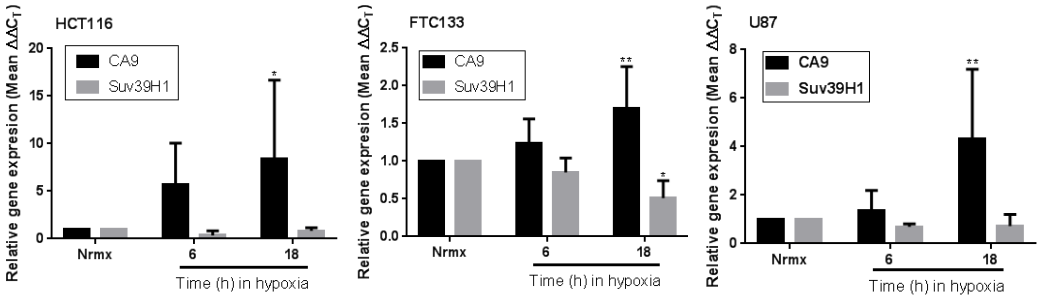

Figure 3.5. Suv39H1 and CA9 relative gene expression in response to hypoxia. HCT116, FTC133 and U87 were exposed for 6 or 18 hours to normoxia (21% O_2) or hypoxia (0.1% O_2). After that time RNA was extracted and analysed by RT-PCR. The relative gene expression represented in the graphs was calculated using HRT1 as the reference housekeeping gene for FTC133 and β-actin for HCT116 and U87. The graph represents the relative gene expression of Suv39H1 and CA9 compared to the normoxic control. Bars represent the mean ± SEM of four independent experiments.

In hypoxia, the mRNA levels of Suv39H1 decreased only slightly after the 6 hours exposure time in both HCT116 and U87. This decrease was more marked after the 18 hours exposure time in both cell lines. In the FTC133 cell line, Suv39H1 mRNA was minimally downregulated after 6 hours in hypoxia, however a statistically significant downregulation was seen after 18 hours exposure. The levels of CA9 mRNA were somewhat increased after only 6 hours in hypoxia but were greatest after 18 hours exposure in all the cell lines analysed (Fig. 3.5).

3.2.3. PROTEASOME PATHWAY IS INVOLVED IN REGULATING SUV39H1 LEVELS IN HYPOXIA

Exposure to mild levels of hypoxia (1% O_2) failed to induce H3K9me3 in FTC133 cell line. FTC133 cells were incubated for 18 hours in mild hypoxic conditions or normoxia and then fixed and stained for H3K9me3 and DAPI. Images were generated and analysed as described in the section 2.7. Three independent experiments were performed and a representative example of one of them is shown in Figure 3.6A. The graph represents the levels of H3K9me3 in mild hypoxia compared to the normoxic control (Fig. 3.6A). The levels of Suv39H1 were also analysed in FTC133 cell line exposed for 18 hours to mild hypoxia by Western blot. Densitometry analysis was performed using data generated by three independent experiments; a representative image of one membrane is shown in Figure 3.6B. The graph in Figure 3.6B represents the levels of Suv39H1 standardised to β-actin as the loading control and normalised to normoxia. HIF-1α was used as hypoxic control (Fig 3.6B). The levels of H3K9me3 or Suv39H1 were not affected by mild hypoxia in FTC133 cells.

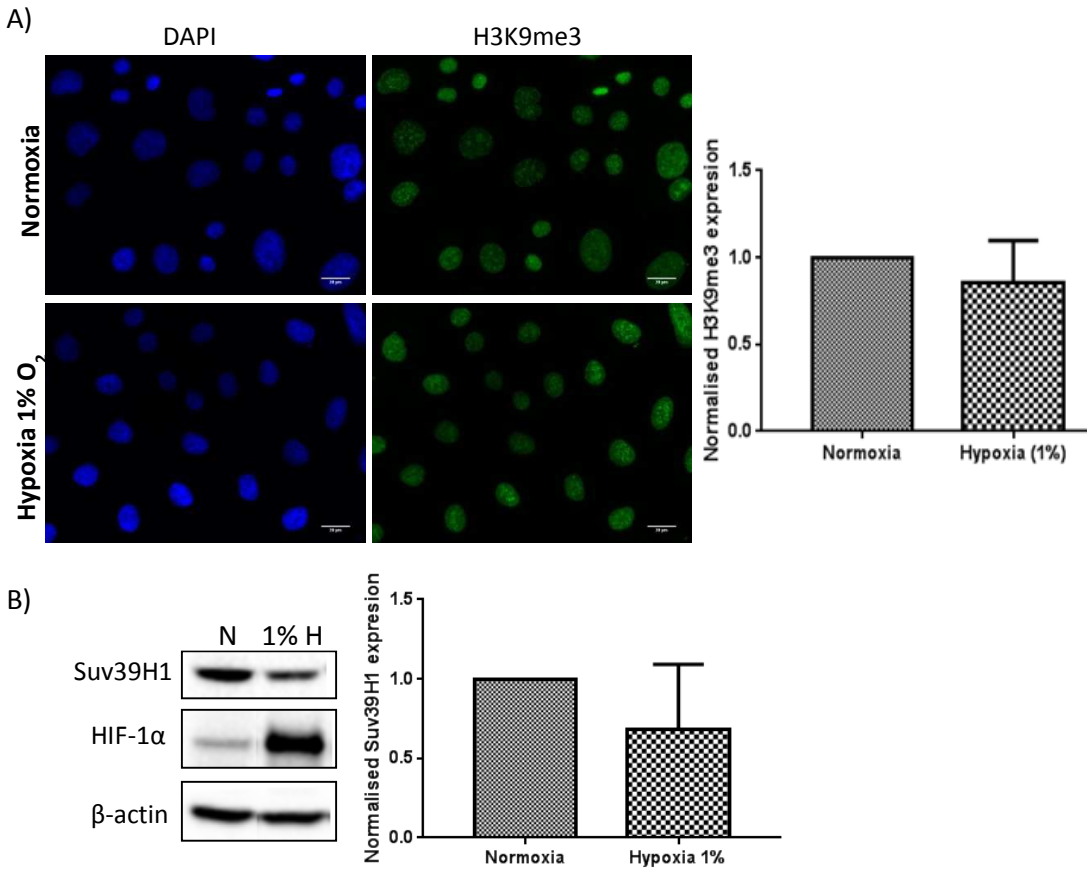

Figure 3.6. Mild levels of hypoxia (1%) failed to induce H3K9me3 and Suv39H1 in FTC133 cell line. FTC133 cells were exposed to normoxia (21% O_2) or mild levels of hypoxia (1% O_2) for 18 hours, fixed and stained for H3K9me3 (green) and DAPI (blue). The graph represents the mean fluorescence of H3K9me3 normalised to the normoxic control. Bars represent the mean ± SEM of three independent experiments (A). Western blot was performed after exposing FTC133 cell to mild hypoxia for 18 hours. Treatment with mild hypoxia is indicated by "1% H" and normoxia by an "N". HIF-1α was used as a control for hypoxic condition and β-actin as a loading control. The graphs represent the densitometry of Suv39H1 expression normalised by the loading control and normoxia. Bars represent the mean ± SEM of three independent experiments (B).

To assess if, in response to hypoxia, Suv39H1 levels are regulated by a proteasome pathway, FTC133 cells was exposed to mild levels of hypoxia or normoxia for a total of 18 hours. Four hours of the exposure time included 30 µM of the proteasome inhibitor MG132 or DMSO, as the vehicle control for the drug. After the treatment the cells were lysed and the protein expression of Suv39H1 was analysed by Western blot. An example of the Western blot membranes is presented in Figure 3.6. Image analysis was carried out by densitometry, using images generated by three independent experiments, to calculate the level of Suv39H1 expression in relation to the loading control. The graph represents Suv39H1 expression with MG132 (red) or with DMSO (blue) (Fig. 3.6).

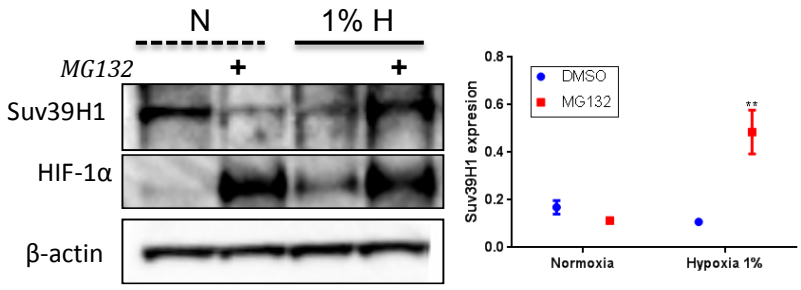

Figure 3.7. Treatment with proteasome inhibitor MG132 induced an upregulation of the protein levels of Suv39H1 in mild hypoxia. FTC133 cells were exposed for a total of 18 hours to normoxia (21% O_2), indicated by an N, or mild hypoxia (1% O_2) indicated by 1% H and treated for 4 hours with 30 µM of MG132 or DMSO. Cell lysates were prepared after the treatment time and analysed by Western blot. The graph represents the expression of Suv39H1 normalised with β-actin with MG132 (red) or DMSO (blue). Bars represent the mean ± SEM of three independent experiments.

HIF-1α was used as a control for the inhibition of the proteasome pathway as well as for hypoxia. The protein levels of HIF-1α were highly upregulated in normoxia and 1% hypoxia in the presence of MG132. The levels of Suv39H1 were significantly upregulated in mild hypoxia when the cells were treated with the proteasomal inhibitor MG132. However, in normoxia the treatment with MG132 had the opposite effect (Fig. 3.6). The results obtained suggest that the ubiquitin proteasome pathway is the principal mechanism regulating the stability of Suv39H1 in hypoxia.

3.3. Discussion

Analysis of H3K9me3 expression revealed that this heterochromatic mark is up-regulated in response to hypoxia. The levels of H3K9me3 were statistically significantly higher in hypoxia compared to normoxia, as shown by analysing data obtained by immunofluorescence and Western blot (Fig. 3.1 and 3.2). As Suv39H1 is thought to be the main methyltransferase responsible for the catalysis of H3K9me3, the expression of Suv39H1 was also analysed. Suv39H1 expression was up-regulated in hypoxia in several cancer cell lines (Fig. 3.3). The correlation of H3K9me3 expression with Suv39H1 expression in response to hypoxia points to the involvement of Suv39H1 in the induction of H3K9me3.

Interestingly, hypoxic induction of Suv39H1 is not observed in all cell lines. In the study of Olcina et al (2013) Suv39H2 and SETDB1, and not Suv39H1 were found to be upregulated by hypoxia in RKO cells [22]. In the same study MEFs lacking Suv39H1 and

2 or lentiviral knockdown of both isoforms prevented H3K9me3 induction in hypoxia. Taken together, these data perhaps suggest cell dependency in the role of Suv39H1 versus Suv39H2 in H3K9me3 regulation in hypoxia. For the present work, three different cell lines were used: U87, FTC133, and HCT116. It was found that in the U87 cell line, Suv39H2 was not responsive to changes in oxygen levels (data not shown) and the FTC133 cell line expresses only the Suv39H1 isoform, lending a greater focus towards Suv39H1. The induction of heterochromatin in response to stress is a common cellular mechanism [162] and redundancy within the system is perhaps reflective of the important role it plays in facilitating survival in such conditions.

Transient heterochromatin formation helps the cell to save energy by diminishing gene transcription, a process that can also be more error-prone under stress conditions. Heterochromatin also helps to protect the DNA from damaging agents. Hypoxia *per se* is not a DNA damaging agent, but DNA damage can be caused by re-oxygenation [164]. Solid tumour cells undergo periods of cycling hypoxia followed by re-oxygenation [165]. Therefore, the up-regulation of mechanisms that induce heterochromatin formation in hypoxia might represent an important advantage for cancer cells.

To further study the mechanism behind the upregulation of Suv39H1 in response to hypoxia, the levels of Suv39H1 mRNA were analysed. The results obtained with RT-PCR showed that the mRNA levels of Suv39H1 in hypoxia were lower than in normoxia. RNA extracted from two different time points (6 and 18 hours) in hypoxia was used. The levels of Suv39H1 mRNA decreased proportionally to the time the cells spent in hypoxia. This trend was observed in all cell lines analysed (Fig. 3.5). The decrease in the levels of Suv39H1 mRNA was only marginally in U87 and HCT116 cells. The outcome of prolonged exposure to hypoxia was much more pronounced in the levels of Suv39H1 mRNA in FTC133 cells. This trend may be the result of a decrease in transcription rate in response to hypoxic stress. Various cell specific mechanisms of transcriptional repression in response to hypoxia have been described [166]. Although Suv39H1 is a ubiquitously expressed protein and no-specific evidence regarding its transcriptional repression has been previously reported. However, the induction of H3K9me3 is associated with general transcriptional repression, which might be responsible for the decline in the levels of Suv39H1 mRNA observed. Hypoxia-induced gene repression is an adaptation mechanism that helps to redirect energetic resources to essential housekeeping functions [167].

The obtained results regarding the mRNA levels of Suv39H1 (Fig. 3.5) suggests a post-translational regulation mechanism of Suv39H1 protein levels in response to hypoxic stress.

When exposed to mild levels of hypoxia, FTC133 cells, failed to induce H3K9me3 formation and did not up-regulate Suv39H1 (Fig. 3.6). To evaluate the involvement of the proteasome pathway in the regulation of Suv39H1, FTC133 cells were treated with proteasome inhibitor MG132. MG132 treatment in normoxia induced a modest reduction in the protein levels of Suv39H1. A possible explanation to these is that the autophagy pathway has been upregulated as a result of blocking proteasome dependent degradation. However, under hypoxic conditions the treatment with MG132 induced a significant upregulation of Suv39H1. The results of this study are suggestive that the ubiquitin proteasome pathway might be the mechanism involved in regulating Suv39H1 stability in hypoxia. The main component of the ubiquitin proteasome pathway is MDM2. MDM2 is an E3 ubiquitin ligase, involved in regulating the stability of more than 100 different proteins [168]. In the next chapter the involvement of MDM2 in regulating the stability of Suv39H1 under hypoxic condition will be addressed.

4. CHAPTER 4: REGULATION OF SUV39H1 IN HYPOXIA

4.1. INTRODUCTION

Suv39H1 is a ubiquitously expressed lysine methyltransferase (KMT)- part of the SET domain family of proteins. These enzymes are responsible for transferring a methyl group from S-adenosyl-L-methionine onto the ε amino group of the lysine residue on the substrate. The SET-domain family of proteins contain a chromodomain that helps recognise methylated lysines. Suv39H1 preferentially binds to the monomethylated form of H3K9 and catalyses demethylation or trimethylation of H3K9 [62].

Suv39H1 plays a fundamental role in regulating heterochromatin formation and genome stability. Knockout mice show an increase genetic instability and an increased risk of late onset B-cell lymphomas as a result of defects in pericentric heterochromatin [169]. Suv39H1 plays an important role in many cellular processes such as: differentiation, development, migration, proliferation and senescence. Genetic deletion of Suv39H1 stimulates tumour progression by inactivating senescence and activating proliferation [170, 171]. Additionally, Suv39H1 mediated induction of H3K9me3 has been related to migration of breast and colon cancer cells *in vitro* [172]. Suv39H1 activity and stability is regulated mainly by post-transcriptional modifications [73, 157, 173].

The stability of Suv39H1 is mainly regulated by ubiquitin-proteasome pathway. Sirt1 has been implicated in increasing the half-life of Suv39H1 by inhibiting its polyubiquitination by MDM2 in response to oxidative stress [73]. MDM2 is an ubiquitin E3 ligase responsible for regulating the stability of many proteins involved in a variety of cellular processes [168]. MDM2 is considered a “hub protein” as a result of being capable of interacting with a large variety of distinct partners. The most well studied downstream target of MDM2 is p53 [60, 173-176]. To complete such variety of different functions, MDM2 is subjected to multiple post-translational modifications. One of such posttranscriptional modifications is the ATM dependent phosphorylation of MDM2 on Serine 394, in response to DNA damage. MDM2 activity is negatively regulated by ATM, which leads to the stabilization of p53 [174, 175]. It has been previously shown that ATM is activated in response to hypoxia [24]. However, the effect of ATM activation in response to hypoxia on MDM2 activity and consequentially on Suv39H1 hasn’t been addressed to date.

Suv39H1 is a critical determinant of cell fate decision and tumour progression. Aberrant expression of this methyltransferase has been reported in a number of solid tumours [177]. Considering that Suv39H1 is dependent on S-adenosyl methionine as a cofactor, its role in linking tumorigenesis and metabolism is of high importance. It is also known that the essential enzyme responsible for the catalysis of S-adenosylmethionine, methionine adenosyltransferase 2A (Mat2A), is transcriptionally upregulated by HIF-1α [178]. However, not much is known about the regulation of Suv39H1 in response to hypoxic stress.

This study addresses the mechanism behind the observed upregulation of Suv39H1 (see Chapter 3). Firstly, the levels of MDM2 and Sirt1 were analysed in hypoxia. After this, the effect of ATM-dependent regulation of MDM2 function was established using an ATM specific inhibitor, Ku55933. Finally, the effect of MDM2 knockdown in combination with ATM inhibition on the levels of Suv39H1 was determined.

4.2. RESULTS

4.2.1. MDM2 PROTEIN LEVELS IN HYPOXIA

Suv39H1 is a target for MDM2 dependent polyubiquitination and subsequent degradation. To investigate if the observed upregulation of Suv39H1 in hypoxia is related to changes in MDM2, the protein levels of MDM2 were studied in response to hypoxia. FTC133, HCT116 and U87 cells were incubated in normoxia (21% O_2) or hypoxia (0.1% O_2) for 18 hours prior to lysis and Western blot analysis. Images of three independent experiments were analysed by densitometry to calculate the level of MDM2 expression in relation to the levels of the loading control (β-actin). A representative image of the experiment is shown in Figure 4.1A. The graphs represent normalised MDM2 expression in relation to the normoxic control (Fig. 4.1B). The blot of HIF-1α used for the HCT116 cells is the same one used in the Figure 3.3, as both MDM2 and Suv39H1 data shown were obtained from the same lysis but run in two different gels. One gel was blot against Suv39H1 and HIF-1α and the other one against MDM2, the β-actin shown is the one used to quantify the Suv39H1 and MDM2 bands, HIF-1α was used only as a control for hypoxia and the data presented was not quantified.

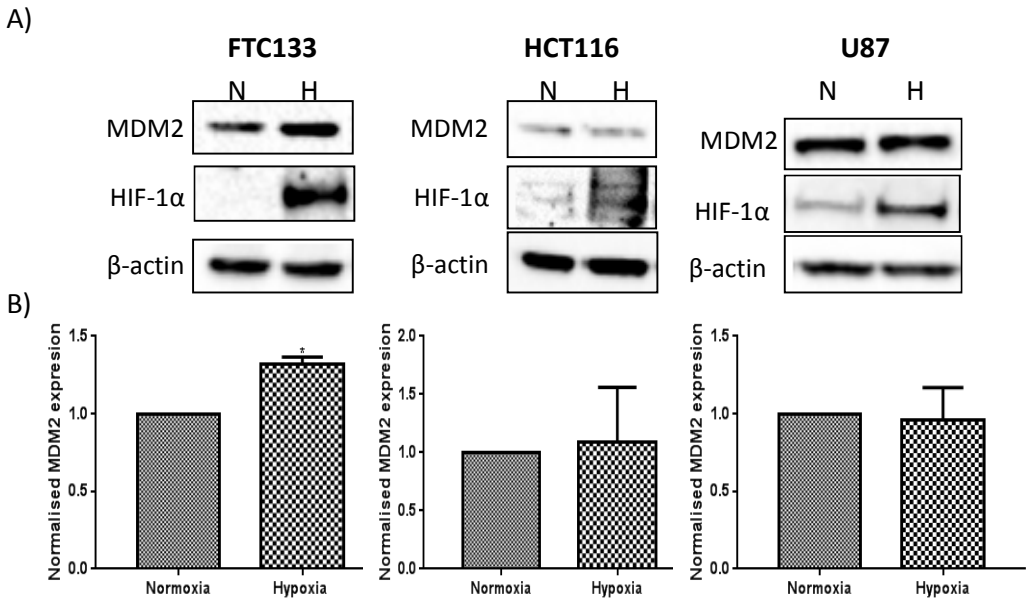

Figure 4.1. MDM2 expression in response to hypoxia. Cells were incubated in normoxia (N; 21% O_2) or hypoxia (H; 0.1% O_2) for 18 hours prior to lysis and Western blotting. HIF-1α was used as a control for hypoxic condition and β-actin as a loading control (A). The graphs represent the densitometry of Suv39H1 expression normalised by the loading control and normoxia (B). Bars represent the mean ± SEM of three independent experiments.

A significant increase of MDM2 was detected in response to hypoxia in FTC133 cell line. The levels of MDM2 were not significantly affected by hypoxia in HCT116 and U87 cell lines.

4.2.2. SIRT1 IS DOWNREGULATED IN HYPOXIA

It has been previously reported that Sirt1 is involved in regulating Suv39H1 stability [73]. Thus, to determinate if Sirt1 is involved in increasing the half-life of Suv39H1 in hypoxia, by inhibiting MDM2 dependent polyubiquitination, the levels of Sirt1 were studied in FTC133, HCT116 and U87 cell lines. Cells were incubated for 18 hours in normoxia or hypoxia and the results of three independent experiments analysed as described in the section above. An example of one of the Western blot membranes is presented in Figure 4.2A. Figure 4.2B shows the graphical representation of the normalised levels of Sirt1 in hypoxia compared to the normoxic control.

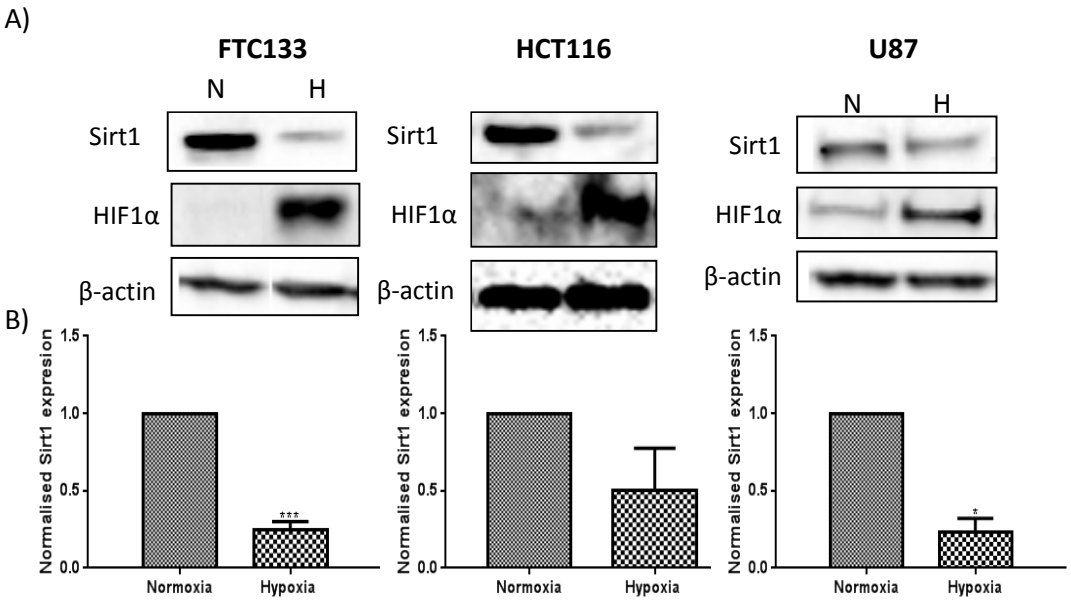

Figure 4.2. Sirt1 is downregulated in response to hypoxia. Cells were incubated in normoxia (N; 21% O_2) or hypoxia (H; 0.1% O_2) for 18 hours prior to lysis and Western blot analysis. HIF-1α was used as a control for hypoxic condition and β-actin as a loading control (A). The graphs represent the densitometry of Sirt1 expression normalized by the loading control and normoxia (B). Bars represent the mean ± SEM of three independent experiments.

The levels of Sirt1 are marginally downregulated in HCT116 but this downregulation is statistically significant in FTC133 and U87 cell lines.

4.2.3. ATM INVOLVEMENT IN REGULATING SUV39H1

4.2.3.1. ATM SPECIFIC INHIBITOR KU55933

To establish the part that ATM potentially plays in regulating MDM2 and subsequently Suv39H1, an ATM specific inhibitor, Ku55933, was used. A detailed description of Ku55933 is presented in *Section 2.4*. The efficacy of ATM inhibition in response to treatment with Ku55933 was established in two different cell models. FTC133 and HCT116 cells were incubated in normoxia or hypoxia with 10 µM of Ku55933 or DMSO for 6 or 18 hours. Cells in normoxia were incubated with Ku55933 for 18 hours only. After treatment, the cells were lysed and the levels of the catalytically active form of ATM, phosphorylated at Serine 1981 (ATM pSer1981), were determined by Western blot. Cells irradiated with 4 Gy were used as a positive control for ATM activation (*see Section 2.5 for details*). Here cells were treated for 18 hours with Ku55933 prior to being irradiated (x-rays). In Figure 4.3A a representative Western blot of FTC133 cells is presented. The

levels of ATM-pSer1981 were quantified by densitometry and normalised to the total amount of ATM and β-actin. Fold change in the levels of ATM-pSer1981, in cells treated with Ku55933, were quantified by standardising the expression levels to the control (DMSO) for each condition (Fig 4.3B). The phosphorylated form of p53 in Serine 15 (p53-pSer15) is an ATM specific downstream target, and was used as control for ATM activity. The levels of p53-pSer15 were quantified using the total amount of p53 and β-actin. The fold change between treated, with Ku55933, and untreated cells is represented in Figure 4.3C.

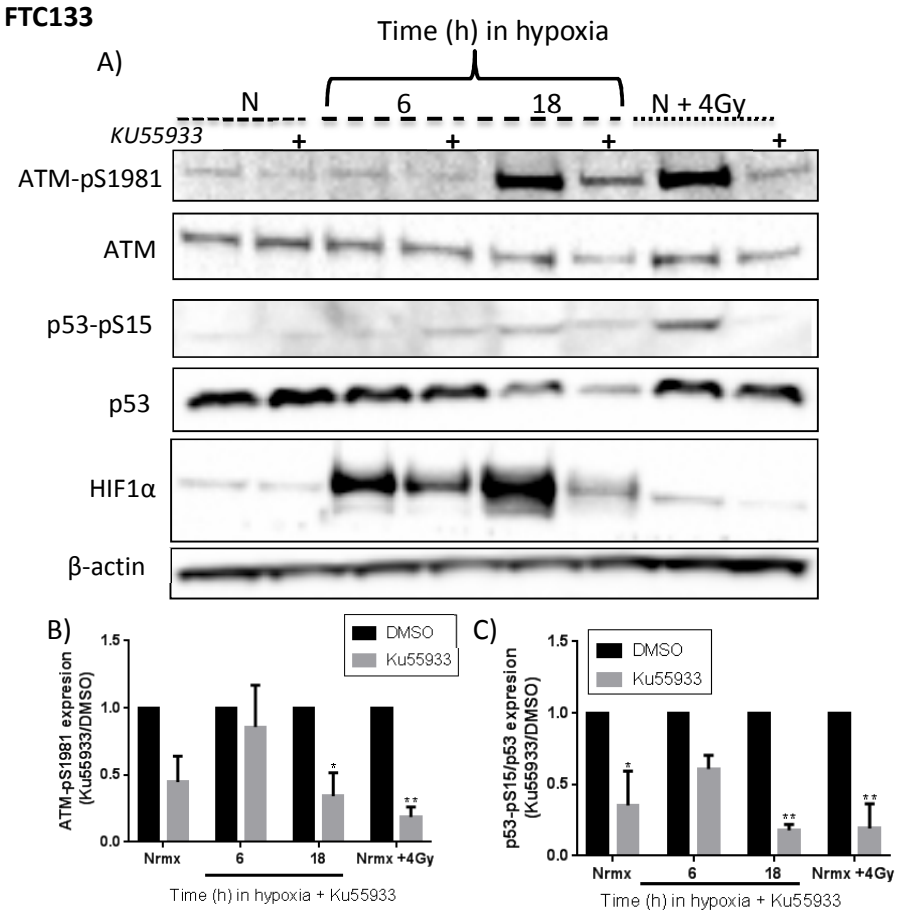

Figure 4.3. The efficiency of Ku55933 (ATM inhibitor) in FTC133 cells. Cells were incubated with or without 10 μM of Ku55933 in normoxia (21% O_2) or hypoxia (0.1% O_2) for 6 or 18 hours prior to lysis and Western blotting. Cells in normoxia were only treated for 18 hours with Ku55933. Treatment with Ku55933 is indicated with the symbol (+). Normoxia is indicated with "N" and cells irradiated with 4 Gy as "N + 4 Gy". HIF-1α was used as a control for hypoxia and β-actin as a loading control (A). The graphs represent the densitometry of ATM-pSer1981 normalized by total amount of ATM, β-actin and standiresed to the non-treated control (DMSO) for each condition (B), and the densitometry of p53-pSer15 normalized by total amount of p53, β-actin and to the non-treated control (DMSO) for each condition (C). Bars represent the mean ± SEM of three independent experiments.

In Figure 4.4A a representative Western blot for HCT116 cells is presented. The levels of ATM-pSer1981 were quantified as described above.

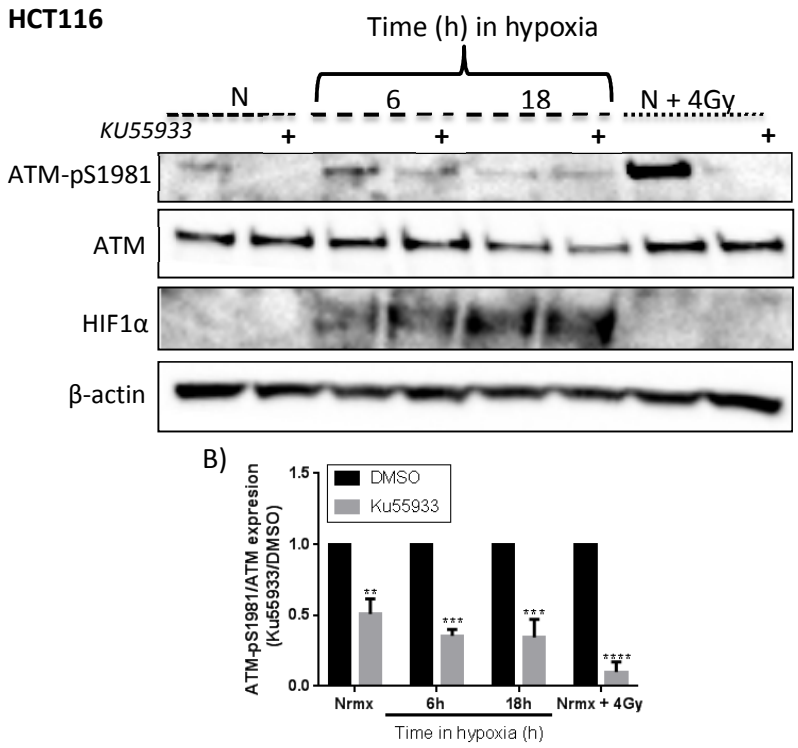

Figure 4.4. The efficiency of Ku55933 (ATM inhibitor) in HCT116 cells. Cells were incubated with or without 10 µM of Ku55933 in normoxia (N; 21% O_2) or hypoxia (H; 0.1% O_2) for 6 or 18 hours prior to lysis and Western blotting. Cells in normoxia were only treated for 18 hours with Ku55933. Treatment with Ku55933 is indicated with the symbol (+). Normoxia is indicated cells irradiated with 4 Gy as "N + 4 Gy". HIF-1α was used as a control for hypoxia and β-actin as a loading control (A). The graph represents the densitometry of ATM-pSer1981 normalized by total amount of ATM, β-actin and to the non-treated control (DMSO) for each condition (B). Bars represent the mean ± SEM of three independent experiments.

The treatment with Ku55933 of FTC133 cells had a significant effect in the levels of ATM-pSer1981 and the downstream target p53-pSer15 only after 18 hours of treatment in hypoxia and normoxia (Fig. 4.3). However, the treatment with Ku55933 in HCT116 cells was more efficient in reducing the levels of ATM-pSer1981. The reduction on the levels of ATM-pSer1981 was significant even after 6 hours of treatment in hypoxia. Treatment with Ku55933 for 18 hours showed to be significant in normoxia and in irradiated cells in both cell lines (Fig. 4.4).

4.2.3.2. THE EFFECT OF ATM INHIBITION ON THE PROTEIN LEVELS AND FUNCTION OF MDM2

In order to evaluate the consequences of ATM inhibition on the levels and function of MDM2, cells were treated with 10 µM of Ku55933 and incubated in normoxia or hypoxia as described in the previous section. Protein levels of MDM2 and p53 were analysed by Western blot. The levels of p53 were used as a control of MDM2 activity. Figure 4.5A and Figure 4.6A represent one of the three membranes analysed for FTC133 and HCT116 cell lines, respectively. Densitometry of normalised MDM2 and p53 expression in FTC133 cells is represented in the graph 4.5B and 4.5C, respectively, and in graphs 4.6B and 4.6C for HCT116 cells. Densitometry analysis was done as described in *Section 4.2.3.1*. p53 densitometry analysis in FTC133 cells, presented in Figure 4.5, was also used when analysing the expression of p53-pS15 (Fig. 4.3).

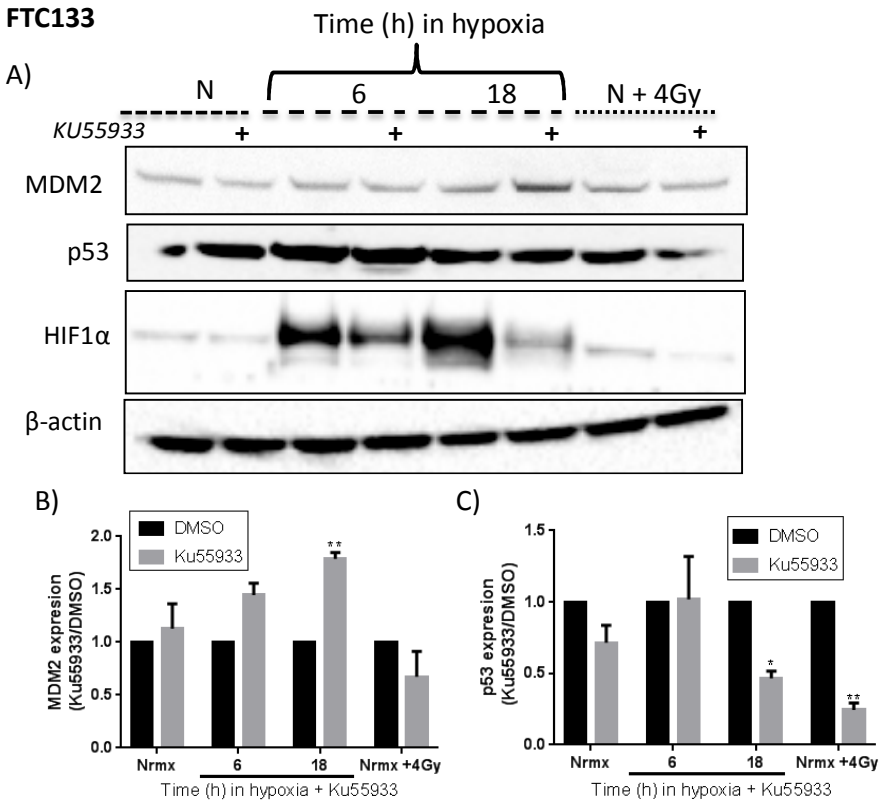

Figure 4.5. Effect of ATM inhibition on the levels and function of MDM2 in FTC133 cells. Cells were incubated with or without 10 µM of Ku55933 in normoxia (21% O_2) or hypoxia (0.1% O_2) for 6 or 18 hours prior to lysis and Western blotting. Cells in normoxia were treated for 18 hours with Ku55933. Treatment with Ku55933 is indicated with the symbol (+). Normoxia is indicated with "N" and cells irradiated with 4 Gy as "N + 4 Gy". HIF-1α was used as a control for hypoxia and β-actin as a loading control (A). The graphs represent the densitometry of MDM2 normalized with β-actin and the non-treated control (DMSO) for each condition (B) and the densitometry of p53 normalized by β-actin and the

non-treated control (DMSO) for each condition (C). Bars represent the mean ± SEM of three independent experiments.

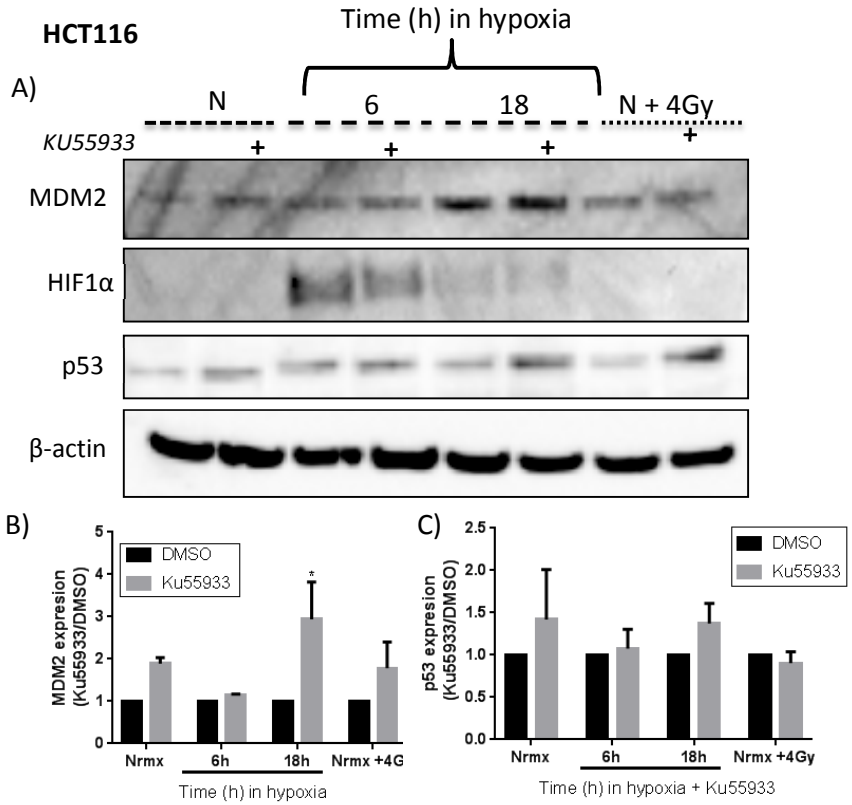

Figure 4.6. Effect of ATM inhibition on the levels and function of MDM2 in HCT116 cells. Cells were incubated with or without 10 µM of Ku55933 in normoxia (21% O_2) or hypoxia (0.1% O_2) for 6 or 18 hours prior to lysis and Western blotting. Cells in normoxia were treated for 18 hours with Ku55933. Treatment with Ku55933 is indicated with the symbol (+). Normoxia is indicated with "N" and cells irradiated with 4 Gy as "N + 4 Gy". HIF-1α was used as a control for hypoxia and β-actin as a loading control (A). The graphs represent the densitometry of MDM2 normalized with β-actin and the non-treated control (DMSO) for each condition (B) and the densitometry of p53 normalized by β-actin and the non-treated control (DMSO) for each condition (C). Bars represent the mean ± SEM of three independent experiments.

ATM inhibition culminated in a significant upregulation of MDM2 expression after 18 hours of treatment in hypoxia in both cell lines analysed. However, the levels of p53 were only negatively affected by Ku55933 in the FTC133 cell line, showing a significant reduction after 18 hours of treatment in hypoxia and in irradiated cells. The effect of ATM inhibition on the levels of p53 was opposite to what was expected in HCT116 cells, showing an upregulation after treatment with Ku55933 in all the conditions studied. On the other hand after 6 hours of treatment, with Ku55933, the levels of p53 didn't seem to be affected in FTC133 cells, which correlates with a less pronounced induction of MDM2

(Fig 4.5B) and poor inhibition of ATM observed after 6 hours of treatment in FTC133 cells (Fig 4.3A).

4.2.3.3. THE EFFECT OF ATM INHIBITION ON THE PROTEIN LEVELS OF SUV39H1

After evaluating the outcome of ATM inhibition on the protein levels and function of MDM2, the effect of this inhibition on the levels of Suv39H1 was studied. FTC133 and HCT116 cells were incubated as described in the previous section and the protein levels of Suv39H1 were examined by Western blot. Figure 4.7A and 4.8A show a representative experiment for FTC133 and HCT116 cell lines, respectively. Densitometry analysis was performed using data obtained from three independent experiments and the graphs represent the expression of Suv39H1 standardised with β-actin and normalised with the untreated control for each condition (Fig. 4.7C and 4.8C).

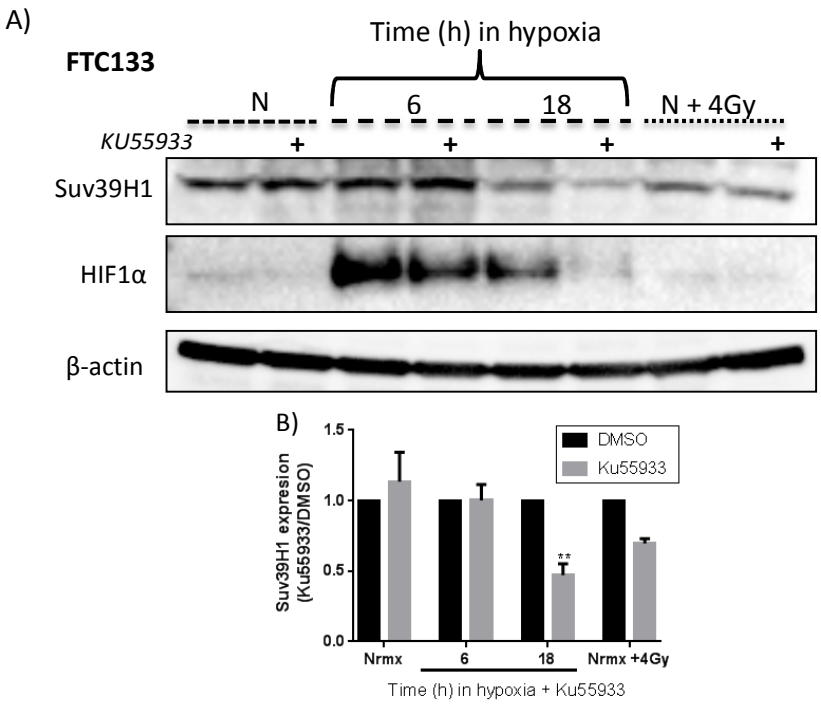

Figure 4.7. Effect of ATM inhibition on Suv39H1 protein levels in FTC133 cells. Cells were incubated with or without 10 μM of Ku55933 in normoxia (21% O_2) or hypoxia (0.1% O_2) for 6 or 18 hours prior to lysis and Western blotting. Treatment with Ku55933 is indicated with the symbol (+). Normoxia is indicated with "N" and cells irradiated with 4 Gy as "N + 4 Gy". HIF-1α was used as a control for hypoxia and β-actin as a loading control (A). The graph represents the densitometry of Suv39H1 standardised with β-actin and normalised to the non-treated control (DMSO) (B) for each condition. Bars represent the mean ± SEM of three independent experiments.

The levels of Suv39H1 were significantly reduced by ATM inhibition after 18 of treatment in hypoxia in the FTC133 cell line. The same trend was also observed in response to irradiation but didn't reach statistical significance. On the other hand, normoxia without radiation had the opposite effect, as the levels of Suv39H1 were slightly increased after treatment with Ku55933 (Fig 4.7).

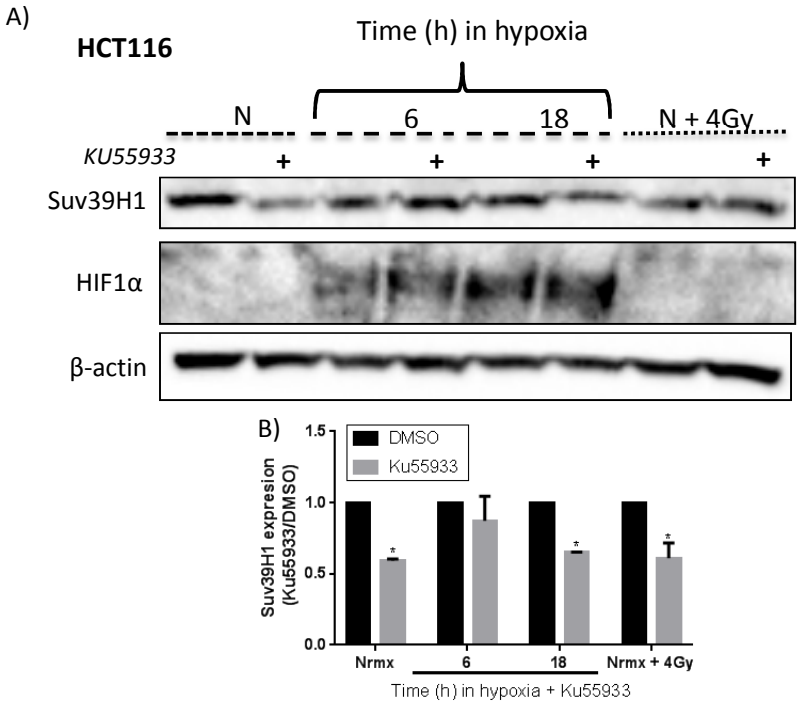

Figure 4.8. Effect of ATM inhibition on Suv39H1 protein levels in HCT116. Cells were incubated with or without 10 μM of Ku55933 in normoxia (21% O_2) or hypoxia (0.1% O_2) for 6 or 18 hours prior to lysis and Western blotting. Treatment with Ku55933 is indicated with the symbol (+). Normoxia is indicated with "N" and cells irradiated with 4 Gy as "N + 4 Gy". HIF-1α was used as a control for hypoxia and β-actin as a loading control (A). The graphs represent the densitometry of Suv39H1 standardised with β-actin and normalised to the non-treated control (DMSO) for each condition. Bars represent the mean ± SEM of three independent experiments.

HCT116 cells showed a significant downregulation of Suv39H1 after 18 hours of treatment with Ku55933 in all the conditions analysed. The levels of Suv39H1 were only marginally affected by Ku55933 after 6 hours of treatment in hypoxia (Fig. 4.8).

4.2.4. ATM AND MDM2 INVOLVEMENT IN REGULATING SUV39H1

4.2.4.1. MDM2 KNOCKDOWN

After evaluating the involvement of ATM in regulating the protein levels of Suv39H1 in a MDM2 dependent manner, in the next section the direct effect of MDM2 on the levels of Suv39H1 was investigated. Firstly, to determinate the involvement of MDM2 in regulating the stability of Suv39H1, MDM2 knockdown was performed (*as described in Section 2.9*). The efficiency of the knockdown was verified by RT-PCR. FTC133 cells were transfected with 20 nmol of pre-designed MDM2 siRNA or a non-specific control siRNA. After transfection, cells were incubated in hypoxia for 18 hours and the RNA was extracted after

a total of 72 hours post transfection. The extracted RNA was converted to cDNA and analysed by RT-PCR using pre-design Taq-man probes for MDM2 and CA9 (as a control for hypoxia), as described in *Section 2.8*. The validity of HRT1 and β-actin as possible housekeeping genes was corroborated by comparing the C_T values of HRT1 and β-actin between transfected cells with MDM2 siRNA and the control siRNA as shown in Figure 4.9.

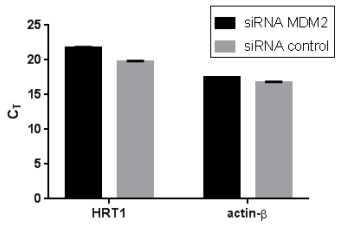

Figure 4.9. C_T values of HRT1 and β-actin in response to MDM2 knockdown in hypoxia. FTC133 cells were transfected with MDM2 siRNA and exposed for 18 hours to hypoxia (0.1% O_2). RNA was extracted after a total of 72 hours post transfection and analysed by RT-PCR. The C_T of HRT1 and β-actin are shown in the graphs. Bars represent the mean ± SEM of three repeats of the same experiment.

The mRNA levels of HRT1 were affected more by the knockdown of MDM2 than the mRNA levels of β-actin (Fig. 4.9). Based on this result, β-actin was selected as the housekeeping gene in order to calculate the relative gene expression of MDM2 and CA9 after transfection. The relative gene expression of Suv39H1 and CA9 is represented in Figure 4.10.

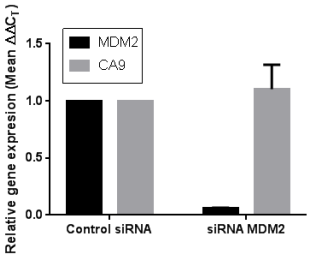

Figure 4.10. MDM2 and CA9 relative gene expression in response to MDM2 knockdown in hypoxia. FTC133 cells were transfected with MDM2 siRNA and exposed for 18 hours to hypoxia (0.1% O_2). RNA was extracted after a total of 72 hours post transfection and analysed by RT-PCR. The relative gene expression represented in the graphs was calculated using β-actin as the reference housekeeping gene. The graph represents the relative gene expression of MDM2 and CA9 compared to the control siRNA. Bars represent the mean ± SEM of three repeats of the same experiment.

The levels of MDM2 mRNA were reduced more than 90% after treatment with MDM2 siRNA compared to the siRNA control. On the other hand, the levels of CA9 mRNA weren't affected by MDM2 siRNA (Fig. 4.10).

In order to determine the effect of MDM2 knockdown on the protein levels of Suv39H1, FTC133 cells were transfected as described above using 20 and 40 pmol of MDM2 siRNA, and incubated in normoxia or hypoxia for 18 hours prior to lysis and Western blot analysis. The cells were lysed after a total of 72 hours post transfection. The levels of Suv39H1 and p53 were evaluated and the results are shown in Figure 4.11.

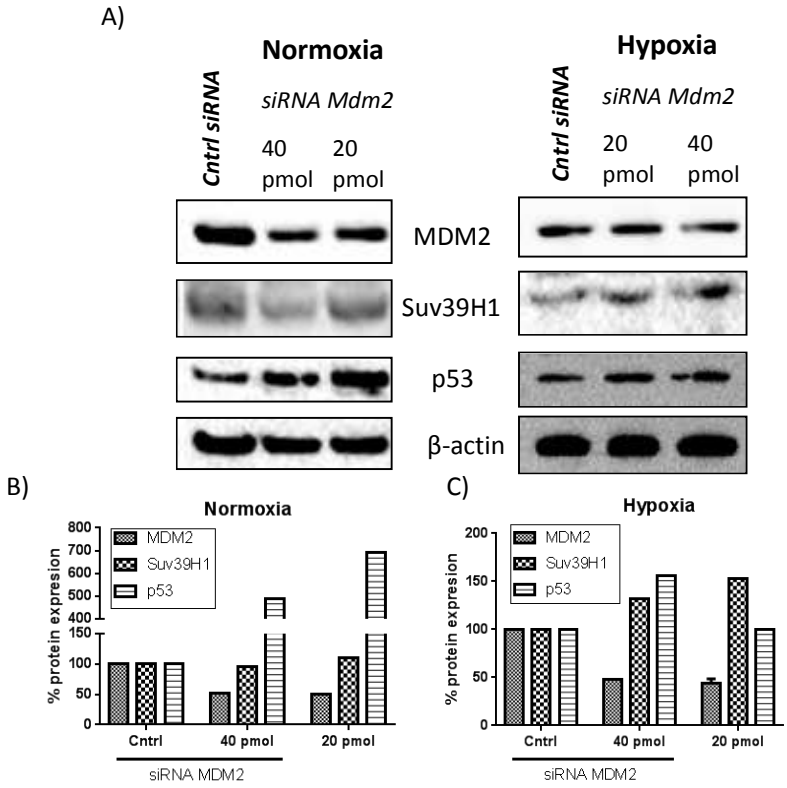

Figure 4.11. Effect of MDM2 knockdown on the protein levels of Suv39H1 and p53. FTC133 cells were transfected with MDM2 siRNA or control siRNA and incubated for 18 hours in normoxia (21% O_2) or hypoxia (0.1% O_2). Cells were lysed after a total of 72 hours post transfection and analysed by Western blot (A). Densitometry analysis of MDM2, Suv39H1 and p53 expression in normoxia (B) and hypoxia (C) is represented in the graphs as a percentage of protein expression by standardising the levels of MDM2, Suv39H1 and p53 with β-actin and control siRNA.

The levels of p53 were upregulated in cells transfected with the siRNA of MDM2 in both conditions. Conversely, the levels of Suv39H1 were only evidently upregulated in response to MDM2 knockdown in hypoxia. Under hypoxic conditions the effect of MDM2

knockdown was slightly higher in Suv39H1 than p53 levels when using 20 pmol of siRNA but not when using 40 pmol of MDM2 siRNA. The difference between the efficacy of transfection between 20 pmol and 40 pmol of siRNA on the protein levels of MDM2 were negligible in both conditions, presenting a reduction of approximately 50% with both concentrations of siRNA used.

4.2.4.2. Effect of MDM2 siRNA and ATM inhibition on the levels of Suv39H1

The effect of MDM2 knockdown on the levels of Suv39H1 and p53 was not very pronounced in hypoxia. This may be due to the fact that MDM2 is not completely functional under this experimental condition, because of the presence of the active form of ATM, which is a negative regulator of MDM2. Considering this, the levels of Suv39H1 and p53 were studied using a combination of MDM2 siRNA with Ku55933 in normoxia and hypoxia. FTC133 cells were transfected with 20 pmol of MDM2 siRNA or a control siRNA. After the transfection the cells were re-seeded and treated with 10 µM of Ku55933 or DMSO for 18 hours in normoxia or hypoxia. The cells were lysed after a total of 72 hours post transfection and analysed by Western blot as described in previous sections. A representative membrane of three independent experiments is presented in Figure 4.12.

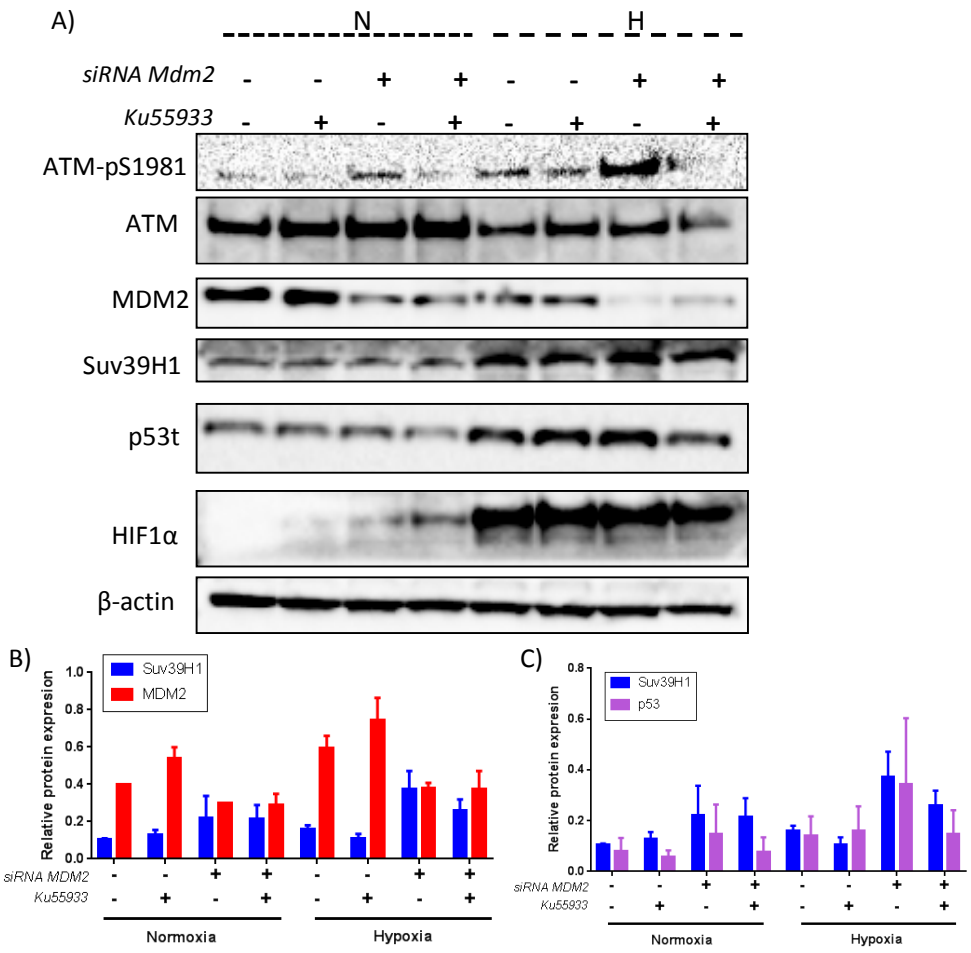

Figure 4.12. Effect of ATM inhibition and MDM2 knockdown on the protein levels of Suv39H1. FTC133 cells were transfected with 20 pmol of MDM2 or a control siRNA and incubated with or without 10 µM of Ku55933 in normoxia (21% O_2) or hypoxia (0.1% O_2) for 18 hours prior to lysis and Western blotting. Treatment with MDM2 siRNA and Ku55933 is indicated with the symbol (+). Normoxia is indicated with an N and hypoxia with an H. HIF-1α was used as a control for hypoxia and β-actin as a loading control (A). The graphs represent the densitometry of Suv39H1 (red) or MDM2 (blue) standardised with β-actin (B) and Suv39H1 (red) or p53 (blue) standardised with β-actin (C) for each condition. Bars represent the mean ± SEM of three independent experiments.

The levels of Suv39H1 were not as significantly affected in normoxia by MDM2 knockdown as the levels of p53. In response to hypoxia, the highest levels of Suv39H1, as well as p53, were found in cells transfected with MDM2 siRNA but without Ku55933. The protein levels of MDM2 were higher in the presence of Ku55933 in normoxia and hypoxia. The highest levels of MDM2 were observed in hypoxia in cells transfected with the control siRNA and incubated with the ATM inhibitor Ku55933.

In order to better interpret the results presented above (Fig.4.12), the obtained data was normalised to the non-treated control (DMSO + NS siRNA) for each condition. The values are presented relative to the non-treated control which was arbitrarily set to 100. The results of this analysis are shown in Figure 4.13.

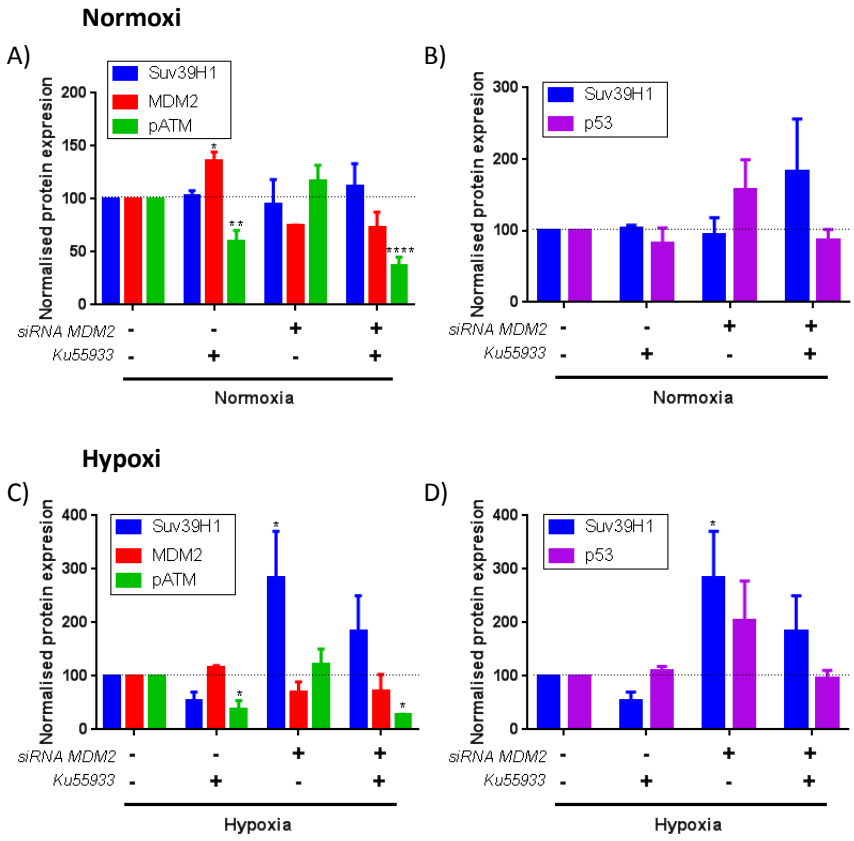

Figure 4.13. Normalised effect of MDM2 knockdown and ATM inhibition on the levels of Suv39H1 and p53 in normoxia and hypoxia. FTC133 cells were transfected with 20 pmol of MDM2 or a control siRNA and incubated with or without 10 µM of Ku55933 in normoxia (21% O_2) or hypoxia (0.1% O_2) for 18 hours prior to lysis and Western blotting. Presented data was obtained by normalising the densitometry values of Suv39H1 (blue), MDM2 (red) and p53 (purple) with β-actin and to the non-treated control for each condition. pATM (green) represents the levels of ATM-pSer1981 standardised to the total amount of ATM and β-actin. Graphs represent the values obtained for Suv39H1, MDM2 and pATM in normoxia (A) and hypoxia (C). Suv39H1 levels were compared to the levels of p53 in normoxia (B) and hypoxia (D).

MDM2 levels were decreased on average 30% in response to treatment with the specific siRNA. However, the observed efficiency of MDM2 siRNA was counteracted by ATM inhibition in normoxia and in hypoxia (Fig. 4.13A and 4.13B). In response to MDM2 knockdown the levels of Suv39H1 were significantly upregulated only in hypoxia. Treatment with Ku55933 decreased the observed upregulation of Suv39H1 in hypoxia

(Fig. 4.13C). A similar trend was observed on the levels of p53 in hypoxia (Fig. 4.13D). The levels of p53 were upregulated in response to MDM2 knockdown in hypoxia as well as in normoxia and this upregulation was negatively affected by the presence of the ATM inhibitor (Fig. 4.13B and 4.13C). Contrastingly, MDM2 knockdown didn't affect the levels of Suv39H1 in normoxia (Fig. 4.13A). As expected, the levels of Suv39H1 were downregulated in response to ATM inhibition in hypoxia. However, ATM inhibition didn't affect the levels of Suv39H1 in normoxia (Fig. 4.13B).

4.3. DISCUSSION

The levels of Suv39H1 in hypoxia have been shown to be largely influenced by the proteasomal pathway (Fig. 3.6). Considering that MDM2 involvement in negatively regulating the protein levels of Suv39H1 has been previously described, the effect of hypoxia on the levels of MDM2 was investigated. Hypoxia didn't exhibit a negative effect on the levels of MDM2 in any of the cell lines analysed; in fact, in FTC133 cells the levels of MDM2 were significantly higher in hypoxia than in normoxia (Fig. 4.1). The up-regulation of MDM2 in response to hypoxia has been previously reported [179, 180].

The presence of high levels of MDM2 in hypoxia suggests that a mechanism involved in negatively regulating MDM2 -dependent degradation of Suv39H1 must be present. Sirt1 has been implicated in increasing the half-life of Suv39H1 by inhibiting its polyubiquitination by MDM2 [73]. However, the levels of Sirt1 were downregulated in response to hypoxia in the cell lines analysed (Fig. 4.2). The negative effect of hypoxia on the levels of Sirt1 was highest in FTC133 and U87 cell lines. Transcriptional downregulation of Sirt1 in response to hypoxia has been previously reported [181].

In view of these findings it was hypothesised that inhibition of MDM2 and consequent upregulation of Suv39H1 may be due to ATM activity in hypoxia. Firstly, the efficiency of the ATM inhibitor, Ku55933, and its effect on MDM2 was assessed in FTC133 and HCT116 cell lines. Ku55933 was only efficient in inhibiting ATM auto-phosphorylation, marked by the presence of ATM-pSer1981, as well as the phosphorylation of p53 (p53-pSer15), after 18 hours of treatment in hypoxia or normoxia in the FTC133 cell line. Shorter time points of incubation with the drug weren't sufficient to inhibit ATM (Fig. 4.3).

In the HCT116 cell line, Ku55933 was able to inhibit the auto -phosphorylation of ATM even after 6 hours of treatment in hypoxia (Fig. 4.4). It is important to point out that HCT116 cells showed lower levels of ATM expression compared to FTC133, and this might be the cause of the observed difference in the efficiency of Ku55933. Thus, increasing the drug concentration may be a way to induce a more rapid and prominent effect of Ku55933 in the FTC133 cell line.

The consequence of ATM inhibition on the levels and function of MDM2 was analysed. Ku55933 induced an upregulation of MDM2 and consequently a downregulation of p53 in FTC133 cells (Fig. 4.5). The effect of ATM inhibition on the protein levels of MDM2 was more evident after 18 hours compared to 6 hours of treatment in hypoxia. This correlates with the results regarding the efficiency of Ku55933 in FTC133 cells (Fig. 4.4).

When irradiated, FTC133 cells presented an increase in MDM2 expression (Fig. 45). The transcriptional induction of MDM2 after irradiation or after other DNA damaging agents has been previously reported. DNA damage leads to p53 stabilisation, which acts as a transcription factor promoting the transcription of a variety of genes, including MDM2 [182]. Treatment with Ku55933 didn't manage to further boost this effect, which correlates with a simultaneous downregulation of p53. Another possible explanation for the observed response may be the activation, in response to x-rays, of other proteins involved in regulating MDM2. One of these proteins may be DNA-PK, as its involvement in regulating MDM2 activity and stability in response to DNA damage has been reported [183].

Contrary to what was expected, ATM inhibition and MDM2 upregulation didn't culminate in p53 downregulation in HCT116 cells (Fig 4.6). These findings imply that p53 stability is regulated by another mechanism in HCT116 cells. This result is supported by previously published data regarding an existence of a defective p53/MDM2 feedback loop in this cell line. The authors of this study showed that neither Ser-15 phosphorylation nor MDM2 is involved in regulating p53 stability or function in HCT116 cells [184].

Similar to FTC133 cells, treatment with Ku55933 lead to an upregulation of MDM2 in HCT116 cells in hypoxia, and this outcome was more pronounced after 18 hours of treatment (Fig. 4.6). These findings correlate with previously published data, regarding regulation of MDM2 stability by ATM. ATM is involved in indirectly regulating auto-ubiquitination and the subsequent degradation of MDM2 by negatively regulating Herpes

virus-associated Ubiquiting-specific protease (HAUSP), a specific deubiquitinase of MDM2 [185]. In contrast to FTC133 cells, treatment of HCT116 cells with Ku55933 resulted in an up-regulation of MDM2 after irradiation (Fig. 4.6). This may be due to the observed differences in the levels of p53 in response to DNA damage and ATM inhibition in these cell lines. In response to Ku55933 and x-rays, FTC133 cells showed a reduction in the levels of p53 which, as mentioned earlier, promotes the transcription of MDM2. On the other hand p53 was found to be upregulated in irradiated HCT116 cells treated with Ku55933, which may cause the observed up-regulation of MDM2.

Next, the effect of ATM inhibition on the levels of Suv39H1 was studied. Consistent with the hypothesis, treatment with Ku55933 lead to a significant reduction of Suv39H1 in hypoxia in both cell lines analysed after 18 hours of treatment. The same effect was shown in response to irradiation in both cell lines, which was more marked in HCT116 cells (Fig. 4.7 and 4.8). As discussed above, the efficiency of ATM inhibition on the downstream target seems to be more effective after longer exposure time to Ku55933.

Under normoxic conditions, the levels of Suv39H1 were minimally upregulated by Ku55933 in FTC133 cell line. However, ATM inhibition led to a significant reduction of Suv39H1 in HCT116 cells in normoxia. These results suggest the existence of a cell dependent mechanism of regulating of Suv39H1 stability in non-stressed cells. A previous study had suggested that Suv39H1 is an indirect transcriptional target of p53. It was shown that p53 negatively regulates the transcription of Suv39H1 through p21 [60]. This might explain the observed positive effect of Ku55933 on the levels of Suv39H1 in normoxia in FTC133 cells (Fig 4.7). Additionally in normoxia, the negative effect of Ku55933 on the levels of Suv39H1 in HCT116 cells may be due to some basal level of ATM activity in non-stressed cells that impact MDM2 stability. Consistent with this, the levels of MDM2 are upregulated in response to Ku55933 treatment in normoxia in HCT116 cells (Fig. 4.6).

In order to further study the mechanism behind Suv39H1 upregulation in hypoxia, the consequence of MDM2 knockdown, together with ATM inhibition, on the levels of Suv39H1 was assessed in FTC133 cells. Firstly, MDM2 knockdown was achieved and its efficiency verified by RT-PCR and Western blot (Fig. 4.10 and 4.11). As expected, cells treated with MDM2 siRNA showed an upregulation of p53 in normoxia and hypoxia. Suv39H1 was upregulated in response to MDM2 knockdown only in hypoxia. In normoxia, MDM2 knockdown only showed to have a minimal effect on the protein levels

of Suv39H1. This result is consistent with the previously presented data (*see Section 3.2.3 and Section 4.2.3.3.3*). This is suggestive of a different regulation mechanism for Suv39H1 in non-stressed FTC133 cells. Secondly, an experiment using MDM2 siRNA together with Ku55933 in normoxia and hypoxia was performed. Consistent with the hypothesis, the higher levels of Suv39H1 and p53 were found in hypoxia with MDM2 knockdown but without Ku55933. As expected, the levels of MDM2 were upregulated in response to Ku559933. Taken together, the results presented in this chapter are indicative of an ATM and MDM2 dependent regulation of Suv39H1 stability in hypoxia.

In summary, the obtained results from both cell lines point to an ATM dependent regulation of Suv39H1 in hypoxia as well as in response to x-rays. ATM involvement in regulating chromatin structure has been previously demonstrated. Specifically, it has been shown that ATM is implicated in inducing changes in chromatin structure in response to DNA damage. ATM dependent phosphorylation of Kap1 induces relaxation of the chromatin structure in response to DNA damage in order to facilitate and promote DNA damage repair. [42]. ATM directly interacts with Kap1, and the consequence of this interaction is the first rapid effect of ATM activation.

Meanwhile, the effect of ATM activation on the levels of Suv39H1 happens through MDM2, and thus likely happens after the first immediate response to ATM activation. The induction of Suv39H1 in response to ATM activation may facilitate the re-building of heterochromatin after the damage has been repaired, and also serves to protect the DNA from future damaging factors.

The involvement of ATM in regulating heterochromatin relaxation in response to DNA damage has been well documented. However, no data regarding ATM function in inducing and re building heterochromatin after the DNA damage repair has been published to date. Although, a study by Burgess [et al] (2014) showed that after DNA damage there is a transitional expansion of the chromatin, followed by an extensive condensation. Condensation of chromatin alone is sufficient for the activation of the DNA damage response, and damage independent upstream signalling [128]. Considering this, it is possible that ATM plays an important role in promoting chromatin condensation by inducing expression of Suv39H1. In support of this hypothesis it has been previously reports that Punkinje neurons obtained from patients with ataxia telangiectasia, which is a

degenerative neurological disease characterised by the autosomal recessive mutation in the ATM gene, are very euchromatic [186].

ATM has also been involved in suppress transcription by regulating chromatin structure in response to DNA damage [187]. The ATM dependent induction of Suv39H1 may be another mechanism by which ATM is involved in repressing transcription. The role of Suv39H1 in negatively regulating gene transcription has been reported [60, 188].

Hypoxic stress induces a persistent activation of ATM without the presence of DNA damage [24]. The absence of DNA damage in hypoxia suppresses the need to induce chromatin relaxation to facilitate repair. In this condition the persistent ATM activation may lead to a general condensation of the chromatin by inducing Suv39H1. In hypoxia, chromatin condensation may serve to repress DNA transcription and to protect the DNA from damage caused by possible future re-oxygenation. This idea is supported by the fact that ATM inhibition under hypoxia sensitises cells to hypoxia/reoxygenation [86]. Therefore indicating the importance of hypoxia induced ATM activation for the survival of cancer cells.

5. CHAPTER 5: ATM ACTIVATION IN HYPOXIA

5.1. INTRODUCTION

ATM is a PI3K –like kinase that plays essential role in the DNA damage response pathway by transducing the damage signal to a wide variety of cellular outcomes through the phosphorylation of a large number of downstream targets [189]. ATM is mainly responsible for orchestrating the repair of DSB [190].

ATM is present in the cell in the form of an inactive homodimer and its activation depends on the action of the acetyltransferase Tip60 that acetylates ATM at Lys3016 [109, 113]. ATM and Tip60 form a heterodimeric complex in the cell. The acetylation of ATM is the first step for its activation. Acetylation dissociates the ATM homodimeric complex and facilitates its trans-auto-phosphorylation, at Ser1981. Subsequently, a dimer to monomer transition leads to the catalytic activation of ATM [109, 114]. ATM is essential for the repair of DNA damage generated in the heterochromatic regions of the genome, characterised by the presence of H3K9me3 [191]. In response to DNA damage, Tip60 is activated by direct interaction with H3K9me3, which leads to the activation of ATM [113, 114].

ATM can also be activated by non DNA damaging stress. DNA damage independent activation of ATM has been reported in response to hypotonic stress, chromatin modifying agents, heat and hypoxia [118, 192, 193]. In response to hypoxia, ATM activation has been related to the formation of stalled replication forks in the context of H3K9me3 chromatin modification [22, 24]. The involvement of Tip60 in the hypoxic dependent activation of ATM has not been tested to date.

The levels of Tip60, as well as its activity, are negatively regulated by Sirt1 [194, 195]. The downregulation of Sirt1 in the experimental conditions used in this study has been shown in Section 4.2.2. Additionally, the involvement of Tip60 in the transcription of some of the HIF-1α target genes has been documented [196]. Taken together the observations mentioned above suggest that Tip60 is an important part of the DNA damage signalling in hypoxic conditions. Considering this, Tip60 involvement in the hypoxia induced activation of ATM was tested.

Firstly, the activation of ATM in hypoxia was verified by Western blot. To verify lack of DNA damage in the experimental conditions immunohistochemical analysis was carried out following the DNA damage markers γH2AX and 53BP1. Finally, in order to test the

involvement of Tip60 in the hypoxia induced activation of ATM, the levels of Tip60 were determined by Western blot in the presence of the Tip60 inhibitor TH1834 [146].

The Tip60 specific inhibitor, TH1834, was designed, characterised and kindly provided by Dr. James Brown's group from the National University of Ireland, Galway. To validate the efficacy of TH1834 in the model used in this study, a dose response experiment was performed using the formation of γH2AX after x-rays as a control for Tip60 activity. The activity of TH1834 was also validated in hypoxia using ATM-pSer1981 as the specific downstream target. Lastly, FTC133 and HCT116 cells were treated with TH1834 and the levels of ATM-pSer1981 were analysed by Western blot.

5.2. RESULTS

5.2.1. ACTIVATION OF ATM IN RESPONSE TO HYPOXIA IN THE ABSENCE OF DNA DAMAGE

In order to determinate if ATM is activated in response to hypoxia, the levels of ATM-pSer1981 were assessed in FTC133 and HCT116 cell lines. Cells were incubated in normoxia (21% O_2) or hypoxia (0.1% O_2) for 18 hours prior to lysis, and Western blot analysis was then carried out. Images of three independent experiments were analysed by densitometry to calculate the levels of ATM-pSer1981 in relation to the levels of total ATM and the loading control (β-actin). A representative image of the experiment is shown in Figure 5.1A. The graphs represent normalised ATM-pSer1981 expression in relation to the normoxic control (Fig. 5.1B).

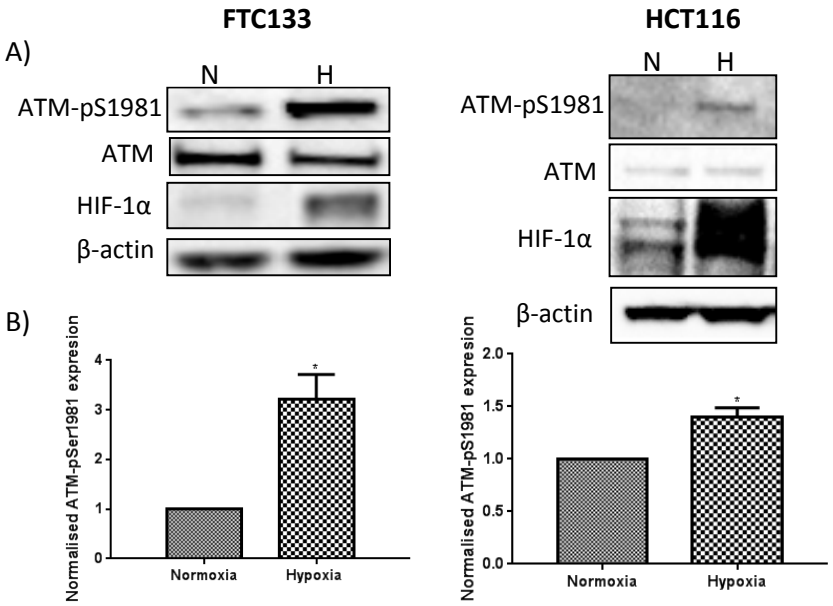

Figure 5.1. ATM-pSer1981 protein levels in response to hypoxia. Cells were incubated in normoxia (N; 21% O_2) or hypoxia (H; 0.1% O_2) for 18 hours prior to lysis and Western blotting. HIF-1α was used as a control for hypoxia and β-actin as a loading control. The graphs represent the densitometry of ATM-pSer1981 normalised to the total amount of ATM, β-actin and the normoxic control. Bars represent the mean ± SEM of three independent experiments.

A significant increase in the levels of the catalytically active form of ATM was found in both cell lines analysed.

To verify the lack of DNA damage in the cells in hypoxia, FTC133 cells were immunohistochemically stained for phosphorylated γH2AX. Cells were incubated for 18 hours in normoxia or hypoxia. After treatment the cells were fixed and stained with γH2AX specific antibody and DAPI was used as a nuclear marker. Cell irradiated with 4Gy of x-rays were used as a positive control for DNA damage foci (*see section 2.5 for details*). Three independent experiments were performed and a representative image of γH2AX staining is presented in Figure 5.2. The mean fluorescence of γH2AX is represented in the graph and was calculated as described in the section 2.7.

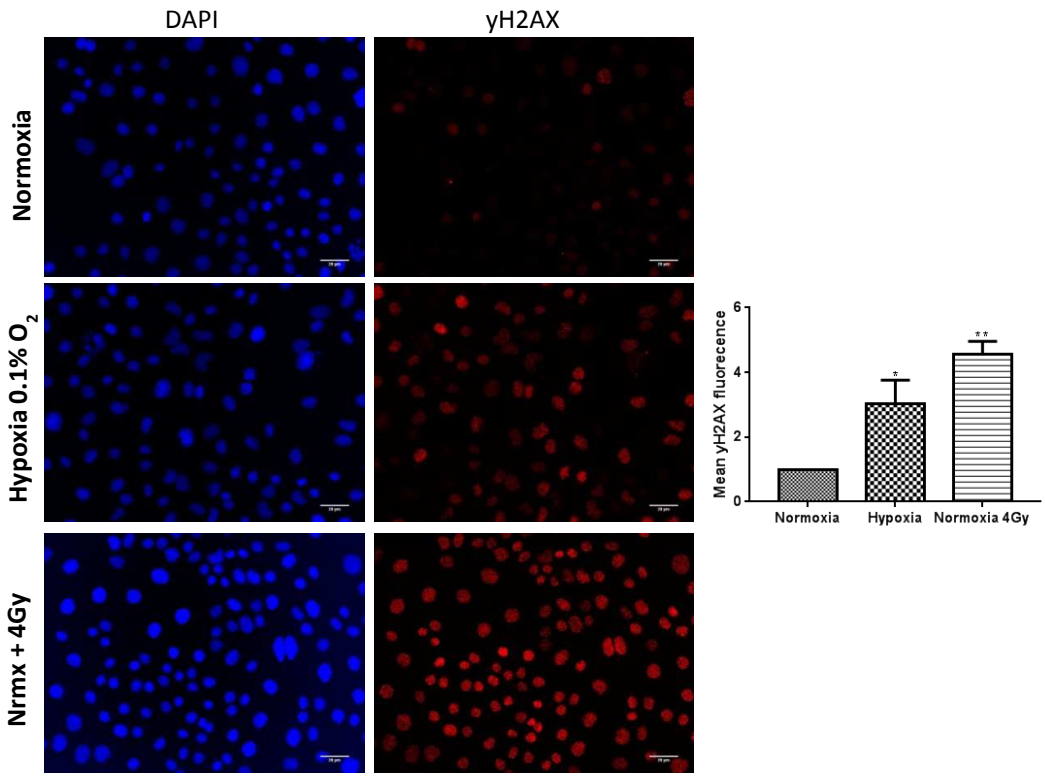

Figure 5.2. Phosphorylated γH2AX levels in response to hypoxia. FTC133 cells were incubated for 18 hours in normoxic (21% O_2) or hypoxic (0.1% O_2) conditions. Cells irradiated with 4Gy cells were used as positive control (Nrmx + 4 Gy). Cells were stained for γH2AX (red) and DAPI (blue). The graph represents the mean expression of γH2AX. Three independent experiments were performed and the bars represent the mean ± SEM.

The expression of γH2AX was significantly induced in response to hypoxia, but this induction was much more prominent after x-rays.

53BP1 was used as an indicator of DNA damage. FTC133 cells were treated and stained as described above and one representative image out of three independent experiments is presented in the Figure 5.3. Images were analysed by counting the amount of 53BP1 foci per cell as described in the section 2.7.3.1., and the results are presented in the graph (Fig. 5.3).

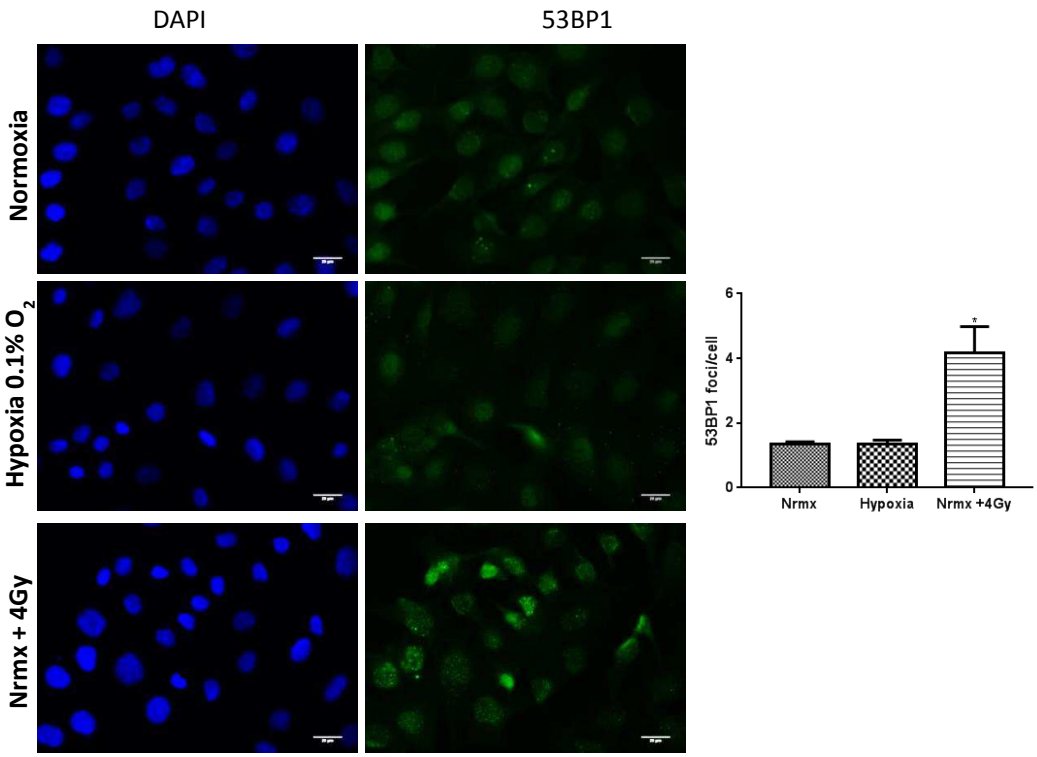

Figure 5.3. The levels of 53BP1 foci in response to hypoxia. FTC133 cells were incubated for 18 hours in normoxic (21% O_2) or hypoxic (0.1% O_2) conditions. Cells irradiated with 4Gy were used as positive control (Nrmx + 4 Gy). Cells were stained for 53BP1 (green) and DAPI (blue). The graph represents the number of 53BP1 foci per cell. Three independent experiments were performed and the bars represent the mean ± SEM.

Contrary to γH2AX, 53BP1 foci weren't induced in response to hypoxia. On the other hand, irradiation with 4 Gy of x-rays did induce a significant upregulation of 53BP1 foci.

5.2.2. UPREGULATION OF TIP60 IN RESPONSE TO HYPOXIA

In order to test the involvement of Tip60 in the hypoxia-induced activation of ATM, firstly the levels of Tip60 were analysed by Western blot. FTC133 and HCT116 cells were incubated for 18 hours in hypoxia or normoxia and Western blot analysis was carried out as described in the previous section. Three independent experiments were performed and a representative image is shown in Figure 5.4A. Graphical representation of densitometric analysis of Tip60 expression is presented in Figure 5.4B.

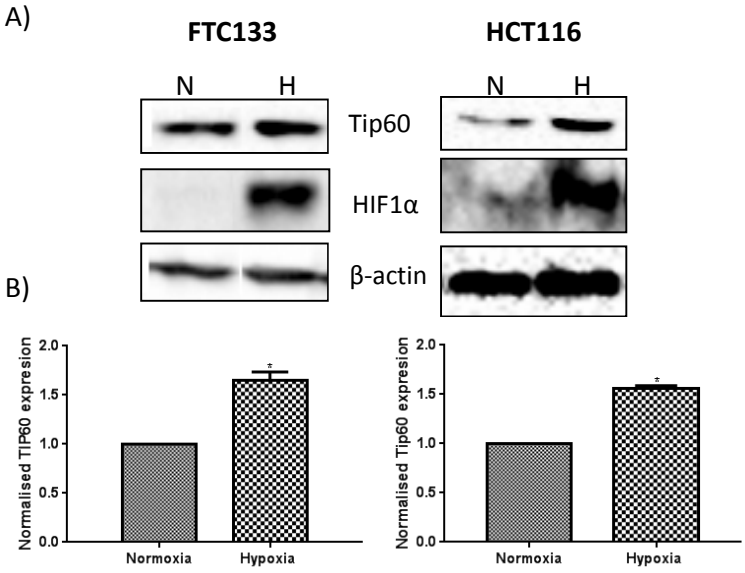

Figure 5.4. Tip60 protein levels in response to hypoxia. Cells were incubated in normoxic (N; 21% O_2) or hypoxic (H; 0.1% O_2) conditions for 18 hours prior to lysis and Western blot analysis. HIF-1α was used as a control for hypoxic condition and β-actin as a loading control (A). The graphs represent the densitometry of Tip60 expression normalised by the loading control and normoxia (B). Bars represent the mean ± SEM of three independent experiments.

The protein levels of Tip60 were significantly upregulated in response to hypoxia in both cell lines analysed.

5.2.3. DOSE RESPONSE ANALYSIS OF TIP60 SPECIFIC INHIBITOR: TH1834

Previous studies provided evidence regarding the involvement of Tip60 in the formation of γH2AX foci after irradiation [197]. Additionally, γH2AX foci were used as a downstream marker by the group of Dr. James Brown to test the efficacy of TH1834 [146]. The efficiency of Tip60 inhibition by TH1834 was assessed in x-ray radiated FTC133 cells in the presence of 1, 10 or 20 µM of the inhibitor following the γH2AX levels.

FTC133 cells were incubated with 1, 10 or 20 µM of TH1834 or DMSO for 18 hours. After this, the cells were irradiated at 4 Gy with x-rays and were fixed 30 minutes post irradiation. Staining with γH2AX antibody was performed as described in the section 2.7. Three independent experiments were performed and the images acquired using a 3D-Histech Pannoramic-250 microscope slide-scanner (*see section 2.7.3 for details*). A representative image is presented in Figure 5.5. γH2AX mean fluorescence was quantified and analysed using Image J software (Fig. 5.5).

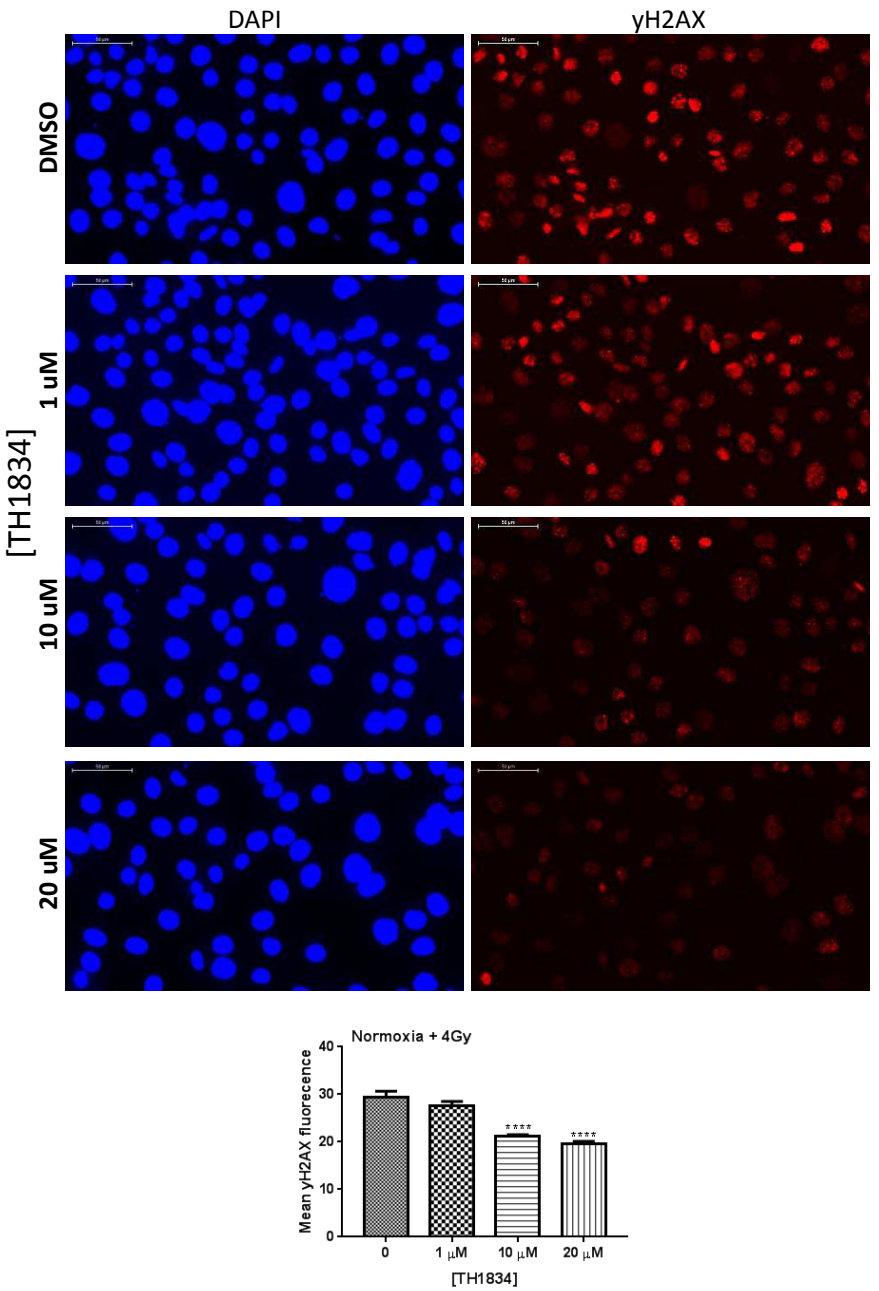

Figure 5.5. γH2AX foci in irradiated FTC133 cells treated with different concentrations of TH1834. FTC133 cells were incubated with 1, 10 or 20 μM of TH1834 or DMSO for 18 hours. Cells were irradiated with 4Gy and fixed 30 minutes post irradiation. Cells were stained for γH2AX (red) and DAPI (blue). The graph represents γH2AX mean fluorescence. Three independent experiments were performed and the bars represent the mean ± SEM.

The formation of γH2AX foci in response to x -rays was reduced in cells pre-treated with TH1834. This reduction was significant with 10 and 20 μM of the drug. Treatment with 10 and 20 μM of TH1834 were equally significant.

5.2.4. THE EFFECT OF TIP60 INHIBITION ON THE ACTIVATION OF ATM IN HYPOXIA

In order to evaluate the effect of Tip60 inhibition on the levels of ATM-pSer1981 immunohistochemical analysis was performed in FTC133 cells and the images were obtained as described in the previous section. FTC133 cells were incubated with 1, 5 or 10 µM of TH1834 or DMSO for 18 hours in hypoxia. After this, the cells were stained for ATM-pSer1981 and DAPI as a nuclear marker. Three independent experiments were performed and a representative image is presented in Figure 5.6.

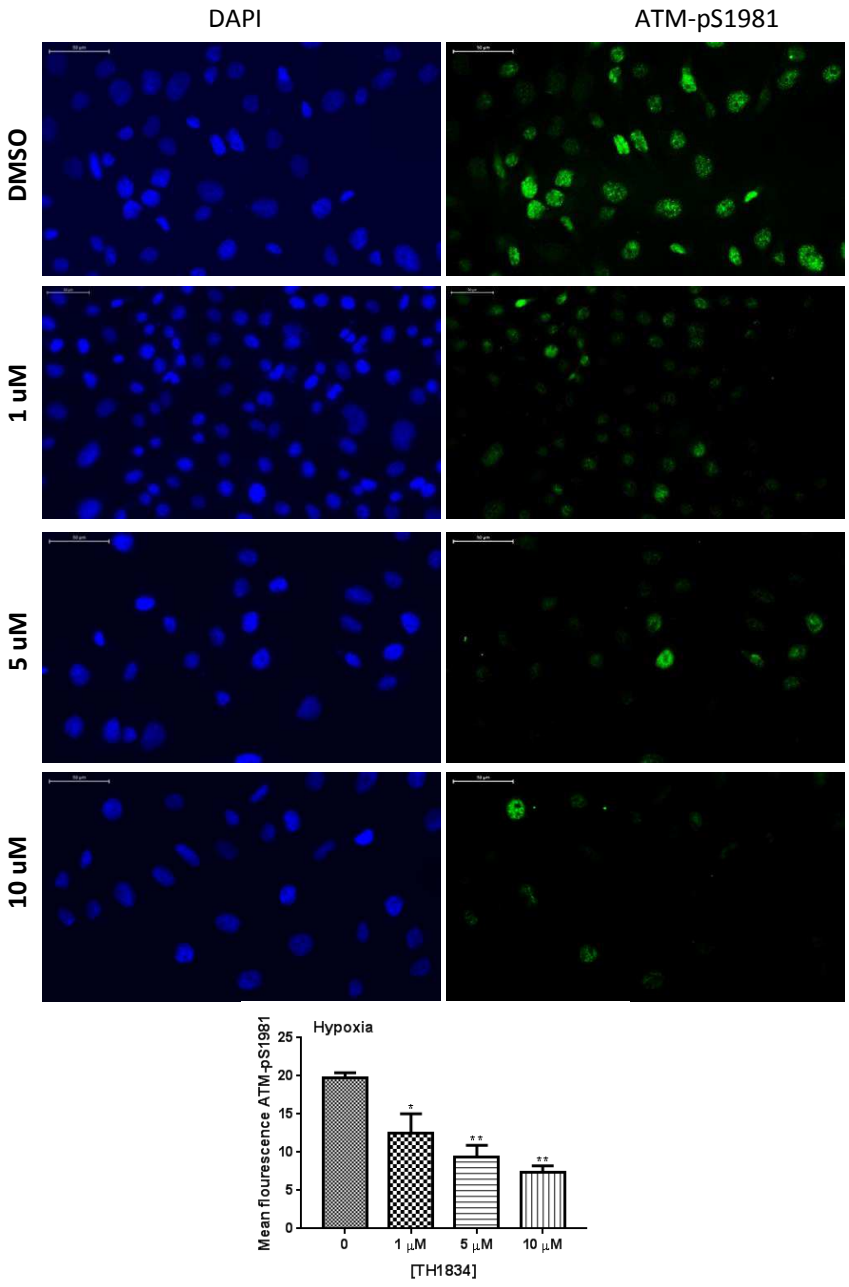

Figure 5.6. The levels of ATM-pSer1981 in FTC133 cells treated with different concentrations of TH1834 in hypoxia. FTC133 cells were incubated with 1, 5 or 10 µM of TH1834 or DMSO for 18 hours in hypoxia (0.1% O_2). Cells were stained for ATM-pSer1981 (green) and DAPI (blue). The graph represents ATM-pSer1981 mean fluorescence. The bars represent the mean ± SEM of three independent experiments.

The levels of ATM-pSer1981 were significantly reduced in the presence of the Tip60 inhibitor in hypoxia. The greatest effect was shown using 10 µM of TH1834.

Data were corroborated by Western blot. Here both FTC133 and HCT116 cells were treated with 10 µM of TH1834. Cells were treated for 6 or 18 hours in hypoxia. Cells in normoxia were treated for 18 hours before Western blot analysis. Cells irradiated with 4 Gy of x-rays were treated for 18 hours with the drug prior to being irradiated (*see section 2.5 for details*). Western blot analysis was carried out as described in the previous section. A representative image for FTC133 and HCT116 cells is presented in Figure 5.7A and Figure 5.7C, respectively.

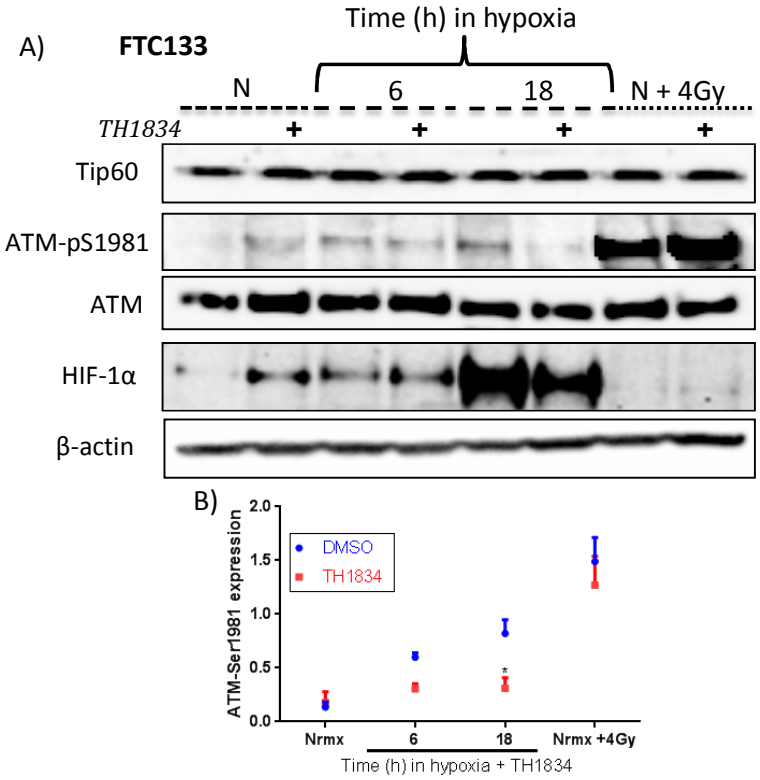

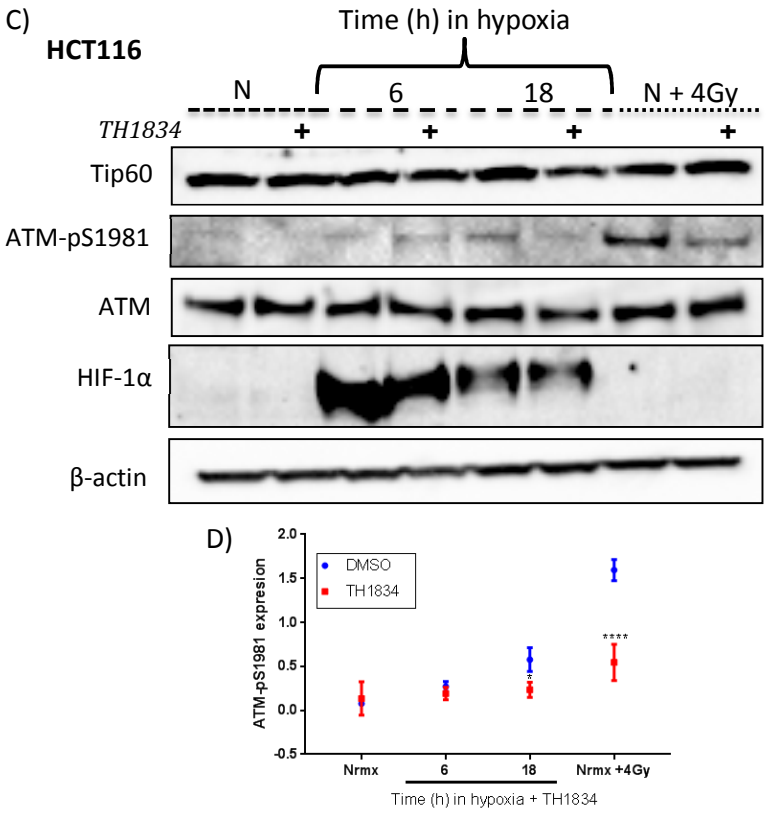

Figure 5.7. Effect of Tip60 inhibition on ATM-pSer1981 protein levels in FTC133 and HCT116 cells. FTC133 (A) and HCT116 (C) cells were incubated with or without 10 µM of TH1834 in normoxia (21% O_2) or hypoxia (0.1% O_2) for 6 or 18 hours prior to lysis and Western blotting. FTC133 Treatment with TH1834 is indicated with the symbol (+). Normoxia is indicated with an N and cells irradiated with 4 Gy as N + 4 Gy. HIF-1α was used as a control for hypoxia and β-actin as a loading control. The graphs represent the densitometry of ATM-pSer1981 standardised to the total amount of ATM and β-actin in the presence of TH1834 (red) or DMSO (blue) for FTC133 (B) and HCT116 (D). Bars represent the mean ± SD of three independent experiments.

Tip60 inhibition had only a small effect on the levels of ATM-pSer1981 after 6 hours of treatment. However, after 18 hours of treatment the levels of ATM-pSer1981 were significantly reduced in both cell lines analysed. On the other hand, treatment with TH1834 only reduced the levels of ATM-pSer1981 in irradiated HCT116 cells, but did not have any significant effect in irradiated FTC133 (Fig. 5.7).

5.2.5. The effect of Tip60 inhibition on the activation of ATM in response to X-rays in FTC133 cells

Treatment with 10 µM of TH1834 did not affect the levels of ATM-pSer1981 in irradiated FTC133 cells (Fig. 5.7). Thus, FTC133 cells were treated with different concentration of TH1834 to assess ATM-pSer1981 levels in response to radiation. FTC133 cells were

incubated with 10, 20 or 30 µM of TH1834 for 18 hours and then irradiated with 4 Gy x-rays. Cell lysates were analysed by Western blot and a representative experiment is presented in Figure 5.8

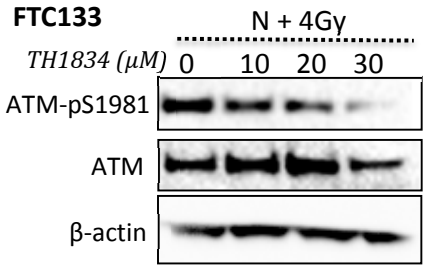

Figure 5.8. The levels of ATM-pSer1981 in irradiated FTC133 cells treated with different concentrations of TH1834. Cells were irradiated at 4 Gy x-rays (N + 4Gy) and then incubated with 10, 20 or 30 µM of TH1834 or DMSO (marked with 0) in normoxia (21% O_2) for 18 hours. Cells were lysed and analysed by Western blot post radiation.

In the irradiated FTC133 cells, the levels of ATM-pSer1981 progressively decreased with an increasing concentration of the drug (Fig. 5.8).

5.2.6. THE EFFECT OF TIP60 INHIBITION ON THE ACTIVATION OF ATM IN HYPOXIA IS INDEPENDENT OF DNA DAMAGE

Co-staining with ATM-pSer1981 and 53BP1 was performed in FTC133 cells treated with TH1834 to ensure that the observed downregulation of ATM-pSer1981 is independent of DNA damage. Cells were treated with 10 µM of TH1834 for 6 or 18 hours in hypoxia. Irradiation with 4 Gy was used as a positive control for 53BP1 foci. FTC133 cells were fixed, stained and images acquired as described in the section 2.7. The results of this experiment are presented in Figure 5.9

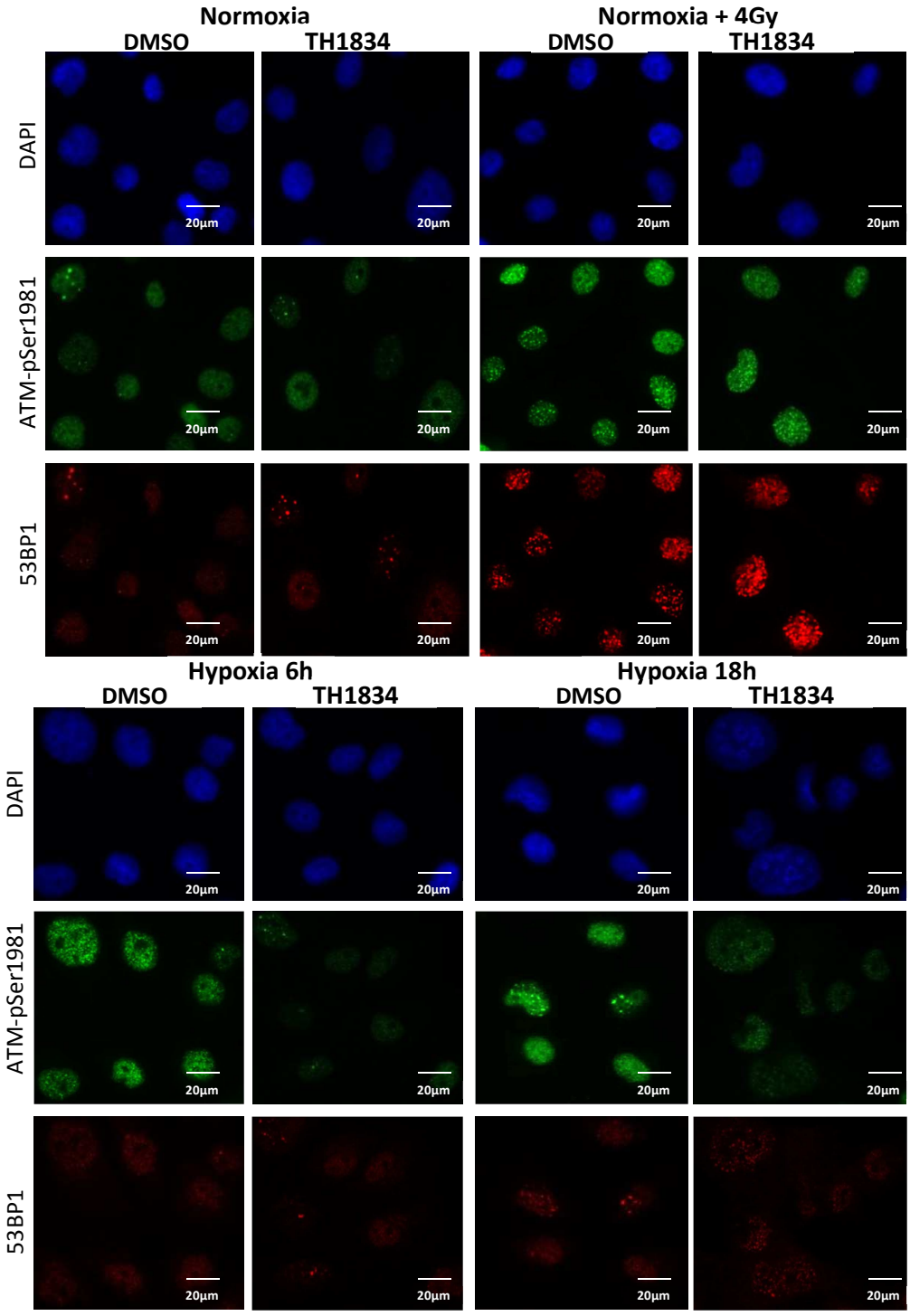

Figure 5.9. The levels of ATM-pSer1981 and 53BP1 foci in FTC133 cells treated with TH1834. FTC133 cells were incubated with 10 µM of TH1834 or DMSO for 18 hours in normoxia (21% O_2) or hypoxia (0.1% O_2). Cells irradiated with 4Gy were used as positive control. Cells were stained for ATM-pSer1981 (green), 53BP1 (red) and DAPI (blue).

Mean fluorescence of ATM-pSer1981 was quantified using Image J software, and the results are shown in Figure 5.10A. The number of 53BP1 foci per cell were quantified as described in Section 2.7 and the outcome is presented in Figure 5.10B. In order to determine if the differences observed in the levels of ATM-pSer1981 were independent of DNA damage, ATM-pSer1981 mean fluorescence was quantified excluding all cells with 53BP1 foci (Fig. 5.10C).

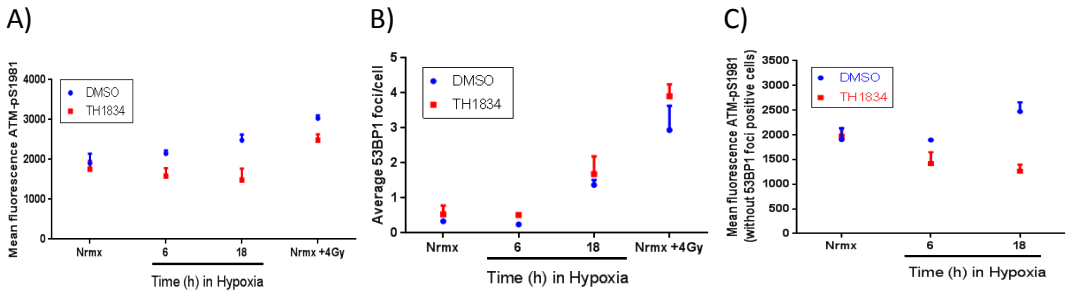

Figure 5.10. ATM-pSer1981 fluorescence and 53BP1 foci in FTC133 cells treated with TH1834. FTC133 cells were incubated with 10 µM of TH1834 (red) or DMSO (blue) for 18 hours in normoxia (21% O_2) or hypoxia (0.1% O_2). Cells were stained for ATM-pSer1981 and 53BP1. ATM-pSer1981 mean fluorescence (A) and the number of 53BP1 foci per cell (B) were quantified using ImageJ software. To exclude ATM-pSer1981 associated with DNA damage, ATM-pSer1981 mean fluorescence was quantified excluding cells with 53BP1 foci (C).

In hypoxia, treatment with Tip60 inhibitor did not induce the formation of more 53BP1 foci. Conversely, in response to x-ray, FTC133 cells treated with TH1834 presented higher levels of 53BP1 compared with the control. The levels of ATM-pSer1981 were evidently lower in the cells treated with TH1834 after 18 hours of treatment in hypoxia, even when the cells with DNA damage were removed from the analysis.

5.3. DISCUSSION

ATM activation in response to hypoxia was observed in FTC133 and HCT116 cells (Fig.5.1). Hypoxia induced activation of ATM has been previously reported [22, 24, 83]. Hypoxia induced γH2AX phosphorylation but 53BP1 foci were not formed (Fig. 5.2 and 5.3) suggesting that γH2AX phosphorylation in response to hypoxia is not related to DNA damage. Induction of γH2AX in response to hypoxia as part of the DNA damage response pathway activation has been previously reported [85, 198]. It has been suggested that DNA damage independent γH2AX phosphorylation in response to hypoxia (0.02% O_2) is associated with the formation of stalled replication forks and consequent activation of ATR

[85]. Evidence that induction of γH2AX in response to mild hypoxia (0.2% O_2) depends on HIF-1α activity *in vitro* and *in vivo* has also been recently shown [198].

Tip60 plays an important role in hypoxia, as a co-activator of HIF-1α, being involved in the regulation of cellular response to hypoxic stress [196]. To further investigate the role of Tip60 in hypoxia, the protein levels of Tip60 in hypoxia were assessed. Tip60 was upregulated in response to hypoxia in FTC133 and HCT116 cells (Fig.5.4). Sirt1 negatively regulates Tip60 stability [194, 195]. The detected downregulation of Sirt1 in these cell lines (*see Chapter 4*), might explain the Tip60 upregulation in hypoxic cells. Sirt1 has also been implicated in regulating Tip60 auto-acetylation and consequently modulation of its acetyltransferase activity (HAT). Sirt1 dependent deacetylation of Tip60 negatively regulates its HAT activity and induces its ubiquitination and subsequent degradation [194]. The downregulation of Sirt1 in response to hypoxia together with the observed upregulation of Tip60, points to the presence of a catalytically active Tip60 under hypoxia.

Activation of the DDR pathway in response to hypoxia plays a crucial role in tumour progression [23, 24, 86, 199]. Tip60 plays an essential role in the DNA damage response pathway after exposure to DNA damaging agents [59, 109, 113]. However, the contribution of Tip60 in the activation of the DDR in response to hypoxia hasn't been tested to date. The involvement of Tip60 in the observed activation of ATM in response to hypoxia (Fig. 5.1) was tested using the Tip60 specific inhibitor, TH1834.

Firstly, TH1834 efficiency was assessed following γH2AX phosphorylation in response to x-rays as a downstream target of Tip60. Significant reduction of γH2AX phosphorylation was observed in FTC133 cells after radiation in the presence of 10 and 20 μM of TH1834. No significant difference in the levels of γH2AX was evident in FTC133 cells treated with 10 or 20 μM of TH1834 alone (Fig. 5.5). The low sensitivity of the assay used to detect γH2AX, or the fact that dose/response curve reached a plateau around 10 μM due to the saturation of the system cannot be excluded.

Next, the involvement of Tip60 in hypoxia induced activation of ATM was tested using 1, 5 and 10 μM of TH1834 in FTC133 cells. Levels of ATM-pSer1981 were significantly downregulated with all the concentrations of TH1834 used. As expected, this downregulation was most pronounced in cells treated with 10 μM of TH1834 (Fig. 5.6).

Tip60 inhibition had a more prominent effect on the levels of ATM-pS1981 in hypoxia than after x-rays in FTC133. On one hand, the observed differences may be due to varying mechanisms of downstream target modification (ATM-pSer1981 vs γH2AX). However, the observed difference is most likely the result of the induction of other mechanisms leading to γH2AX phosphorylation in the presence of DNA damage.

To further investigate the effect of Tip60 on the activation of ATM under hypoxic conditions, FTC133 and HCT116 cells were treated with 10 μM of TH1834 and ATM-pSer1981 was followed. Reduced ATM-pSer1981 levels were detected in FTC133 cells after 6 hours of treatment in hypoxia. Modest reduction of ATM-pSer1981 the levels were also observed in HCT116 after 6 hours of treatment in hypoxia. However, significant reduction of ATM-pSer1981 levels was evident in both cell lines treated with TH1834 for 18 hours in hypoxia (Fig. 5.7).

Significant downregulation of the ATM-pSer1981 levels was recorded in pre-treated with TH1834 HCT116 cells in response to radiation. In FTC133 cells on the other hand, the effect of Tip60 inhibition on the levels of ATM-pSer1981in response to radiation was not as evident (Fig. 5.7). The lack of response in FTC133 might be due to low efficiency of the drug in a condition where the levels of expression of ATM-pSer1981 are much higher. To test this hypothesis, FTC133 cells were treated with higher concentrations of TH1834 which resulted in a more pronounced downregulation of ATM-pSer1981 in cells treated with 20 and 30 μM of the drug (Fig. 5.8).

To exclude the possibility that the observed effect of TH1834 in hypoxia is dependent on DNA damage present in the cells, FTC133 cells were co-stained for ATM-pSer1981 and 53BP1 after treatment (Fig. 5.9). As expected, the analysis showed that the levels of 53BP1 foci after 6 and 18 hours of treatment with TH1834 in hypoxia were very similar to those detected in the untreated cells. The levels of ATM-pSer1981 were downregulated in response to Tip60 inhibition, even after excluding cells with 53BP1 foci from the analysis (Fig. 5.10). These results suggest that Tip60 is involved in the DNA damage independent activation of ATM.

In response to x-ray irradiation, the levels of 53BP1 were higher in FTC133 cells treated with TH1834 compared to the control (Fig. 5.10). The observed consequence of Tip60 inhibition in irradiated cells may be due to faulty DNA damage repair as a consequence of

ATM inhibition. In support of this hypothesis, it has been previously reported that ATM is involved in the dissociation of the 53BP1 foci from the sites of DNA damage [200].

Downregulation of the γH2AX phosphorylation and upregulation of the 53BP1 levels was observed in TH1834 treated cells in response to radiation. It is important to point out that γH2AX phosphorylation is a process dependent on the activation of kinases involved in DDR, such as ATM and ATR. Thus, the reduction in the levels of γH2AX in response to Tip60 inhibition may be a direct consequence of ATM inhibition. Reduction of γH2AX foci after treatment with Tip60 siRNA has been previously reported, but the underlying mechanisms leading to this effect have not been addressed [197]. Meanwhile, the formation of 53BP1 foci in response to DNA damage is independent of the action of kinases of the DDR pathway. 53BP1 is one of the proteins that are recruited early to the sites of DNA damage through the recognition and binding to H4K20me2 [201].

In conclusion, data presented in this chapter suggest that Tip60 plays a crucial role in the hypoxia dependent activation of ATM. Existing data link the activation of ATM to S-phase arrest as well as to the induction of H3K9me3 in hypoxia [22]. It has been shown that hypoxia induced activation of ATM is independent of the MRN complex [24]. The relationship between Tip60 and MRN in ATM activation is not very clear [202]. Two different studies from the same group reported contradicting results regarding MRN involvement in the Tip60 dependent activation of ATM [59, 113]. The first study reported an MRN independent activation of Tip60 and ATM [113]. However, the follow-up study showed that Tip60 dependent activation of ATM is diminished, but not totally abolished, by Rad50 siRNA in HCT116 cells [59]. This indicated that the role that MRN plays in this mechanism is debatable.

As mentioned above, the presence of H3K9me3 in hypoxia is important for the hypoxia dependent activation of ATM. It has been reported that H3K9me3 acts as an allosteric regulator of Tip60 HAT activity [59]. High levels of H3K9me3 in response to hypoxia might lead to Tip60 activation. Although, previous studies found that hypoxia induced ATM doesn’t localise to chromatin [24]. It may be possible that Tip60 is activated by the interaction with H3K9me3, but the Tip60/ATM complex isn’t retained in the chromatin because MRN, which functions as an adaptor, is not present. This idea is supported by previous published data showing that ATM activation is regulated mainly through changes in the chromatin structure, rather than by direct interaction with the chromatin [106].

However, H3K9me3 is necessary, but not sufficient, for the hypoxia induced activation of ATM, as induction of H3K9me3 in mild hypoxia didn't lead to the activation of ATM [22].

Downregulation of Sirt1 observed in response to hypoxia may be another mechanism of Tip60 activation and subsequent ATM auto-phosphorylation. Given that 2% O_2 does not induce ATM activation [22] future studies should investigate the levels of Sirt1 and its activity, in response to milder levels of hypoxia.

Induction of S-phase arrest, in response to hypoxia, has been shown to be a necessary factor in ATM activation under these conditions. However, treatment only with hydroxyurea, which leads to the induction of S-phase arrest, failed to induce ATM activation. It was shown that the activation of ATM is also dependent on the presence of H3K9me3 [22]. All this suggests that more than one factor must be involved in regulating ATM activity under hypoxic conditions.

6. CONCLUSIONS AND FUTURE DIRECTIONS

6.1. CONCLUSIONS

6.1.1. H3K9ME3 IS INDUCED BY SUV39H1 IN RESPONSE TO HYPOXIA IN FTC133, U87 AND HCT116 CELLS

Heterochromatin features are commonly observed in tumours [212]. Tumour hypoxia induces changes in the chromatin structure, with induction of the heterochromatin mark H3K9me3 frequently found. The expression of the heterochromatin related mark, H3K9me3, was upregulated in FTC133 and U87 exposed for 18 hours to hypoxia (0.1% O_2). The predominance of H3K9me3 coincided with the upregulation of Suv39H1 in FTC133, U87 and HCT116 cells exposed to hypoxic conditions. However, under mild levels of hypoxia (1% O_2) induction of H3K9me3 and Suv39H1 were not evident in FTC133 suggesting that induction of Suv39H1 is a prerequisite for the stimulation of H3K9me3.

mRNA analysis carried out in FTC133, U87 and HCT116 cell lines pointed out that Suv39H1 in hypoxia is regulated at post-translational level. Significant increase of Suv39H1 cellular levels was observed in FTC133 cells treated with the proteasome inhibitor MG132 in mild hypoxia suggesting the involvement of the ubiquitin proteasome pathway in regulating the Suv39H1 protein levels under these conditions. Potential contribution of the E3 ligase MDM2 in these events was investigated in an effort to uncover the regulatory mechanisms behind Suv39H1 upregulation in hypoxia and consequential changes in chromatin structure in response to hypoxic stress. These observations could facilitate the design of more precise therapeutic schemes enabling improved treatment of hypoxic tumour regions.

6.1.2. SUV39H1 IS UPREGULATED IN HYPOXIA VIA ATM DEPENDENT INHIBITION OF MDM2 IN FTC133 AND HCT116 CELLS

The upregulation of Suv39H1 in hypoxia and the involvement of the proteasome pathway in this process were shown in *Chapter 3* of this study. The next aim of this project was to determine the exact mechanism behind this process. As Sirt1 has been previously reported to be involved in inhibiting MDM2 dependent degradation of Suv39H1 [73], the levels of MDM2 and Sirt1 were analysed. There was no significant change of the MDM2 protein levels in HCT116 and U87 cells whereas significant upregulation of this E3 ligase was evident in FTC133 cells. Sirt1 protein levels on the other side were downregulated in

hypoxia, compared to the normoxic control in all the cell lines analysed. In view of these findings it was hypothesised that another mechanism must be involved in negatively regulating MDM2 activity.

The hypoxia induced activation of ATM, as well as its involvement in regulating MDM2 activity, have been previously reported [24, 174, 175]. To address the possible involvement of ATM in the observed upregulation of Suv39H1 in hypoxia, the ATM specific inhibitor Ku55933 was used. After 18 hours of treatment with Ku55933 in hypoxia, the levels of Suv39H1 were significantly reduced in all the cell lines analysed. This indicates that ATM is at least partially involved in the upregulation of Suv39H1 in hypoxia.

To further validate the involvement of ATM and MDM2 in the hypoxia induced upregulation of Suv39H1, MDM2 knockdown in combination with Ku55933 was performed in FTC133 cells. The highest levels of Suv39H1 were recorded in cells transfected with siRNA targeting MDM2 in the absence of Ku55933, in hypoxia. This result further corroborates that ATM as well as MDM2 are involved in regulating Suv39H1 in response to hypoxic stress. The role of ATM in the hypoxia induced heterochromatin points to a new stress-specific role of this protein in promoting tumour cell survival under these conditions.

6.1.3. HYPOXIA INDUCED ACTIVATION OF ATM IS DEPENDENT ON TIP60 ACTIVITY IN FTC133 AND HCT116 CELLS

The final aim of this study was to understand the mechanism of the hypoxia-induced activation of ATM. The involvement of the acetyltransferase Tip60 in the DNA damage induced activation of ATM has been previously reported [113]. However, it is not known if the same mechanism operates in response to hypoxia. It has been previously reported that Sirt1 is involved in negatively regulating Tip60 protein levels as well as its enzymatic activity [194]. The observed downregulation of Sirt1 (see Chapter 4) and upregulation of Tip60 (see Chapter 5) in response to hypoxia suggested the presence of an active form of Tip60 under these conditions. In order to test the involvement of Tip60 in the upregulation of the catalytically active form of ATM (ATM-pSer1981) in response to hypoxia, the Tip60 specific inhibitor TH1834 [146] was used.

FTC133 and HCT116 cells treated with TH1834 in hypoxia, showed a significant reduction in the levels of ATM-pSer1981. In order to exclude the possibility that the

observed effect of TH1834 was due to DNA damage present in the cells, the 53BP1 foci were analysed. The obtained results support the notion that the Tip60 mediated negative effect on the ATM-pSer1981 levels was independent of DNA damage. This result implied that Tip60 is involved in the hypoxia induced activation of ATM. A summarised proposed mechanism is illustrated in Figure 7.1.

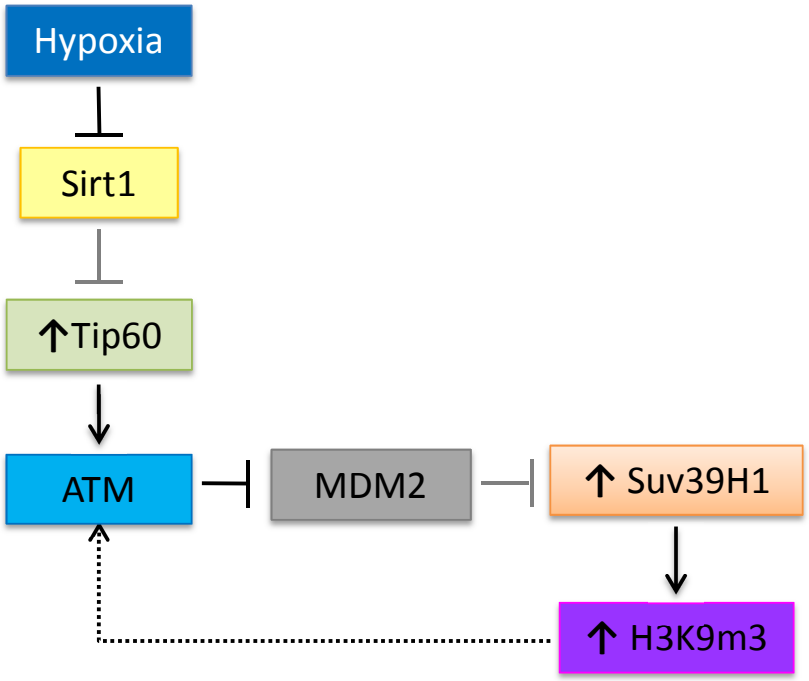

Figure 7.1. Proposed mechanism of hypoxia induced activation of ATM and its consequence

Tip60 has been proposed to link chromatin with the DDR pathway [59]. The role of Tip60 in the induction of ATM in hypoxia further underlines the importance of the chromatin structure in ATM activation. The possible dependence of Tip60 activation on Sirt1 may be an important link between DDR and metabolism in hypoxia. The involvement of ATM in Kap1 dependent chromatin relaxation to promote DNA damage repair has been previously established [191]. This is a direct consequence of ATM activation and happens quickly after ATM activation. However, the induction on Suv39H1 in response to ATM activation seems to be a late response in the DDR activation process as it happens indirectly through MDM2. The importance of ATM in maintaining heterochromatin integrity is well known [191]. The existence of a mechanism that links ATM to heterochromatin formation seems

logical as this helps the cell to re-establish the heterochromatin after the damage has been repaired and protect the genome through chromatin compaction.

6.2. FUTURE DIRECTIONS

Further investigations are needed to unravel the detailed molecular mechanisms governing the regulation of chromatin structure in response to hypoxic stress by the ATM and Suv39H1 interplay. It would be beneficial to perform Suv39H1 knockdown and analyse the effect of this on the levels of H3K9me3 in hypoxia. Existent preliminary data using Suv39H1 siRNA points to Suv39H1 dependent induction of H3K9me3. Further work is still required to confirm this hypothesis.

On the other hand it will also be important to address if the upregulation of H3K9me3 translates to a more compact form of chromatin. This can be done by using a chromatin accessibility assays such as Micrococcal nuclease (MNase) assays. This will provide information about the level of compaction of the chromatin in cells exposed to hypoxia.

In order to understand better the involvement of ATM in heterochromatin formation, it will be necessary to evaluate the levels of heterochromatin factors in ATM $^{-/-}$ cells exposed to hypoxia. Additionally, to provide further support to the data in this study immunohistochemical analysis of pre-existent tumour sections might be useful. It will be interesting to see if tumour sections present co-localised expression of ATM-pSer1981 with Suv39H1 and H3K9me3. It will also be important to evaluate if this correlates with the hypoxic regions of the tumour. This will provide information about the relevance of the mechanism described in this study in 3D tumour models. Demonstrating the importance of these mechanisms in tumour samples would provide insight into possible future therapeutic opportunities, as for example, the use of Suv39H1 as a target to sensitise hypoxic cells to treatment.

Another important aspect of this study is the elucidation of the role of Tip60 in the hypoxia induced activation of ATM. The activation of Tip60 in response to hypoxia might be due to the observed downregulation of Sirt1. It will be important to study further the role that Sirt1 plays in the hypoxia induced activation of the DNA damage response pathway. Sirt1 is a NAD^+ dependent enzyme that might be an important link between tumour metabolism and the DNA damage response pathway. The detailed understanding of this mechanism will facilitate better targeting of the hypoxic regions of the tumour.

REFERENCES

1. The National Cancer Institute. (2014) "Defining cancer" Available at: http://www.cancer.gov/cancertopics/cancerlibrary/what-is-cancer [Accessed on 29/10/2014].
2. Rohwer, N., et al., *The growing complexity of HIF-1alpha's role in tumorigenesis: DNA repair and beyond.* Oncogene, 2013. **32**(31): p. 3569-76.
3. Hanahan, D. and R.A. Weinberg, *The hallmarks of cancer.* Cell, 2000. **100**(1): p. 57-70.
4. Hanahan, D. and R.A. Weinberg, *Hallmarks of cancer: the next generation.* Cell, 2011. **144**(5): p. 646-74.
5. Harris, A.L., *Hypoxia--a key regulatory factor in tumour growth.* Nat Rev Cancer, 2002. **2**(1): p. 38-47.
6. Bertout, J.A., S.A. Patel, and M.C. Simon, *The impact of O2 availability on human cancer.* Nat Rev Cancer, 2008. **8**(12): p. 967-75.
7. Bristow, R.G. and R.P. Hill, *Hypoxia and metabolism. Hypoxia, DNA repair and genetic instability.* Nat Rev Cancer, 2008. **8**(3): p. 180-92.
8. Semenza, G.L., *Expression of hypoxia-inducible factor 1: mechanisms and consequences.* Biochem Pharmacol, 2000. **59**(1): p. 47-53.
9. Weidemann, A. and R.S. Johnson, *Biology of HIF-1alpha.* Cell Death Differ, 2008. **15**(4): p. 621-7.
10. Clarke, M.F., et al., *Cancer stem cells--perspectives on current status and future directions: AACR Workshop on cancer stem cells.* Cancer Res, 2006. **66**(19): p. 9339-44.
11. Schodel, J., D.R. Mole, and P.J. Ratcliffe, *Pan-genomic binding of hypoxia-inducible transcription factors.* Biol Chem, 2013. **394**(4): p. 507-17.
12. Semenza, G.L., *Hypoxia-inducible factor 1: regulator of mitochondrial metabolism and mediator of ischemic preconditioning.* Biochim Biophys Acta, 2011. **1813**(7): p. 1263-8.
13. Kenneth, N.S. and S. Rocha, *Regulation of gene expression by hypoxia.* Biochem J, 2008. **414**(1): p. 19-29.
14. Hu, C.J., et al., *The N-terminal transactivation domain confers target gene specificity of hypoxia-inducible factors HIF-1alpha and HIF-2alpha.* Mol Biol Cell, 2007. **18**(11): p. 4528-42.
15. Wiesener, M.S., et al., *Widespread hypoxia-inducible expression of HIF-2alpha in distinct cell populations of different organs.* FASEB J, 2003. **17**(2): p. 271-3.
16. Boulahbel, H., R.V. Duran, and E. Gottlieb, *Prolyl hydroxylases as regulators of cell metabolism.* Biochem Soc Trans, 2009. **37**(Pt 1): p. 291-4.
17. Rabinowitz, M.H., *Inhibition of hypoxia-inducible factor prolyl hydroxylase domain oxygen sensors: tricking the body into mounting orchestrated survival and repair responses.* J Med Chem, 2013. **56**(23): p. 9369-402.
18. Gordan, J.D. and M.C. Simon, *Hypoxia-inducible factors: central regulators of the tumor phenotype.* Curr Opin Genet Dev, 2007. **17**(1): p. 71-7.
19. Majumder, P.K., et al., *mTOR inhibition reverses Akt-dependent prostate intraepithelial neoplasia through regulation of apoptotic and HIF-1-dependent pathways.* Nat Med, 2004. **10**(6): p. 594-601.
20. Zelzer, E., et al., *Insulin induces transcription of target genes through the hypoxia-inducible factor HIF-1alpha/ARNT.* EMBO J, 1998. **17**(17): p. 5085-94.
21. Richard, D.E., et al., *p42/p44 mitogen-activated protein kinases phosphorylate hypoxia-inducible factor 1alpha (HIF-1alpha) and enhance the transcriptional activity of HIF-1.* J Biol Chem, 1999. **274**(46): p. 32631-7.
22. Olcina, M.M., et al., *Replication stress and chromatin context link ATM activation to a role in DNA replication.* Mol Cell, 2013. **52**(5): p. 758-66.

23. Pires, I.M., et al., *Targeting radiation-resistant hypoxic tumour cells through ATR inhibition.* Br J Cancer, 2012. **107**(2): p. 291-9.
24. Bencokova, Z., et al., *ATM activation and signaling under hypoxic conditions.* Mol Cell Biol, 2009. **29**(2): p. 526-37.
25. Bouquet, F., et al., *A DNA-dependent stress response involving DNA-PK occurs in hypoxic cells and contributes to cellular adaptation to hypoxia.* J Cell Sci, 2011. **124**(Pt 11): p. 1943-51.
26. Cam, H., et al., *mTORC1 signaling under hypoxic conditions is controlled by ATM-dependent phosphorylation of HIF-1alpha.* Mol Cell, 2010. **40**(4): p. 509-20.
27. Fallone, F., et al., *ATR controls cellular adaptation to hypoxia through positive regulation of hypoxia-inducible factor 1 (HIF-1) expression.* Oncogene, 2013. **32**(37): p. 4387-96.
28. Vaupel, P. and A. Mayer, *Hypoxia in cancer: significance and impact on clinical outcome.* Cancer Metastasis Rev, 2007. **26**(2): p. 225-39.
29. Rademakers, S.E., et al., *Molecular aspects of tumour hypoxia.* Mol Oncol, 2008. **2**(1): p. 41-53.
30. Blouw, B., et al., *The hypoxic response of tumors is dependent on their microenvironment.* Cancer Cell, 2003. **4**(2): p. 133-46.
31. Chi, J.T., et al., *Gene expression programs in response to hypoxia: cell type specificity and prognostic significance in human cancers.* PLoS Med, 2006. **3**(3): p. e47.
32. Yu, T., B. Tang, and X. Sun, *Development of Inhibitors Targeting Hypoxia-Inducible Factor 1 and 2 for Cancer Therapy.* Yonsei Med J, 2017. **58**(3): p. 489-496.
33. Koshiji, M., et al., *HIF-1alpha induces cell cycle arrest by functionally counteracting Myc.* EMBO J, 2004. **23**(9): p. 1949-56.
34. Dang, C.V., et al., *The interplay between MYC and HIF in cancer.* Nat Rev Cancer, 2008. **8**(1): p. 51-6.
35. Lovejoy, C.A. and D. Cortez, *Common mechanisms of PIKK regulation.* DNA Repair (Amst), 2009. **8**(9): p. 1004-8.
36. Gray, L.H., et al., *The concentration of oxygen dissolved in tissues at the time of irradiation as a factor in radiotherapy.* Br J Radiol, 1953. **26**(312): p. 638-48.
37. Grimes, D.R. and M. Partridge, *A mechanistic investigation of the oxygen fixation hypothesis and oxygen enhancement ratio.* Biomed Phys Eng Express, 2015. **1**(4): p. 045209.
38. Doktorova, H., et al., *Hypoxia-induced chemoresistance in cancer cells: The role of not only HIF-1.* Biomed Pap Med Fac Univ Palacky Olomouc Czech Repub, 2015. **159**(2): p. 166-77.
39. Watson, J.A., et al., *Epigenetics, the epicenter of the hypoxic response.* Epigenetics, 2010. **5**(4): p. 293-6.
40. Melvin, A. and S. Rocha, *Chromatin as an oxygen sensor and active player in the hypoxia response.* Cell Signal, 2012. **24**(1): p. 35-43.
41. Venkatesh, S. and J.L. Workman, *Histone exchange, chromatin structure and the regulation of transcription.* Nat Rev Mol Cell Biol, 2015. **16**(3): p. 178-89.
42. Cann, K.L. and G. Dellaire, *Heterochromatin and the DNA damage response: the need to relax.* Biochem Cell Biol, 2011. **89**(1): p. 45-60.
43. Weisenberger, D.J., et al., *Analysis of repetitive element DNA methylation by MethyLight.* Nucleic Acids Res, 2005. **33**(21): p. 6823-36.
44. Ramachandran, S., et al., *Epigenetic Therapy for Solid Tumors: Highlighting the Impact of Tumor Hypoxia.* Genes (Basel), 2015. **6**(4): p. 935-56.
45. Kouzarides, T., *Chromatin modifications and their function.* Cell, 2007. **128**(4): p. 693-705.
46. Lu, X., et al., *The effect of H3K79 dimethylation and H4K20 trimethylation on nucleosome and chromatin structure.* Nat Struct Mol Biol, 2008. **15**(10): p. 1122-4.
47. Margueron, R., P. Trojer, and D. Reinberg, *The key to development: interpreting the histone code?* Curr Opin Genet Dev, 2005. **15**(2): p. 163-76.

48. Vettese-Dadey, M., et al., *Acetylation of histone H4 plays a primary role in enhancing transcription factor binding to nucleosomal DNA in vitro.* EMBO J, 1996. **15**(10): p. 2508-18.
49. Hong, L., et al., *Studies of the DNA binding properties of histone H4 amino terminus. Thermal denaturation studies reveal that acetylation markedly reduces the binding constant of the H4 "tail" to DNA.* J Biol Chem, 1993. **268**(1): p. 305-14.
50. Josling, G.A., et al., *The role of bromodomain proteins in regulating gene expression.* Genes (Basel), 2012. **3**(2): p. 320-43.
51. Greer, E.L. and Y. Shi, *Histone methylation: a dynamic mark in health, disease and inheritance.* Nat Rev Genet, 2012. **13**(5): p. 343-57.
52. Lawrence, M., S. Daujat, and R. Schneider, *Lateral Thinking: How Histone Modifications Regulate Gene Expression.* Trends Genet, 2016. **32**(1): p. 42-56.
53. Johansson, C., et al., *The roles of Jumonji-type oxygenases in human disease.* Epigenomics, 2014. **6**(1): p. 89-120.
54. Oike, T., et al., *Chromatin-regulating proteins as targets for cancer therapy.* J Radiat Res, 2014. **55**(4): p. 613-28.
55. Perez-Perri, J.I., J.M. Acevedo, and P. Wappner, *Epigenetics: new questions on the response to hypoxia.* Int J Mol Sci, 2011. **12**(7): p. 4705-21.
56. Barski, A., et al., *High-resolution profiling of histone methylations in the human genome.* Cell, 2007. **129**(4): p. 823-37.
57. Becker, J.S., D. Nicetto, and K.S. Zaret, *H3K9me3-Dependent Heterochromatin: Barrier to Cell Fate Changes.* Trends Genet, 2016. **32**(1): p. 29-41.
58. Dejardin, J., *Switching between Epigenetic States at Pericentromeric Heterochromatin.* Trends Genet, 2015. **31**(11): p. 661-672.
59. Sun, Y., et al., *Histone H3 methylation links DNA damage detection to activation of the tumour suppressor Tip60.* Nat Cell Biol, 2009. **11**(11): p. 1376-82.
60. Mungamuri, S.K., et al., *p53-mediated heterochromatin reorganization regulates its cell fate decisions.* Nat Struct Mol Biol, 2012. **19**(5): p. 478-84, S1.
61. Tschiersch, B., et al., *The protein encoded by the Drosophila position-effect variegation suppressor gene Su(var)3-9 combines domains of antagonistic regulators of homeotic gene complexes.* EMBO J, 1994. **13**(16): p. 3822-31.
62. Dillon, S.C., et al., *The SET-domain protein superfamily: protein lysine methyltransferases.* Genome Biol, 2005. **6**(8): p. 227.
63. Loyola, A., et al., *PTMs on H3 variants before chromatin assembly potentiate their final epigenetic state.* Mol Cell, 2006. **24**(2): p. 309-16.
64. Fritsch, L., et al., *A subset of the histone H3 lysine 9 methyltransferases Suv39h1, G9a, GLP, and SETDB1 participate in a multimeric complex.* Mol Cell, 2010. **37**(1): p. 46-56.
65. Rao, V.K., A. Pal, and R. Taneja, *A drive in SUVs: From development to disease.* Epigenetics, 2017. **12**(3): p. 177-186.
66. Vandel, L., et al., *Transcriptional repression by the retinoblastoma protein through the recruitment of a histone methyltransferase.* Mol Cell Biol, 2001. **21**(19): p. 6484-94.
67. Narita, M., et al., *Rb-mediated heterochromatin formation and silencing of E2F target genes during cellular senescence.* Cell, 2003. **113**(6): p. 703-16.
68. Rao, V.K., et al., *G9a promotes proliferation and inhibits cell cycle exit during myogenic differentiation.* Nucleic Acids Res, 2016. **44**(17): p. 8129-43.
69. Tachibana, K., et al., *Analysis of the subcellular localization of the human histone methyltransferase SETDB1.* Biochem Biophys Res Commun, 2015. **465**(4): p. 725-31.
70. Song, Y.J., J.H. Choi, and H. Lee, *Setdb1 is required for myogenic differentiation of C2C12 myoblast cells via maintenance of MyoD expression.* Mol Cells, 2015. **38**(4): p. 362-72.
71. Hong, W., et al., *Epigenetic involvement of Alien/ESET complex in thyroid hormone-mediated repression of E2F1 gene expression and cell proliferation.* Biochem Biophys Res Commun, 2011. **415**(4): p. 650-5.

72. Khanal, P., et al., *Prolyl isomerase Pin1 negatively regulates the stability of SUV39H1 to promote tumorigenesis in breast cancer.* FASEB J, 2013. **27**(11): p. 4606-18.
73. Bosch-Presegue, L., et al., *Stabilization of Suv39H1 by SirT1 is part of oxidative stress response and ensures genome protection.* Mol Cell, 2011. **42**(2): p. 210-23.
74. Casciello, F., et al., *Functional Role of G9a Histone Methyltransferase in Cancer.* Front Immunol, 2015. **6**: p. 487.
75. Zhang, J., et al., *Down-regulation of G9a triggers DNA damage response and inhibits colorectal cancer cells proliferation.* Oncotarget, 2015. **6**(5): p. 2917-27.
76. Fei, Q., et al., *Histone methyltransferase SETDB1 regulates liver cancer cell growth through methylation of p53.* Nat Commun, 2015. **6**: p. 8651.
77. Watson, J.A., et al., *Generation of an epigenetic signature by chronic hypoxia in prostate cells.* Hum Mol Genet, 2009. **18**(19): p. 3594-604.
78. Johnson, A.B. and M.C. Barton, *Hypoxia-induced and stress-specific changes in chromatin structure and function.* Mutat Res, 2007. **618**(1-2): p. 149-62.
79. Tsai, Y.P. and K.J. Wu, *Epigenetic regulation of hypoxia-responsive gene expression: focusing on chromatin and DNA modifications.* Int J Cancer, 2014. **134**(2): p. 249-56.
80. Muscari, C., et al., *Priming adult stem cells by hypoxic pretreatments for applications in regenerative medicine.* J Biomed Sci, 2013. **20**: p. 63.
81. Krieg, A.J., et al., *Regulation of the histone demethylase JMJD1A by hypoxia-inducible factor 1 alpha enhances hypoxic gene expression and tumor growth.* Mol Cell Biol, 2010. **30**(1): p. 344-53.
82. Park, H., *Hypoxia suffocates histone demethylases to change gene expression: a metabolic control of histone methylation.* BMB Rep, 2017. **50**(11): p. 537-538.
83. Olcina, M.M., et al., *H3K9me3 facilitates hypoxia-induced p53-dependent apoptosis through repression of APAK.* Oncogene, 2015.
84. Hammond, E.M., et al., *Hypoxia links ATR and p53 through replication arrest.* Mol Cell Biol, 2002. **22**(6): p. 1834-43.
85. Hammond, E.M., M.J. Dorie, and A.J. Giaccia, *ATR/ATM targets are phosphorylated by ATR in response to hypoxia and ATM in response to reoxygenation.* J Biol Chem, 2003. **278**(14): p. 12207-13.
86. Olcina, M., P.S. Lecane, and E.M. Hammond, *Targeting hypoxic cells through the DNA damage response.* Clin Cancer Res, 2010. **16**(23): p. 5624-9.
87. Ahuja, N., A.R. Sharma, and S.B. Baylin, *Epigenetic Therapeutics: A New Weapon in the War Against Cancer.* Annu Rev Med, 2016. **67**: p. 73-89.
88. Shen, H. and P.W. Laird, *Interplay between the cancer genome and epigenome.* Cell, 2013. **153**(1): p. 38-55.
89. Coyle, K.M., J.E. Boudreau, and P. Marcato, *Genetic Mutations and Epigenetic Modifications: Driving Cancer and Informing Precision Medicine.* Biomed Res Int, 2017. **2017**: p. 9620870.
90. Kaminskas, E., et al., *FDA drug approval summary: azacitidine (5-azacytidine, Vidaza) for injectable suspension.* Oncologist, 2005. **10**(3): p. 176-82.
91. Azad, N., et al., *The future of epigenetic therapy in solid tumours--lessons from the past.* Nat Rev Clin Oncol, 2013. **10**(5): p. 256-66.
92. Ahuja, N., H. Easwaran, and S.B. Baylin, *Harnessing the potential of epigenetic therapy to target solid tumors.* J Clin Invest, 2014. **124**(1): p. 56-63.
93. McCabe, M.T., et al., *Targeting Histone Methylation in Cancer.* Cancer J, 2017. **23**(5): p. 292-301.
94. Morera, L., M. Lubbert, and M. Jung, *Targeting histone methyltransferases and demethylases in clinical trials for cancer therapy.* Clin Epigenetics, 2016. **8**: p. 57.
95. Rada, M., et al., *Human EHMT2/G9a activates p53 through methylation-independent mechanism.* Oncogene, 2017. **36**(7): p. 922-932.

96. Bittencourt, D., et al., *G9a functions as a molecular scaffold for assembly of transcriptional coactivators on a subset of glucocorticoid receptor target genes.* Proc Natl Acad Sci U S A, 2012. **109**(48): p. 19673-8.
97. Chaudhary, M.W. and R.S. Al-Baradie, *Ataxia-telangiectasia: future prospects.* Appl Clin Genet, 2014. **7**: p. 159-67.
98. Malewicz, M. and T. Perlmann, *Function of transcription factors at DNA lesions in DNA repair.* Exp Cell Res, 2014.
99. Scharer, O.D. and A.J. Campbell, *Wedging out DNA damage.* Nat Struct Mol Biol, 2009. **16**(2): p. 102-4.
100. Hakem, R., *DNA-damage repair; the good, the bad, and the ugly.* EMBO J, 2008. **27**(4): p. 589-605.
101. Hiom, K., *Coping with DNA double strand breaks.* DNA Repair (Amst), 2010. **9**(12): p. 1256-63.
102. Manuel Stucki, J.A.C., Duaa Mohammad, Michael B. Yafee, Stephen J. Smerdon and Stephen P. Jackson *MDC1 Directly Binds Phosphorylated Histone H2AX to Regulate Cellular Responses toDNADouble-Strand Breaks.* Cell, 2005. **127**(7): p. 1213 - 1226.
103. Woods, D. and J.J. Turchi, *Chemotherapy induced DNA damage response: convergence of drugs and pathways.* Cancer Biol Ther, 2013. **14**(5): p. 379-89.
104. Harper, J.W. and S.J. Elledge, *The DNA damage response: ten years after.* Mol Cell, 2007. **28**(5): p. 739-45.
105. Du, F., et al., *Dimer monomer transition and dimer re-formation play important role for ATM cellular function during DNA repair.* Biochem Biophys Res Commun, 2014. **452**(4): p. 1034-9.
106. Bakkenist, C.J. and M.B. Kastan, *DNA damage activates ATM through intermolecular autophosphorylation and dimer dissociation.* Nature, 2003. **421**(6922): p. 499-506.
107. Blanpain, C., et al., *DNA-damage response in tissue-specific and cancer stem cells.* Cell Stem Cell, 2011. **8**(1): p. 16-29.
108. Tichy, A., et al., *Ataxia-telangiectasia mutated kinase (ATM) as a central regulator of radiation-induced DNA damage response.* Acta Medica (Hradec Kralove), 2010. **53**(1): p. 13-7.
109. Sun, Y., et al., *DNA damage-induced acetylation of lysine 3016 of ATM activates ATM kinase activity.* Mol Cell Biol, 2007. **27**(24): p. 8502-9.
110. Sapountzi, V. and J. Cote, *MYST-family histone acetyltransferases: beyond chromatin.* Cell Mol Life Sci, 2011. **68**(7): p. 1147-56.
111. Sapountzi, V., I.R. Logan, and C.N. Robson, *Cellular functions of TIP60.* Int J Biochem Cell Biol, 2006. **38**(9): p. 1496-509.
112. Tang, Y., et al., *Tip60-dependent acetylation of p53 modulates the decision between cell-cycle arrest and apoptosis.* Mol Cell, 2006. **24**(6): p. 827-39.
113. Sun, Y., et al., *A role for the Tip60 histone acetyltransferase in the acetylation and activation of ATM.* Proc Natl Acad Sci U S A, 2005. **102**(37): p. 13182-7.
114. Kaidi, A. and S.P. Jackson, *KAT5 tyrosine phosphorylation couples chromatin sensing to ATM signalling.* Nature, 2013. **498**(7452): p. 70-4.
115. Ghobashi, A.H. and M.A. Kamel, *Tip60: updates.* J Appl Genet, 2018. **59**(2): p. 161-168.
116. Goodarzi, A.A., et al., *Autophosphorylation of ataxia-telangiectasia mutated is regulated by protein phosphatase 2A.* EMBO J, 2004. **23**(22): p. 4451-61.
117. Miyakoda, M., et al., *Activation of ATM and phosphorylation of p53 by heat shock.* Oncogene, 2002. **21**(7): p. 1090-6.
118. Guo, Z., et al., *ATM activation by oxidative stress.* Science, 2010. **330**(6003): p. 517-21.
119. Irarrazabal, C.E., et al., *ATM, a DNA damage-inducible kinase, contributes to activation by high NaCl of the transcription factor TonEBP/OREBP.* Proc Natl Acad Sci U S A, 2004. **101**(23): p. 8809-14.

120. Olcina, M.M., R.J. Grand, and E.M. Hammond, *ATM activation in hypoxia - causes and consequences.* Mol Cell Oncol, 2014. **1**(1): p. e29903.
121. Kumareswaran, R., et al., *Chronic hypoxia compromises repair of DNA double-strand breaks to drive genetic instability.* J Cell Sci, 2012. **125**(Pt 1): p. 189-99.
122. Chen, H., et al., *Hypoxic stress induces dimethylated histone H3 lysine 9 through histone methyltransferase G9a in mammalian cells.* Cancer Res, 2006. **66**(18): p. 9009-16.
123. Bindra, R.S. and P.M. Glazer, *Repression of RAD51 gene expression by E2F4/p130 complexes in hypoxia.* Oncogene, 2007. **26**(14): p. 2048-57.
124. Sprong, D., et al., *Resistance of hypoxic cells to ionizing radiation is influenced by homologous recombination status.* Int J Radiat Oncol Biol Phys, 2006. **64**(2): p. 562-72.
125. Um, J.H., et al., *Association of DNA-dependent protein kinase with hypoxia inducible factor-1 and its implication in resistance to anticancer drugs in hypoxic tumor cells.* Exp Mol Med, 2004. **36**(3): p. 233-42.
126. Ding, G., et al., *HIF1-regulated ATRIP expression is required for hypoxia induced ATR activation.* FEBS Lett, 2013. **587**(7): p. 930-5.
127. To, K.K., et al., *The phosphorylation status of PAS-B distinguishes HIF-1alpha from HIF-2alpha in NBS1 repression.* EMBO J, 2006. **25**(20): p. 4784-94.
128. Burgess, R.C., et al., *Activation of DNA damage response signaling by condensed chromatin.* Cell Rep, 2014. **9**(5): p. 1703-17.
129. O'Connor, M.J., *Targeting the DNA Damage Response in Cancer.* Mol Cell, 2015. **60**(4): p. 547-60.
130. Hosoya, N. and K. Miyagawa, *Targeting DNA damage response in cancer therapy.* Cancer Sci, 2014. **105**(4): p. 370-88.
131. Jackson, S.P. and J. Bartek, *The DNA-damage response in human biology and disease.* Nature, 2009. **461**(7267): p. 1071-1078.
132. Helleday, T., *The underlying mechanism for the PARP and BRCA synthetic lethality: clearing up the misunderstandings.* Mol Oncol, 2011. **5**(4): p. 387-93.
133. Hahn, W.C., et al., *Creation of human tumour cells with defined genetic elements.* Nature, 1999. **400**(6743): p. 464-8.
134. Bartkova, J., et al., *Replication stress and oxidative damage contribute to aberrant constitutive activation of DNA damage signalling in human gliomas.* Oncogene, 2010. **29**(36): p. 5095-102.
135. Halazonetis, T.D., V.G. Gorgoulis, and J. Bartek, *An oncogene-induced DNA damage model for cancer development.* Science, 2008. **319**(5868): p. 1352-5.
136. Hills, S.A. and J.F. Diffley, *DNA replication and oncogene-induced replicative stress.* Curr Biol, 2014. **24**(10): p. R435-44.
137. Ball, H.L., J.S. Myers, and D. Cortez, *ATRIP binding to replication protein A-single-stranded DNA promotes ATR-ATRIP localization but is dispensable for Chk1 phosphorylation.* Mol Biol Cell, 2005. **16**(5): p. 2372-81.
138. Beck, H., et al., *Cyclin-dependent kinase suppression by WEE1 kinase protects the genome through control of replication initiation and nucleotide consumption.* Mol Cell Biol, 2012. **32**(20): p. 4226-36.
139. Chen, D., et al., *Wee1 Inhibitor AZD1775 Combined with Cisplatin Potentiates Anticancer Activity against Gastric Cancer by Increasing DNA Damage and Cell Apoptosis.* Biomed Res Int, 2018. **2018**: p. 5813292.
140. Do, K., et al., *Phase I Study of Single-Agent AZD1775 (MK-1775), a Wee1 Kinase Inhibitor, in Patients With Refractory Solid Tumors.* J Clin Oncol, 2015. **33**(30): p. 3409-15.
141. Liu, S.K., et al., *A novel poly(ADP-ribose) polymerase inhibitor, ABT-888, radiosensitizes malignant human cell lines under hypoxia.* Radiother Oncol, 2008. **88**(2): p. 258-68.
142. Chan, N., et al., *Contextual synthetic lethality of cancer cell kill based on the tumor microenvironment.* Cancer Res, 2010. **70**(20): p. 8045-54.

143. Rao, A.S., et al., *Letter Re: Id1 gene expression in hyperplastic and neoplastic thyroid tissues.* J Clin Endocrinol Metab, 2005. **90**(10): p. 5906.
144. Ponten, J. and E.H. Macintyre, *Long term culture of normal and neoplastic human glia.* Acta Pathol Microbiol Scand, 1968. **74**(4): p. 465-86.
145. Sun, L., et al., *Autocrine transforming growth factor-beta 1 and beta 2 expression is increased by cell crowding and quiescence in colon carcinoma cells.* Exp Cell Res, 1994. **214**(1): p. 215-24.
146. Gao, C., et al., *Rational design and validation of a Tip60 histone acetyltransferase inhibitor.* Sci Rep, 2014. **4**: p. 5372.
147. Hickson, I., et al., *Identification and characterization of a novel and specific inhibitor of the ataxia-telangiectasia mutated kinase ATM.* Cancer Res, 2004. **64**(24): p. 9152-9.
148. Groll, M. and R. Huber, *Inhibitors of the eukaryotic 20S proteasome core particle: a structural approach.* Biochim Biophys Acta, 2004. **1695**(1-3): p. 33-44.
149. Smith, P.K., et al., *Measurement of protein using bicinchoninic acid.* Anal Biochem, 1985. **150**(1): p. 76-85.
150. M, P., *Relative quantification*, in *Real- time PCR* B. SA, Editor. 2004, International University Line: La Jolla, CA. p. 63-82.
151. Bannister, A.J. and T. Kouzarides, *Regulation of chromatin by histone modifications.* Cell Res, 2011. **21**(3): p. 381-95.
152. Falk, M., E. Lukasova, and S. Kozubek, *Chromatin structure influences the sensitivity of DNA to gamma-radiation.* Biochim Biophys Acta, 2008. **1783**(12): p. 2398-414.
153. Takata, H., et al., *Chromatin compaction protects genomic DNA from radiation damage.* PLoS One, 2013. **8**(10): p. e75622.
154. Nakayama, J., et al., *Role of histone H3 lysine 9 methylation in epigenetic control of heterochromatin assembly.* Science, 2001. **292**(5514): p. 110-3.
155. Rea, S., et al., *Regulation of chromatin structure by site-specific histone H3 methyltransferases.* Nature, 2000. **406**(6796): p. 593-9.
156. Hagemann, T.L., D. Mares, and S. Kwan, *Gene regulation of Wiskott-Aldrich syndrome protein and the human homolog of the Drosophila Su(var)3-9: WASP and SUV39H1, two adjacent genes at Xp11.23.* Biochim Biophys Acta, 2000. **1493**(3): p. 368-72.
157. Wang, D., et al., *Methylation of SUV39H1 by SET7/9 results in heterochromatin relaxation and genome instability.* Proc Natl Acad Sci U S A, 2013. **110**(14): p. 5516-21.
158. Tausendschon, M., N. Dehne, and B. Brune, *Hypoxia causes epigenetic gene regulation in macrophages by attenuating Jumonji histone demethylase activity.* Cytokine, 2011. **53**(2): p. 256-62.
159. Lu, Y., et al., *Silencing of the DNA mismatch repair gene MLH1 induced by hypoxic stress in a pathway dependent on the histone demethylase LSD1.* Cell Rep, 2014. **8**(2): p. 501-13.
160. Lu, Y., et al., *Hypoxia-induced epigenetic regulation and silencing of the BRCA1 promoter.* Mol Cell Biol, 2011. **31**(16): p. 3339-50.
161. Benlhabib, H. and C.R. Mendelson, *Epigenetic regulation of surfactant protein A gene (SP-A) expression in fetal lung reveals a critical role for Suv39h methyltransferases during development and hypoxia.* Mol Cell Biol, 2011. **31**(10): p. 1949-58.
162. Jia, S., K. Noma, and S.I. Grewal, *RNAi-independent heterochromatin nucleation by the stress-activated ATF/CREB family proteins.* Science, 2004. **304**(5679): p. 1971-6.
163. Sulli, G., R. Di Micco, and F. d'Adda di Fagagna, *Crosstalk between chromatin state and DNA damage response in cellular senescence and cancer.* Nat Rev Cancer, 2012. **12**(10): p. 709-20.
164. Li, C. and R.M. Jackson, *Reactive species mechanisms of cellular hypoxia-reoxygenation injury.* Am J Physiol Cell Physiol, 2002. **282**(2): p. C227-41.
165. Dewhirst, M.W., Y. Cao, and B. Moeller, *Cycling hypoxia and free radicals regulate angiogenesis and radiotherapy response.* Nat Rev Cancer, 2008. **8**(6): p. 425-37.

166. Cavadas, M.A.S., A. Cheong, and C.T. Taylor, *The regulation of transcriptional repression in hypoxia.* Exp Cell Res, 2017. **356**(2): p. 173-181.
167. Boutilier, R.G., *Mechanisms of cell survival in hypoxia and hypothermia.* J Exp Biol, 2001. **204**(Pt 18): p. 3171-81.
168. Fahraeus, R. and V. Olivares-Illana, *MDM2's social network.* Oncogene, 2014. **33**(35): p. 4365-76.
169. Peters, A.H., et al., *Loss of the Suv39h histone methyltransferases impairs mammalian heterochromatin and genome stability.* Cell, 2001. **107**(3): p. 323-37.
170. Reimann, M., et al., *Tumor stroma-derived TGF-beta limits myc-driven lymphomagenesis via Suv39h1-dependent senescence.* Cancer Cell, 2010. **17**(3): p. 262-72.
171. Albacker, C.E., et al., *The histone methyltransferase SUV39H1 suppresses embryonal rhabdomyosarcoma formation in zebrafish.* PLoS One, 2013. **8**(5): p. e64969.
172. Yokoyama, Y., et al., *Cancer-associated upregulation of histone H3 lysine 9 trimethylation promotes cell motility in vitro and drives tumor formation in vivo.* Cancer Sci, 2013. **104**(7): p. 889-95.
173. Chen, L., et al., *MDM2 recruitment of lysine methyltransferases regulates p53 transcriptional output.* EMBO J, 2010. **29**(15): p. 2538-52.
174. Cheng, Q., et al., *ATM activates p53 by regulating MDM2 oligomerization and E3 processivity.* EMBO J, 2009. **28**(24): p. 3857-67.
175. Gannon, H.S., B.A. Woda, and S.N. Jones, *ATM phosphorylation of Mdm2 Ser394 regulates the amplitude and duration of the DNA damage response in mice.* Cancer Cell, 2012. **21**(5): p. 668-79.
176. Ravi, R., et al., *Regulation of tumor angiogenesis by p53-induced degradation of hypoxia-inducible factor 1alpha.* Genes Dev, 2000. **14**(1): p. 34-44.
177. Ozdag, H., et al., *Differential expression of selected histone modifier genes in human solid cancers.* BMC Genomics, 2006. **7**: p. 90.
178. Liu, Q., et al., *Hypoxia induces genomic DNA demethylation through the activation of HIF-1alpha and transcriptional upregulation of MAT2A in hepatoma cells.* Mol Cancer Ther, 2011. **10**(6): p. 1113-23.
179. Nardinocchi, L., et al., *Targeting hypoxia in cancer cells by restoring homeodomain interacting protein-kinase 2 and p53 activity and suppressing HIF-1alpha.* PLoS One, 2009. **4**(8): p. e6819.
180. Salehi-Abargouei, A., et al., *Dietary diversity score and obesity: a systematic review and meta-analysis of observational studies.* Eur J Clin Nutr, 2016. **70**(1): p. 1-9.
181. Lim, J.H., et al., *Sirtuin 1 modulates cellular responses to hypoxia by deacetylating hypoxia-inducible factor 1alpha.* Mol Cell, 2010. **38**(6): p. 864-78.
182. Barak, Y., et al., *Regulation of mdm2 expression by p53: alternative promoters produce transcripts with nonidentical translation potential.* Genes Dev, 1994. **8**(15): p. 1739-49.
183. Mayo, L.D., J.J. Turchi, and S.J. Berberich, *Mdm-2 phosphorylation by DNA-dependent protein kinase prevents interaction with p53.* Cancer Res, 1997. **57**(22): p. 5013-6.
184. Kaeser, M.D., S. Pebernard, and R.D. Iggo, *Regulation of p53 stability and function in HCT116 colon cancer cells.* J Biol Chem, 2004. **279**(9): p. 7598-605.
185. Khoronenkova, S.V., et al., *ATM-dependent downregulation of USP7/HAUSP by PPM1G activates p53 response to DNA damage.* Mol Cell, 2012. **45**(6): p. 801-13.
186. Fernandez-Capetillo, O. and A. Nussenzweig, *ATM breaks into heterochromatin.* Mol Cell, 2008. **31**(3): p. 303-4.
187. Shanbhag, N.M., et al., *ATM-dependent chromatin changes silence transcription in cis to DNA double-strand breaks.* Cell, 2010. **141**(6): p. 970-81.
188. Mungamuri, S.K., et al., *USP7 Enforces Heterochromatinization of p53 Target Promoters by Protecting SUV39H1 from MDM2-Mediated Degradation.* Cell Rep, 2016. **14**(11): p. 2528-37.

189. Ciccia, A. and S.J. Elledge, *The DNA damage response: making it safe to play with knives.* Mol Cell, 2010. **40**(2): p. 179-204.
190. Zou, L. and S.J. Elledge, *Sensing DNA damage through ATRIP recognition of RPA-ssDNA complexes.* Science, 2003. **300**(5625): p. 1542-8.
191. Goodarzi, A.A., et al., *ATM signaling facilitates repair of DNA double-strand breaks associated with heterochromatin.* Mol Cell, 2008. **31**(2): p. 167-77.
192. Hunt, C.R., et al., *Hyperthermia activates a subset of ataxia-telangiectasia mutated effectors independent of DNA strand breaks and heat shock protein 70 status.* Cancer Res, 2007. **67**(7): p. 3010-7.
193. Kanu, N. and A. Behrens, *ATMIN defines an NBS1-independent pathway of ATM signalling.* EMBO J, 2007. **26**(12): p. 2933-41.
194. Peng, L., et al., *SIRT1 negatively regulates the activities, functions, and protein levels of hMOF and TIP60.* Mol Cell Biol, 2012. **32**(14): p. 2823-36.
195. Wang, J. and J. Chen, *SIRT1 regulates autoacetylation and histone acetyltransferase activity of TIP60.* J Biol Chem, 2010. **285**(15): p. 11458-64.
196. Perez-Perri, J.I., et al., *The TIP60 Complex Is a Conserved Coactivator of HIF1A.* Cell Rep, 2016. **16**(1): p. 37-47.
197. Chailleux, C., et al., *Physical interaction between the histone acetyl transferase Tip60 and the DNA double-strand breaks sensor MRN complex.* Biochem J, 2010. **426**(3): p. 365-71.
198. Wrann, S., et al., *HIF mediated and DNA damage independent histone H2AX phosphorylation in chronic hypoxia.* Biol Chem, 2013. **394**(4): p. 519-28.
199. Hammond, E.M., M.J. Dorie, and A.J. Giaccia, *Inhibition of ATR leads to increased sensitivity to hypoxia/reoxygenation.* Cancer Res, 2004. **64**(18): p. 6556-62.
200. Gupta, A., et al., *MOF phosphorylation by ATM regulates 53BP1-mediated double-strand break repair pathway choice.* Cell Rep, 2014. **8**(1): p. 177-89.
201. Mallette, F.A., et al., *RNF8- and RNF168-dependent degradation of KDM4A/JMJD2A triggers 53BP1 recruitment to DNA damage sites.* EMBO J, 2012. **31**(8): p. 1865-78.
202. Squatrito, M., C. Gorrini, and B. Amati, *Tip60 in DNA damage response and growth control: many tricks in one HAT.* Trends Cell Biol, 2006. **16**(9): p. 433-42.
203. Liu, L., et al., *Hypoxia-induced energy stress regulates mRNA translation and cell growth.* Mol Cell, 2006. **21**(4): p. 521-31.
204. Gordan, J.D., et al., *HIF-2alpha promotes hypoxic cell proliferation by enhancing c-myc transcriptional activity.* Cancer Cell, 2007. **11**(4): p. 335-47.
205. Xenaki, G., et al., *PCAF is an HIF-1alpha cofactor that regulates p53 transcriptional activity in hypoxia.* Oncogene, 2008. **27**(44): p. 5785-96.
206. Gardner, L.B., et al., *Hypoxia inhibits G1/S transition through regulation of p27 expression.* J Biol Chem, 2001. **276**(11): p. 7919-26.
207. Xie, L., et al., *PHD3-dependent hydroxylation of HCLK2 promotes the DNA damage response.* J Clin Invest, 2012. **122**(8): p. 2827-36.
208. Richards, R., et al., *Cell cycle progression in glioblastoma cells is unaffected by pathophysiological levels of hypoxia.* PeerJ, 2016. **4**: p. e1755.
209. Foskolou, I.P., et al., *Ribonucleotide Reductase Requires Subunit Switching in Hypoxia to Maintain DNA Replication.* Mol Cell, 2017. **66**(2): p. 206-220 e9.
210. Kolberg, M., et al., *Structure, function, and mechanism of ribonucleotide reductases.* Biochim Biophys Acta, 2004. **1699**(1-2): p. 1-34.
211. Fang, Z., et al., *Ribonucleotide reductase large subunit M1 plays a different role in the invasion and metastasis of papillary thyroid carcinoma and undifferentiated thyroid carcinoma.* Tumour Biol, 2016. **37**(3): p. 3515-26.
212. Di Micco, R., et al., *Interplay between oncogene-induced DNA damage response and heterochromatin in senescence and cancer.* Nat Cell Biol, 2011. **13**(3): p. 292-302.